6. PHASE DIAGRAMS

The starting compositions were based on the phase diagrams of Bruwer (1996). At low Fe concentrations (< 10 wt% Fe), the quaternary phase diagrams is not expected to deviate much from the ternary (Cu-Ni-S) phase diagrams. This means that the major stability fields in the Cu-Ni-S system are anticipated to remain in existence in the Cu-Ni-Fe-S system but will possibly change in size and shape.

Phase diagrams are grouped in temperature classes and sub-grouped according to the starting Fe-content (i.e. 1, 3, 5 and 10 wt% Fe). The average and standard deviations for EMP analyses of phases are listed in Appendix C according to the relevant starting Fe-content. Appendix D groups the experiment labels according to the starting Fe-content in the different stability fields for each isothermal section.

6.1 The 1200°C isothermal sections

The specific isothermal sections are presented in Figures 6.1 to 6.4. At 1200°C (and different Fe contents), the assemblage consists of two phases, a melt and an alloy. At less than ~ 20 wt% sulphur and more than ~ 20 wt% Ni, an alloy phase will be stable in the melt. The compositions of the alloy and coexisting melt depend on the starting composition: with an increase in the starting Fe-content, the composition of the coexisting melt increases in sulphur content. The composition of the melt coexisting with pure Ni-alloy is inferred, using the diagram of Bruwer (1996) as a guideline.

Experiments 12I5 and 12I6 display deviations from the starting composition, and because the precision and accuracy of analysis were high, it can reasonably be argued that the polished surface do not display all the phases present at the specified temperature. In these experiments the sulphur values are notably higher and the metals lower than the starting composition. It can, therefore, be expected that an alloy phase is part of the assemblage, although not detected in the specific section of the experiment.

At starting compositions containing more than 50 wt% Cu and less than ~ 20 wt% sulphur, the melt separates into two immiscible melts with different sulphur contents. The two immiscible melts do not co-exist with an alloy phase. The position of the (2-melt)-field is indicated with a dotted field boundary line after the position and shape of this field in the Fe-free system. The shape and size of the (2 melt)-field were not of interest for the purpose of this study. Therefore, it was not investigated in detail and only a small amount of data points are available.

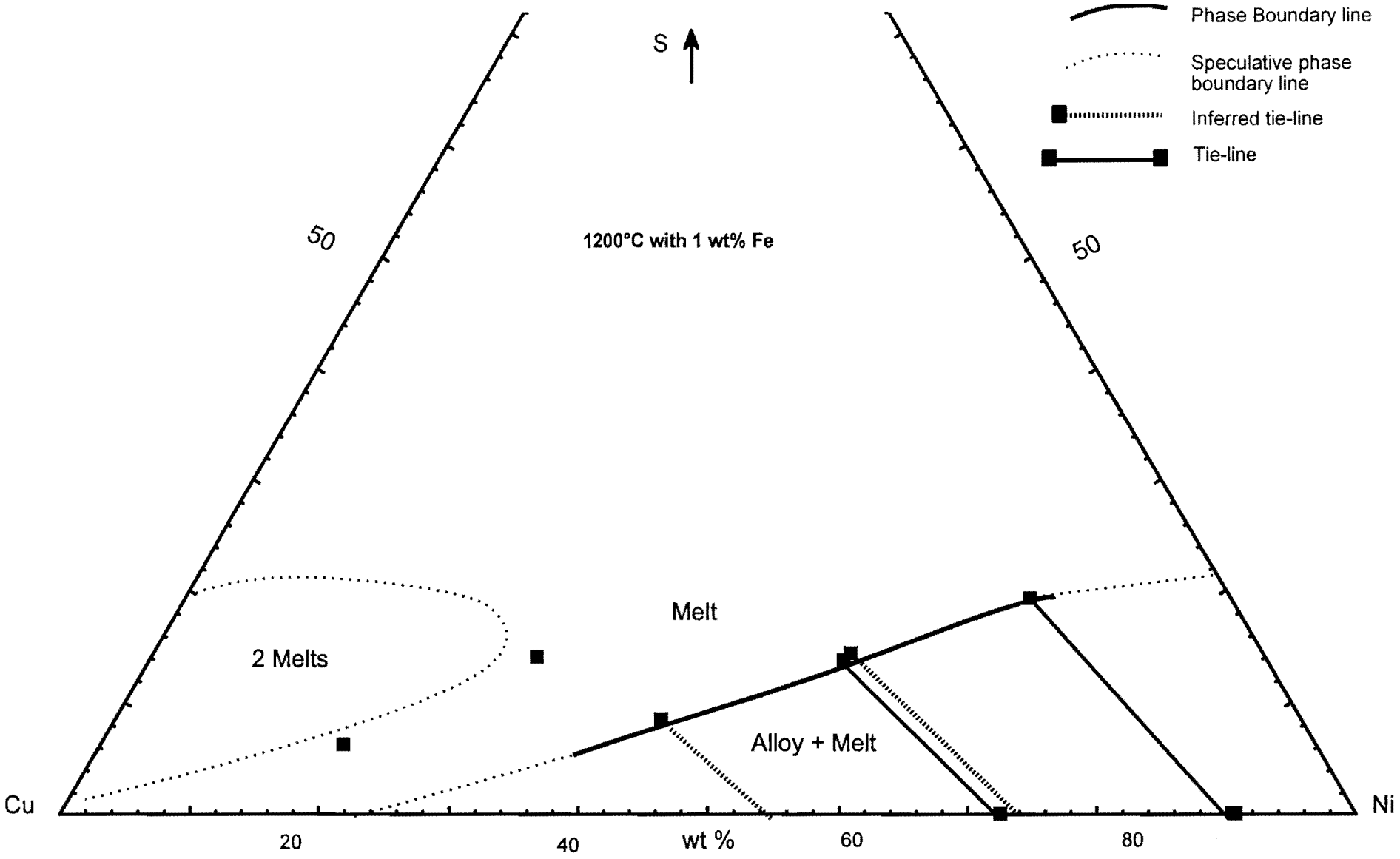

Figure 6.1: Phase relations at 1200°C and 1 wt% Fe in starting compositions.

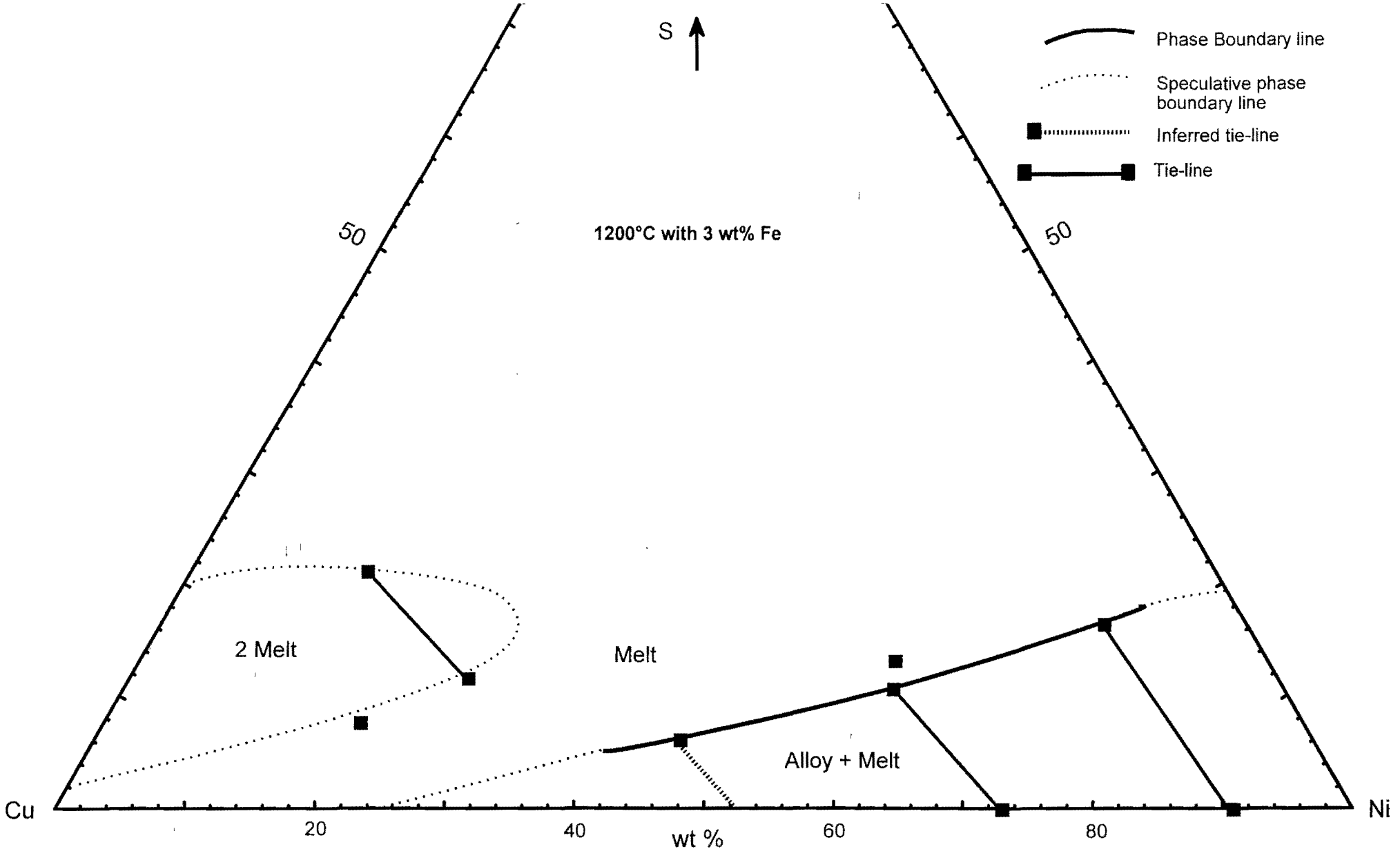

Figure 6.2: Phase relations at 1200°C and 3 wt% Fe in starting compositions.

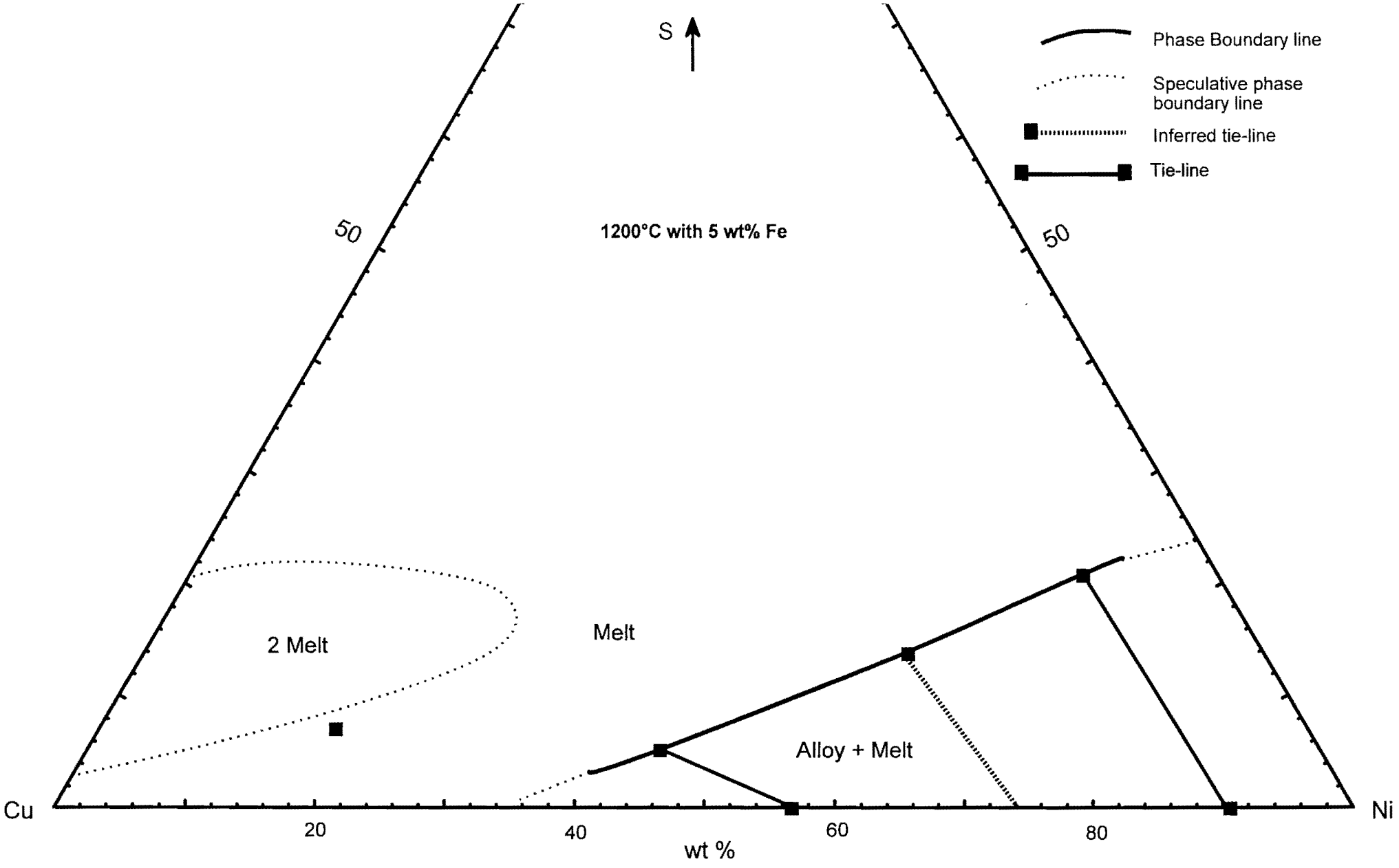

Figure 6.3: Phase relations at 1200°C and 5 wt% Fe in starting compositions.

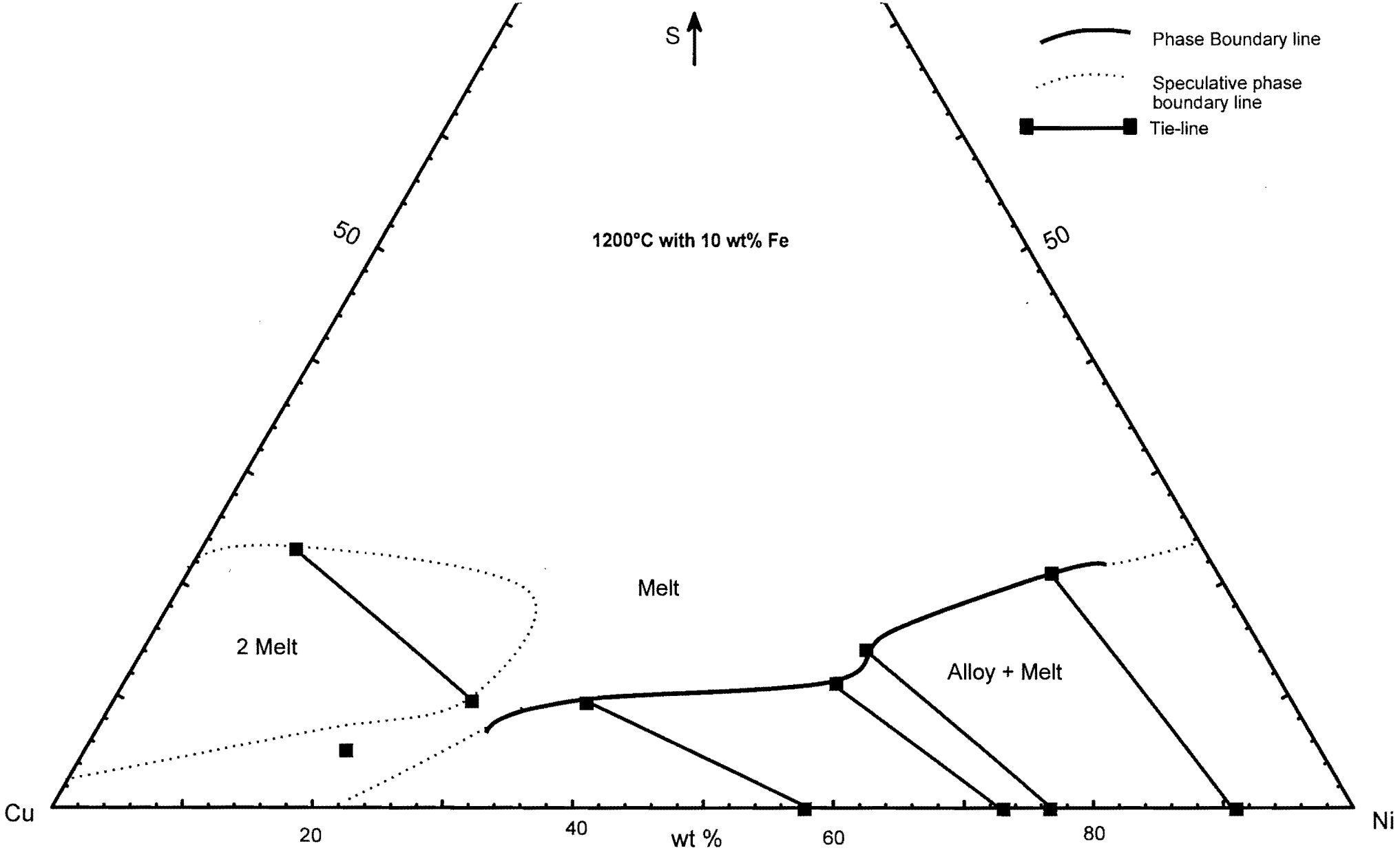

Figure 6.4: Phase relations at 1200°C and 10 wt% Fe in starting compositions.

6.2 The 1100°C isothermal sections

The isothermal sections at 1100°C are presented in Figures 6.5 to 6.8. At 1100°C and compositions containing ≤ 5 wt% Fe, a maximum of two possible phases can exist, a melt and an alloy phase. The melt coexisting with alloy changes composition with a change in the bulk metal content. Alloys with higher Ni-contents coexist with higher sulphur-content melts and higher Fe in the starting composition leads to more sulphur rich compositions of the coexisting melt. Melts with more than ~ 50 wt% Cu and less than ~ 20 wt% sulphur separate into two immiscible melts. Only at less than 10 wt% sulphur in the starting composition would the melt coexist with a Cu-rich alloy.

If the starting composition contains 10 wt% Fe, digenite exists at starting compositions higher than ~ 50 wt% Cu and sulphur contents lower than ~ 20 wt%. Digenite coexists with a Cu-rich alloy at starting compositions containing more than ~ 60 wt% Cu and coexists with a Cu-rich alloy and a melt phase at compositions between ~ 50 and 60 wt% Cu.

When digenite becomes stable it also presents the "problem of apparently crossing tie-lines". In a three-component system, this would indicate that the experiments involved were either in dis-equilibrium or that analyses were unreliable. In this four-component system, however, crossing tie-lines are a result of a three-dimensional projection onto a two-dimensional surface. Digenite from different experiments contains different amounts of Fe that can not be displayed successfully in these diagrams. The effect of projecting data points from a volume representing an imaginable phase field for digenite is shown in Figure 6.9.

6.3 The 1000°C isothermal sections

The isothermal sections at 1000°C are presented in Figures 6.10 to 6.13. Depending on the bulk composition, a Cu-Ni-sulphide assemblage will comprise a maximum of three phases, i.e. alloy, digenite and melt. Ni-rich starting compositions with less than ~ 20 wt% sulphur will result in an alloy coexisting with a melt phase. A bulk composition rich in Cu and between 10 and 20 wt% sulphur will produce digenite coexisting with either alloy, melt, or (alloy+melt). The composition of the melt coexisting with alloy increases in sulphur-content with the increase of Fe in the bulk composition. Similarly, the melt composition coexisting with digenite increases in sulphur-content with the increase in Fe-content.

The change in composition of the melt and alloy coexisting with digenite (referred to as the "cotectic-alloy" and "cotectic-melt") is of interest. Monitoring these two phases with the change in temperature and Fe-content of the bulk gives an indication of the crystallization path of the melt at any given starting composition.

Again, crossing tie-lines are explained by the projection of a three-dimensional phase field onto a two-dimensional diagram.

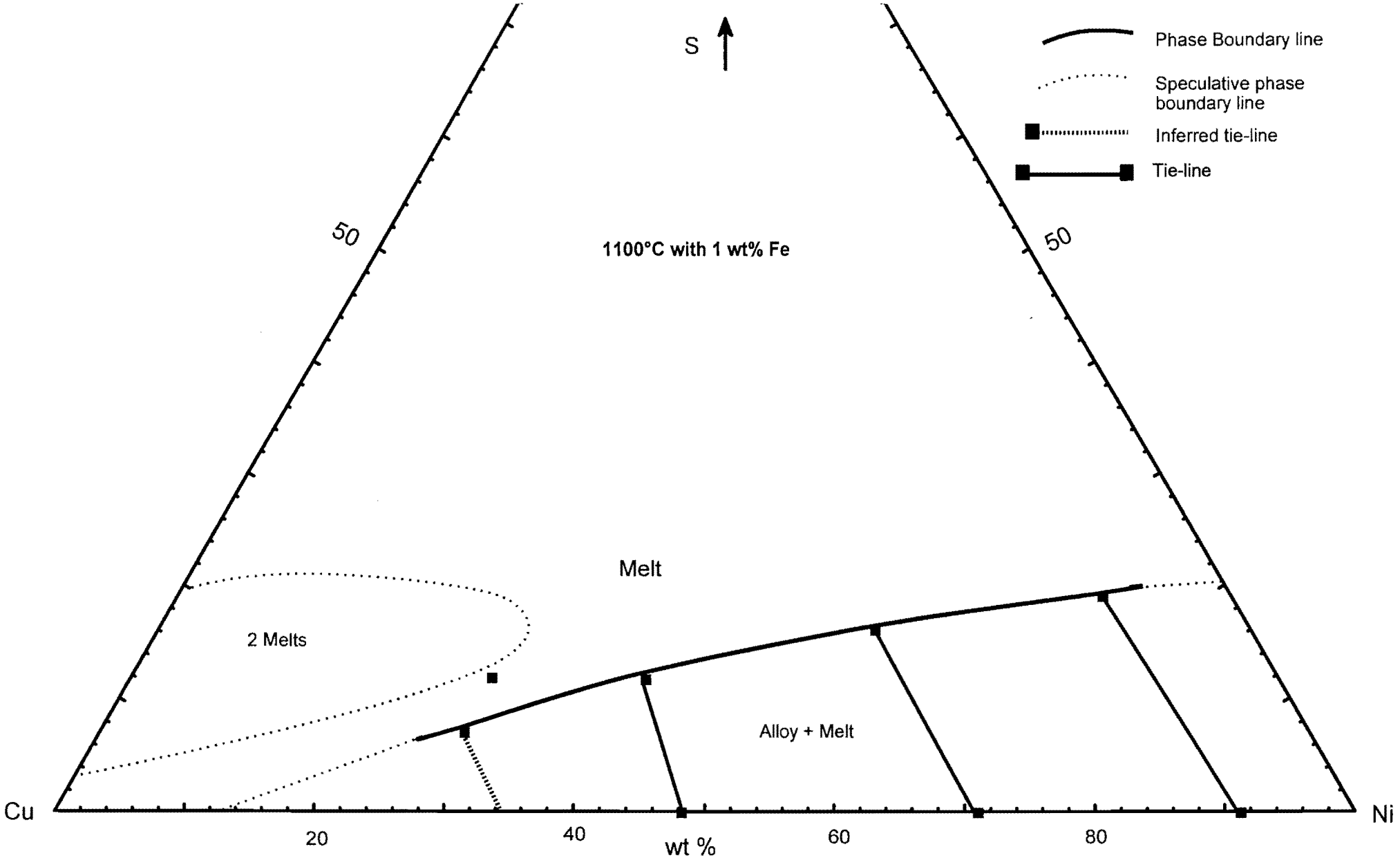

Figure 6.5: Phase relations at 1100°C and 1 wt% Fe in starting compositions.

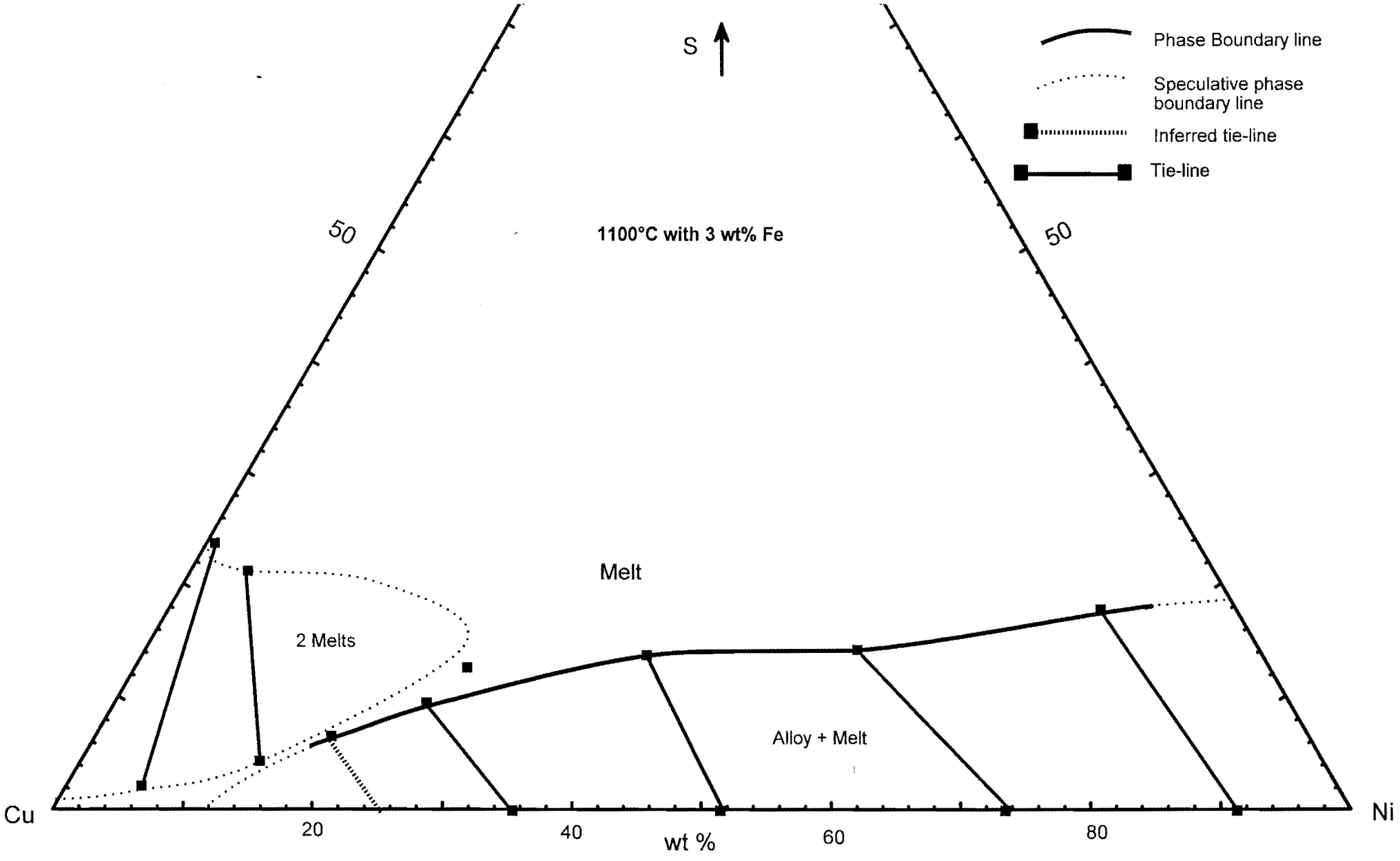

Figure 6.6: Phase relations at 1100°C and 3 wt% Fe in starting compositions.

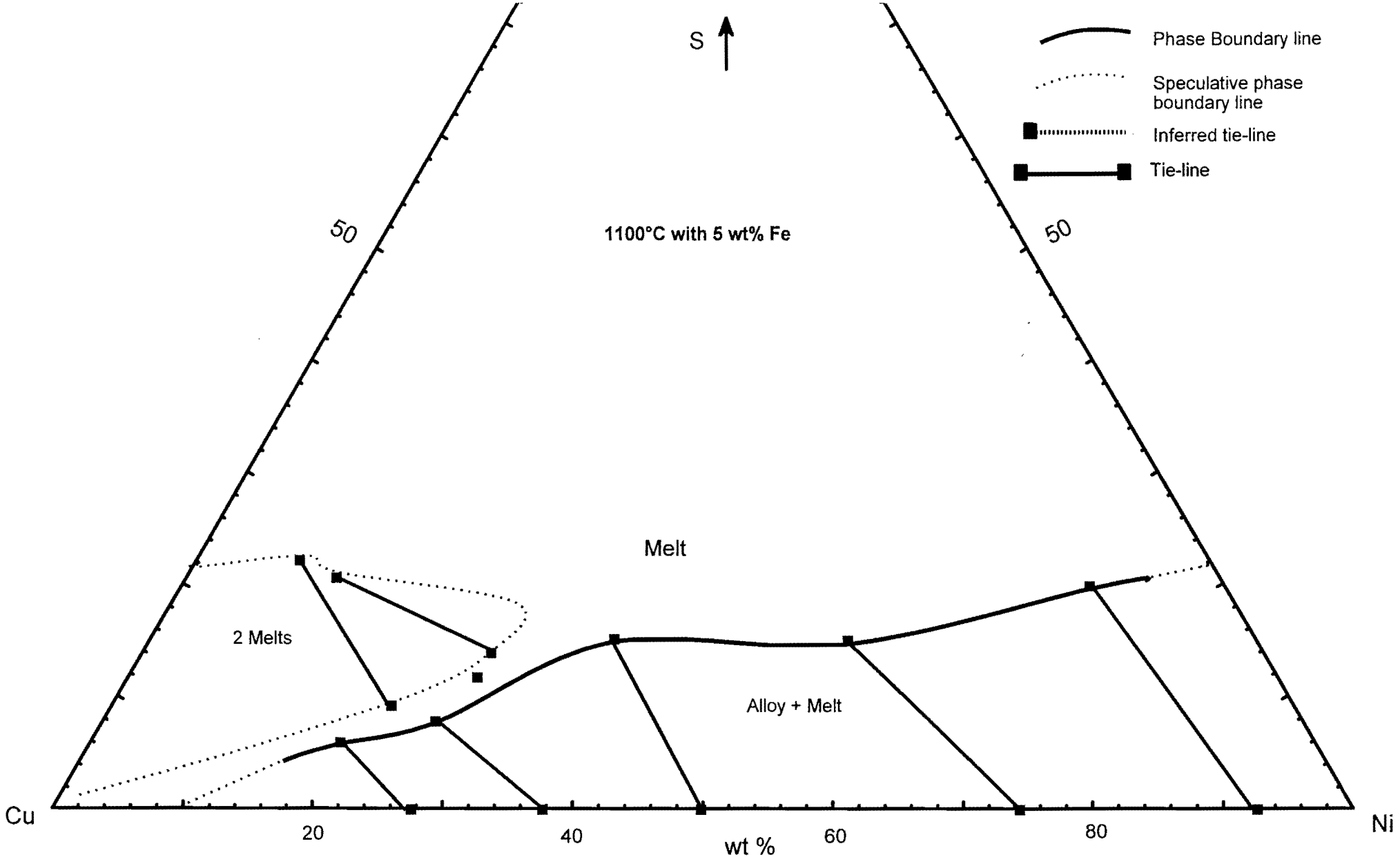

Figure 6.7: Phase relations at 1100°C and 5 wt% Fe in starting compositions.

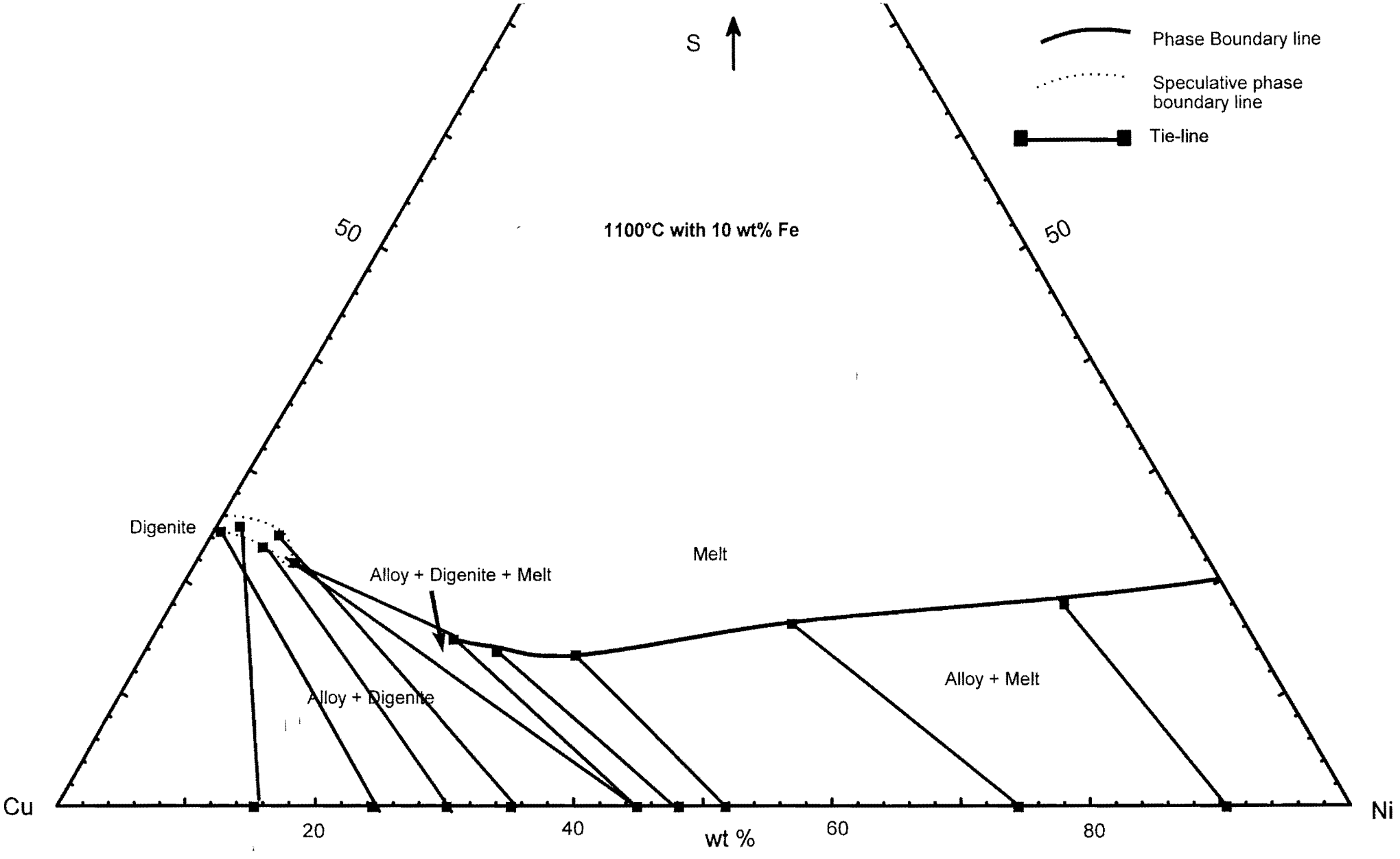

Figure 6.8: Phase relations at 1100°C and 10 wt% Fe in starting compositions.

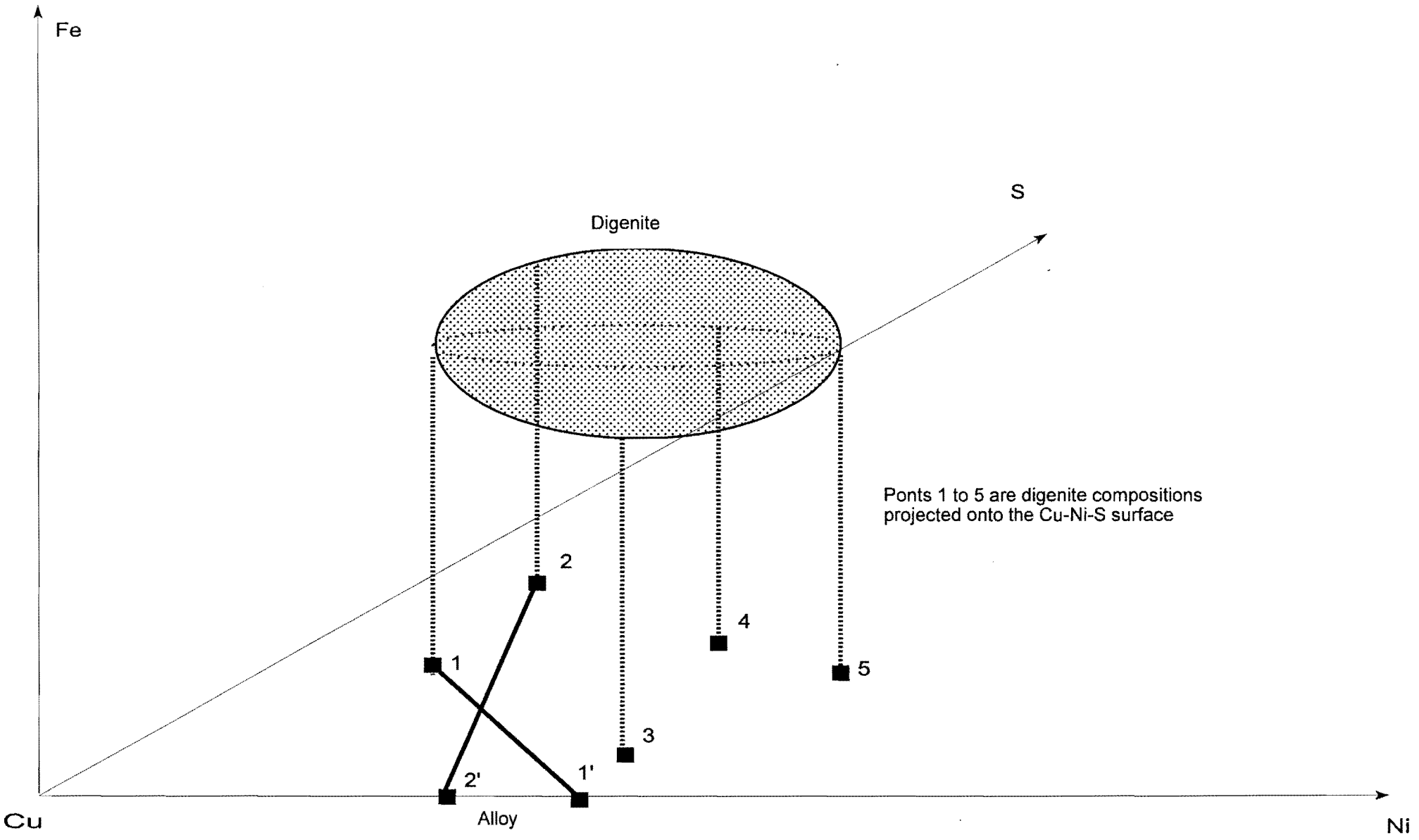

Figure 6.9: Projection of a three-dimensional volume representing an imaginary phase field of digenite, onto a two-dimensional surface. A tie-line from point 2 to 2' (a Cu-rich alloy) would seemingly cross with a tie-line from 1 to 1' (a slightly more Ni-rich alloy). In the third dimension these two tie-lines would not cross.

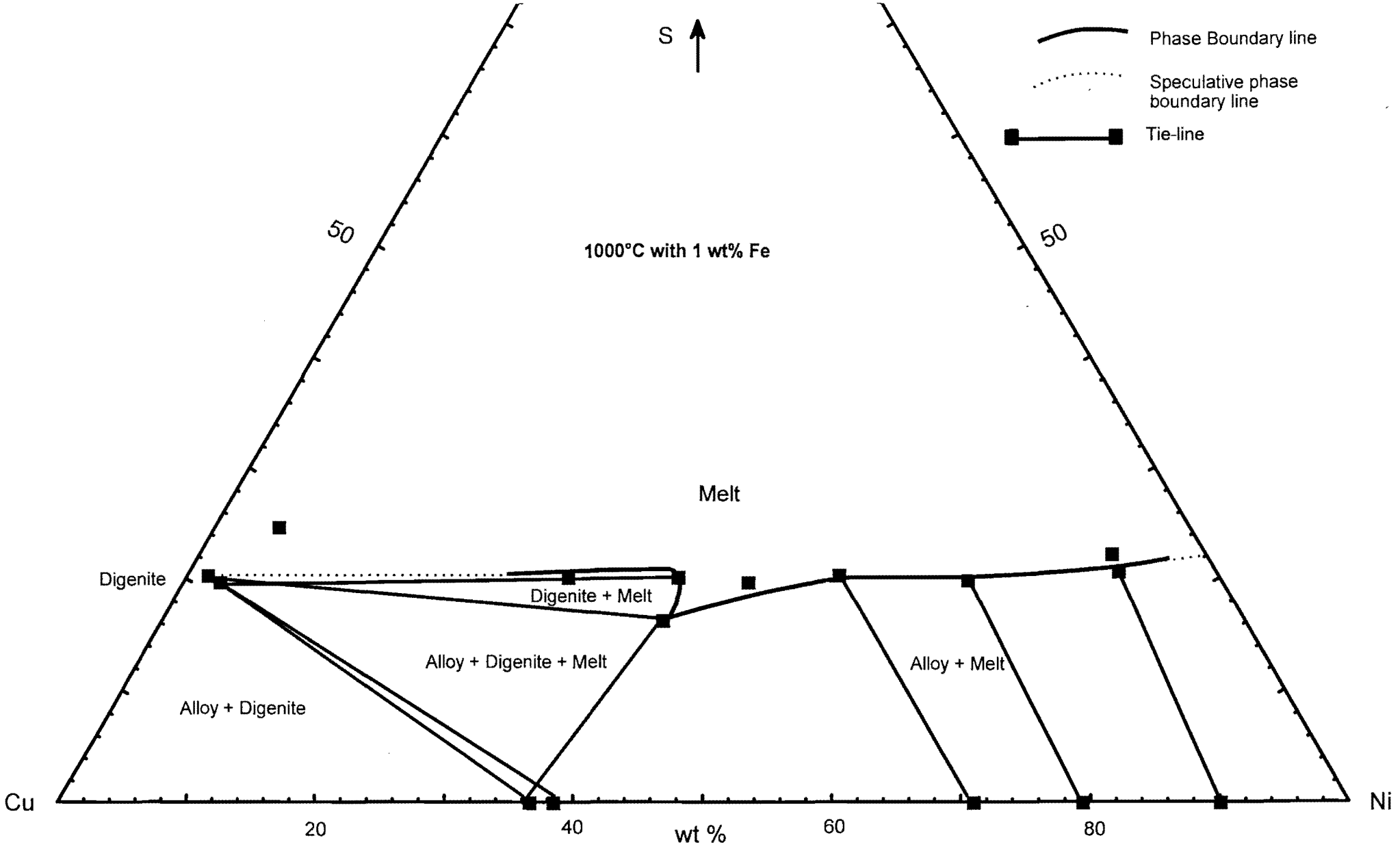

Figure 6.10: Phase relations at 1000°C and 1 wt% Fe in starting compositions.

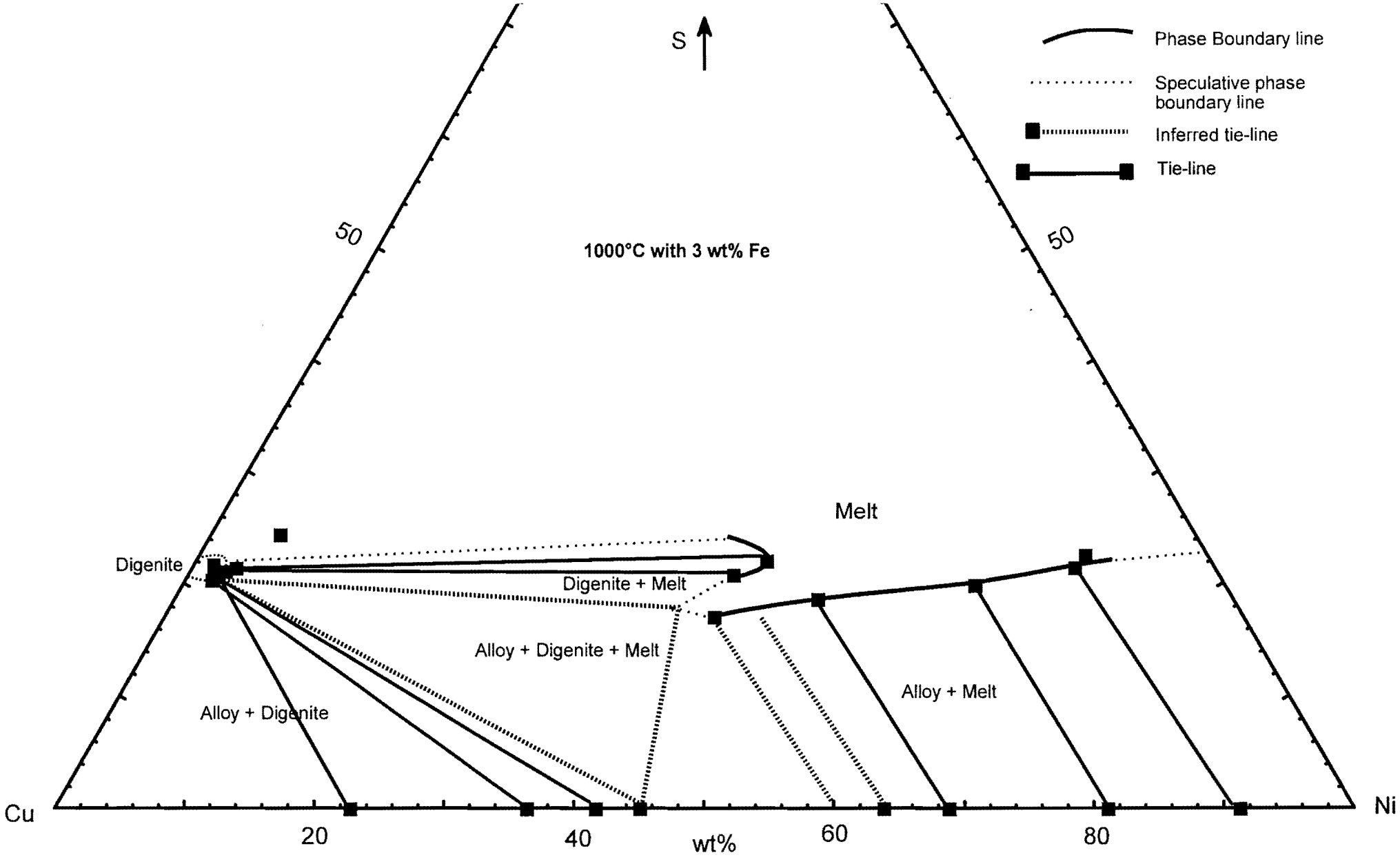

Figure 6.11: Phase relations at 1000°C and 3 wt% Fe in starting compositions.

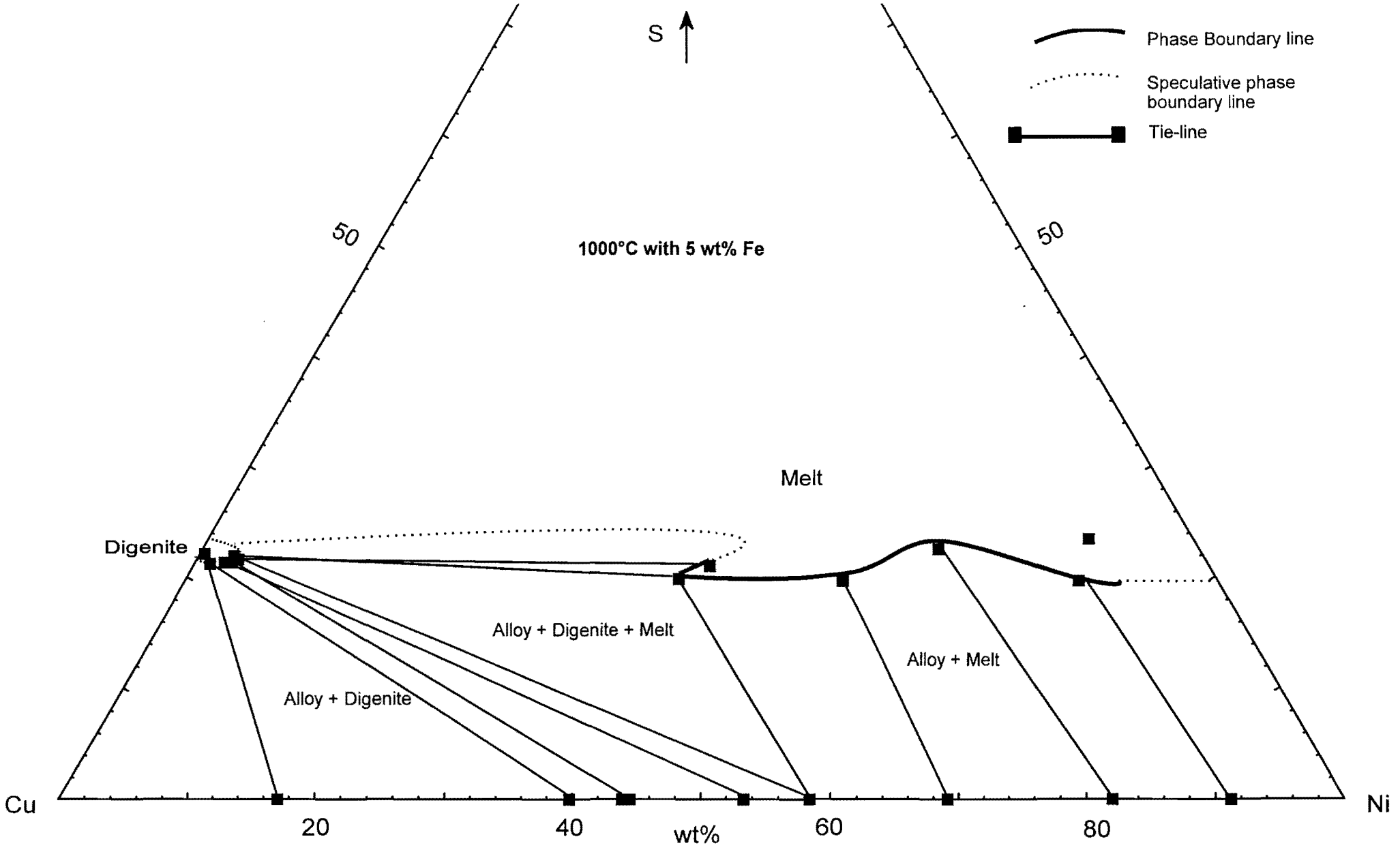

Figure 6.12: Phase relations at 1000°C and 5 wt% Fe in starting compositions.

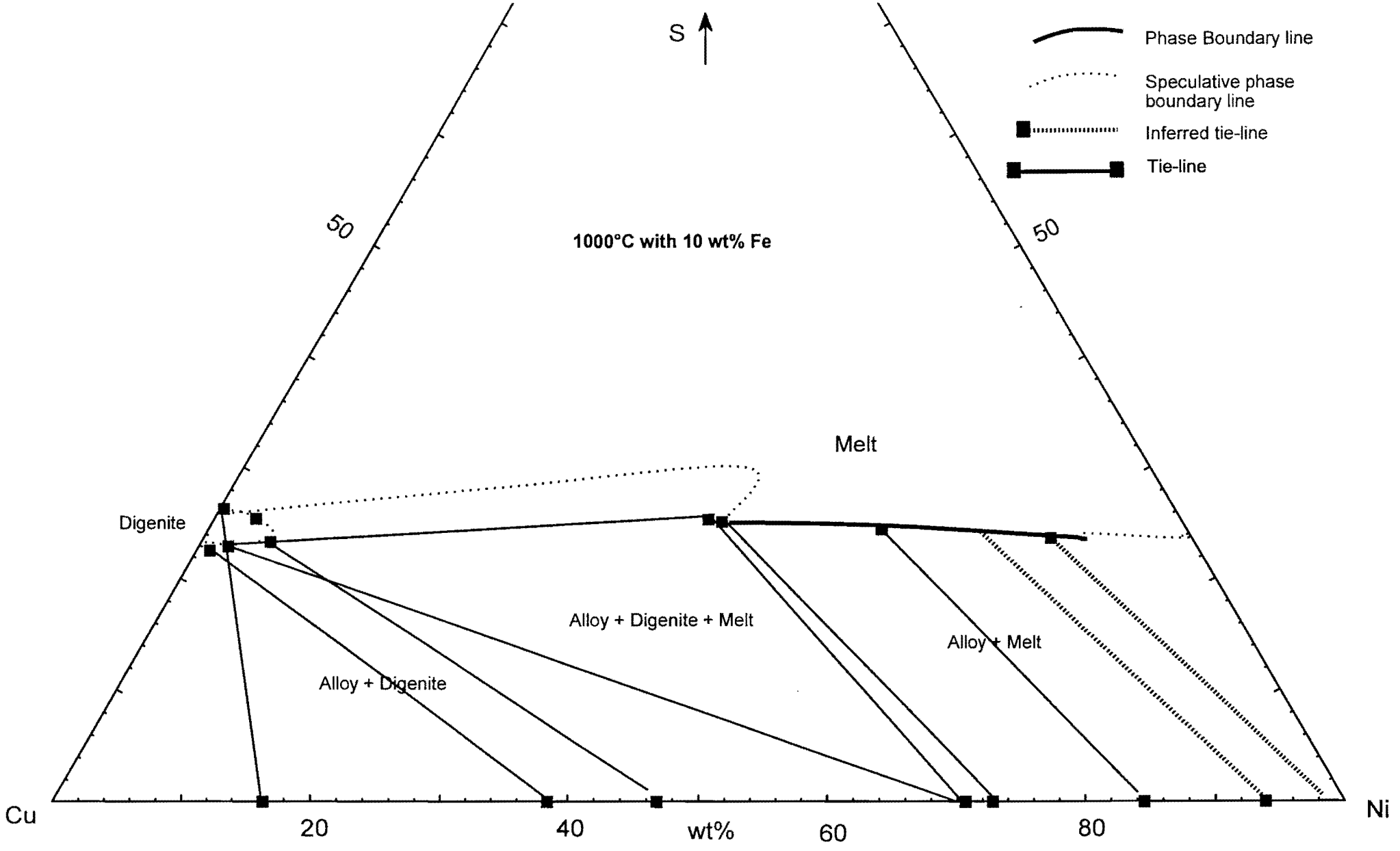

Figure 6.13: Phase relations at 1000°C and 10 wt% Fe in starting compositions.

6.4 The 900°C isothermal sections

The isothermal sections at 900°C are presented in Figures 6.14 to 6.17. An enlargement of the area around digenite appears in the insert. At 900°C, a Cu-Ni-sulphide assemblage will produce four possible phases at low sulphur (< ~ 25 wt%) and three possible phases at high sulphur-contents (> ~ 30 wt%) and low Cu-contents (< ~20 wt%).

At low concentrations of sulphur in the bulk, an alloy phase will coexist with digenite, melt, or (digenite+melt). The composition of the average cotectic alloy and cotectic melt increases in Ni-content with the increase in the concentration of Fe in the starting composition. At sulphur-contents of approximately 25 wt%, and Cu-contents more than ~ 50 wt%, two phases will coexist: a Cu-sulphide and melt. The Cu-sulphide is either digenite or a phase with higher sulphur and Ni-contents defined earlier as "β-phase". Digenite and β-phase were never observed in the same experiment. However, this may just be a result of starting compositions that did not favor these two phases to coexist. Starting compositions that could reflect such an assemblage are very limited and not encountered in this study.

At higher sulphur-contents and low Cu concentrations, crystallization from a Cu-Ni-sulphide melt will result in a three phase assemblage depending on the starting composition; (millerite+vaesite+melt), (millerite+melt) or (millerite+vaesite). With an increase in the Fe-content of the bulk, the melt coexisting with millerite and vaesite becomes enriched in Cu.

6.5 The 800°C isothermal sections

The isothermal sections at 800°C are presented in Figures 6.18 to 6.21. At low sulphur-contents, the phase assemblages at 800°C are very similar with respect to those at 900°C. An alloy phase will coexist with either digenite, (digenite+melt), or only melt, depending on the starting composition. The composition of the cotectic melt does not change much with the addition of Fe to the bulk composition, but the cotectic alloy increases in Ni content with the increase of Fe. The composition of the melt coexisting with an alloy phase does not show a significant increase in sulphur content with an increase in the Fe concentration of the bulk.

In the Fe-free system (Bruwer, 1996), a Cu-rich melt field forms at sulphur contents of ~ 30 wt%. A similar melt exists at low (1 wt%) Fe concentrations but was not encountered in the higher Fe content assemblages. Three possibilities arise: firstly the composition of this melt could change at higher Fe concentrations of the bulk, secondly this melt could disappear completely on addition of Fe to the bulk, or thirdly, the proportion of melt to solids is so small that the likelihood of intersecting this phase in a polished section is very small.

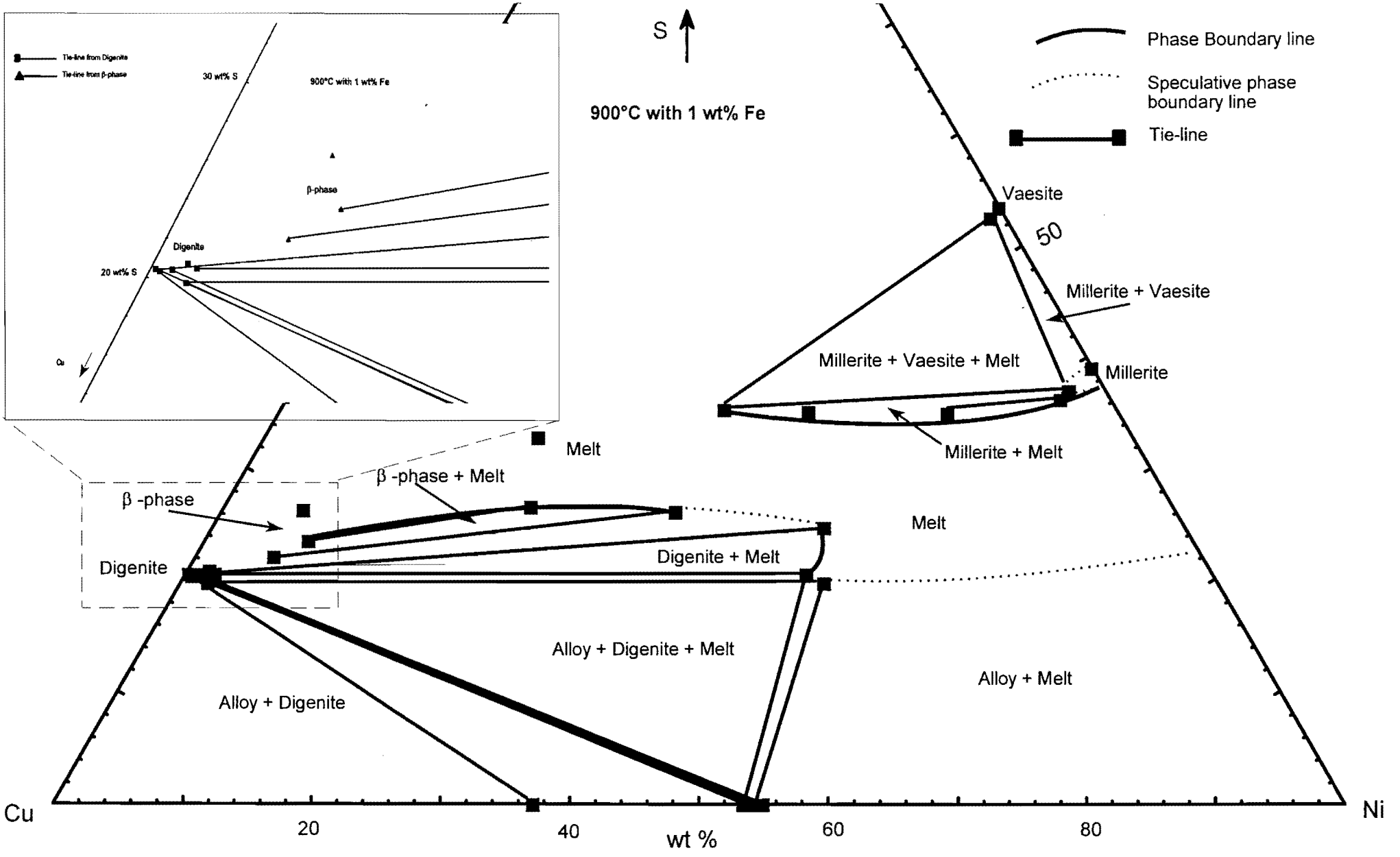

Figure 6.14: Phase relations at 900°C and 1 wt% Fe in starting compositions. The insert shows the area where digenite and the β -phase plot.

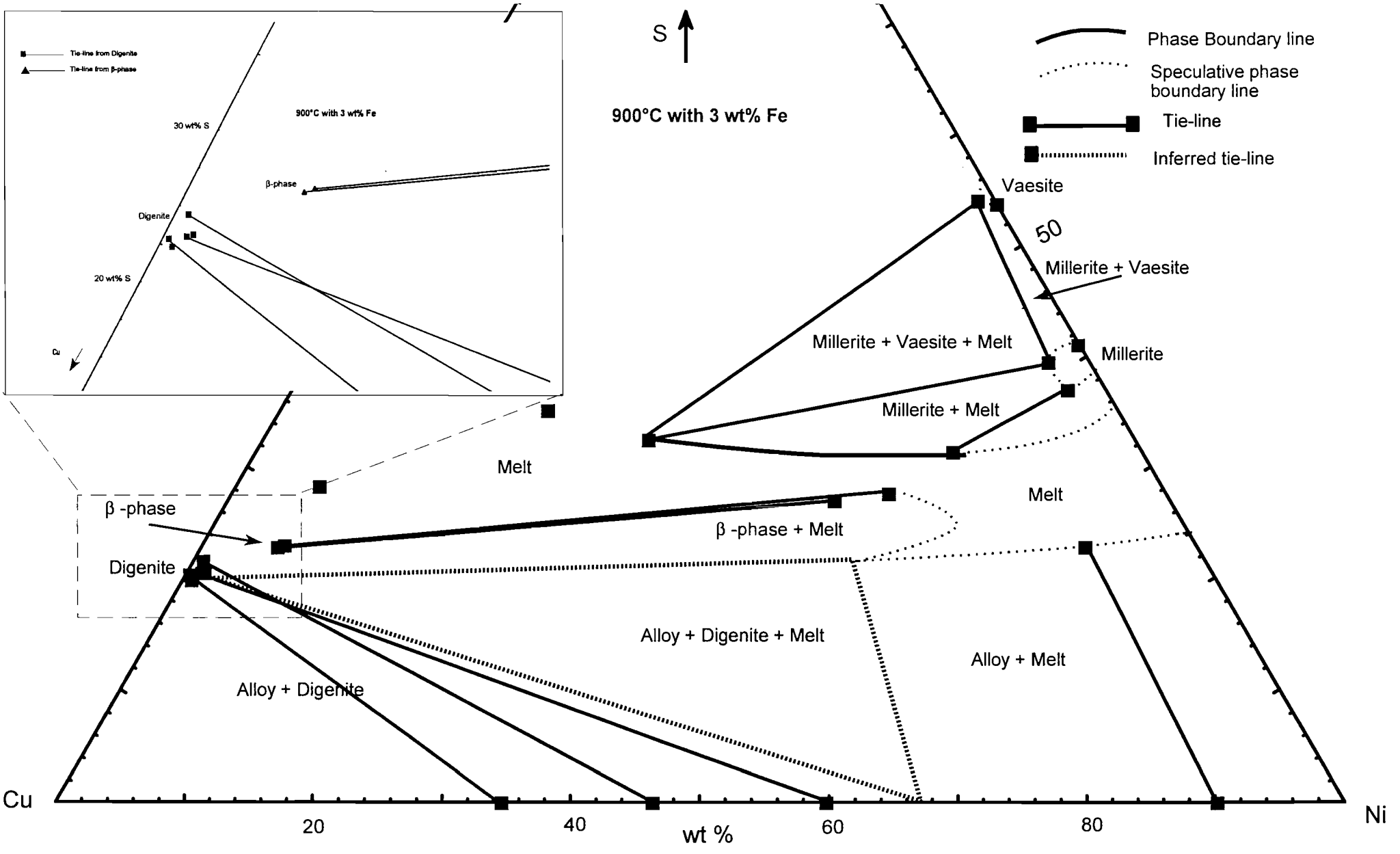

Figure 6.15: Phase relations at 900°C and 3 wt% Fe in starting compositions. The insert shows the area where digenite and the β -phase plot.

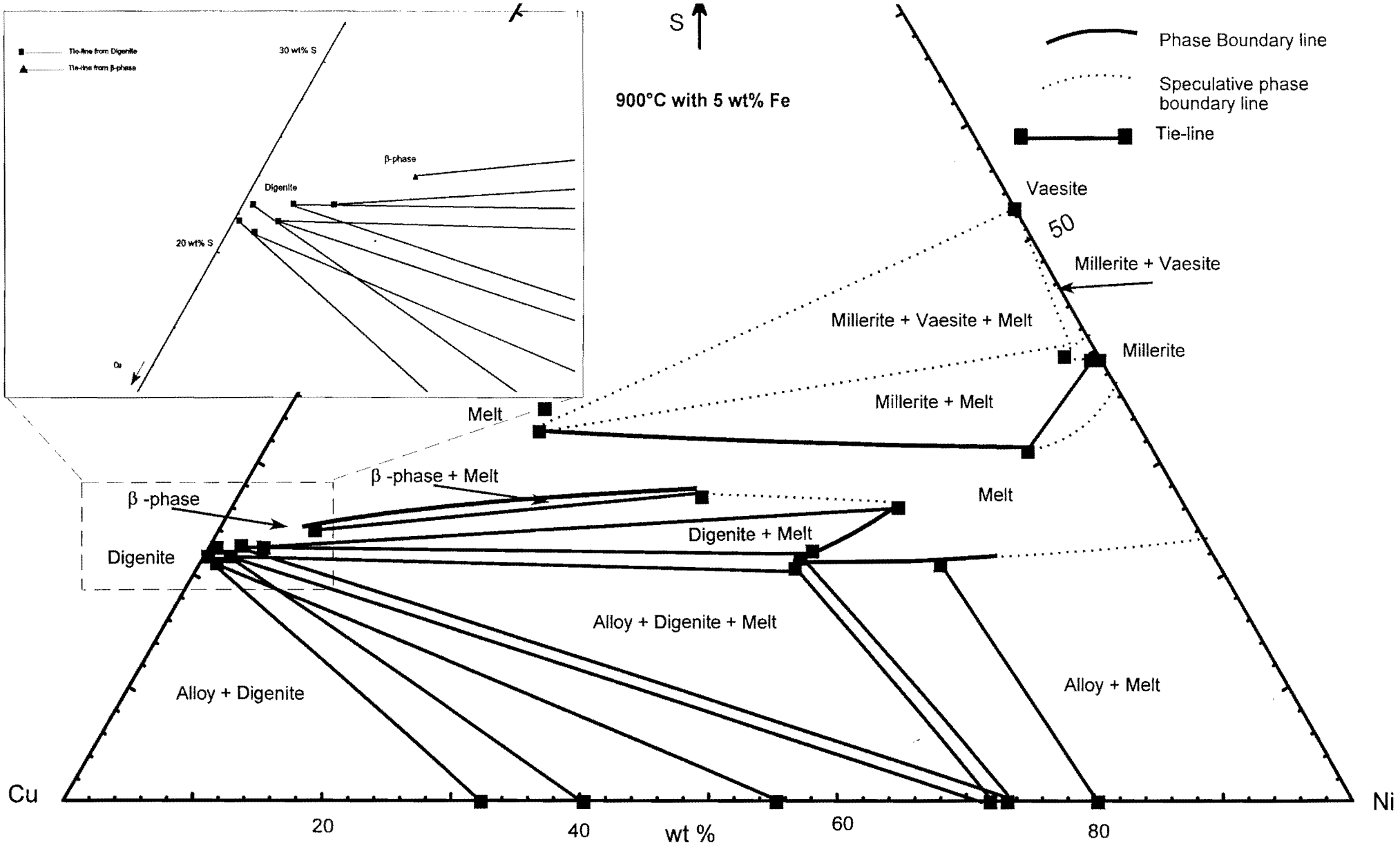

Figure 6.16: Phase relations at 900°C and 5 wt% Fe in starting compositions. The insert shows the area where digenite and the β -phase plot.

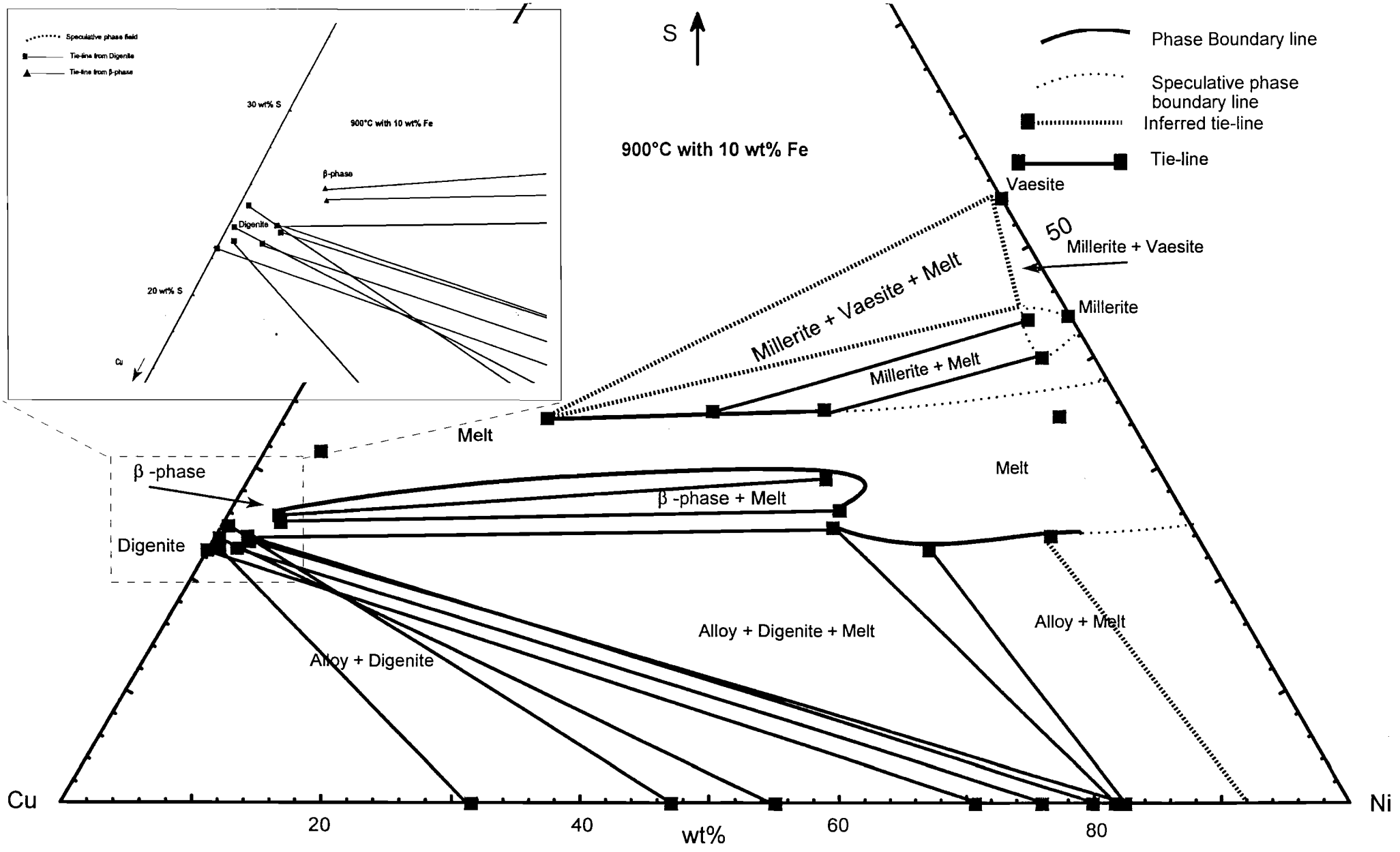

Figure 6.17: Phase relations at 900°C and 10 wt% Fe in starting compositions. The insert shows the area where digenite and the β -phase plot.

If such a Cu-rich melt exists, the assemblages of phases coexisting with the sulphide-melt at sulphur concentrations 30 – 50 wt% become very complex. The aim of this project is not to investigate this part of the system systematically. Therefore, the phase relations are indicated with stippled lines due to a lack of sufficient data. An interesting aspect is the coexistence of millerite, vaesite and a Ni-rich melt with the β-phase, but not with digenite. With an increase in the bulk Fe concentration, the sulphur content of the β-phase and millerite also increases.

Heazlewoodite was described by Bruwer (1996) at temperatures 800°C and lower. This Ni-sulphide was, however, never observed in this study. It is possible that starting compositions were never favourable to encounter heazlewoodite, or, when it did crystallize, that the polished sections did not include it. It is assumed (based on previous studies, section 2.1.1) that this phase would indeed crystallize from 800°C downwards, although the exact composition in the Cu-Ni-Fe-S system is undetermined.

6.6 The 700°C isothermal sections

The isothermal sections at 700°C are presented in Figures 6.22 to 6.25. At low sulphur contents, the phase assemblages remain the same as in the higher temperature isotherms. At high (~ 30 – ~ 50 wt%) sulphur contents three phases are stable: β-phase, millerite and vaesite. The phase relations at ~ 20 to ~ 40 wt% sulphur are superimposed from the high temperature isotherms, and indicated by stippled lines. Again the presence of heazlewoodite is unconfirmed by this investigation.

In all of the experiments, a distinct compositional difference between digenite and β-phase was observed, but the phase relation between these two Cu-sulphides could not be determined. Digenite appears to have a smaller compositional variation than the β-phase (see chapter 7).

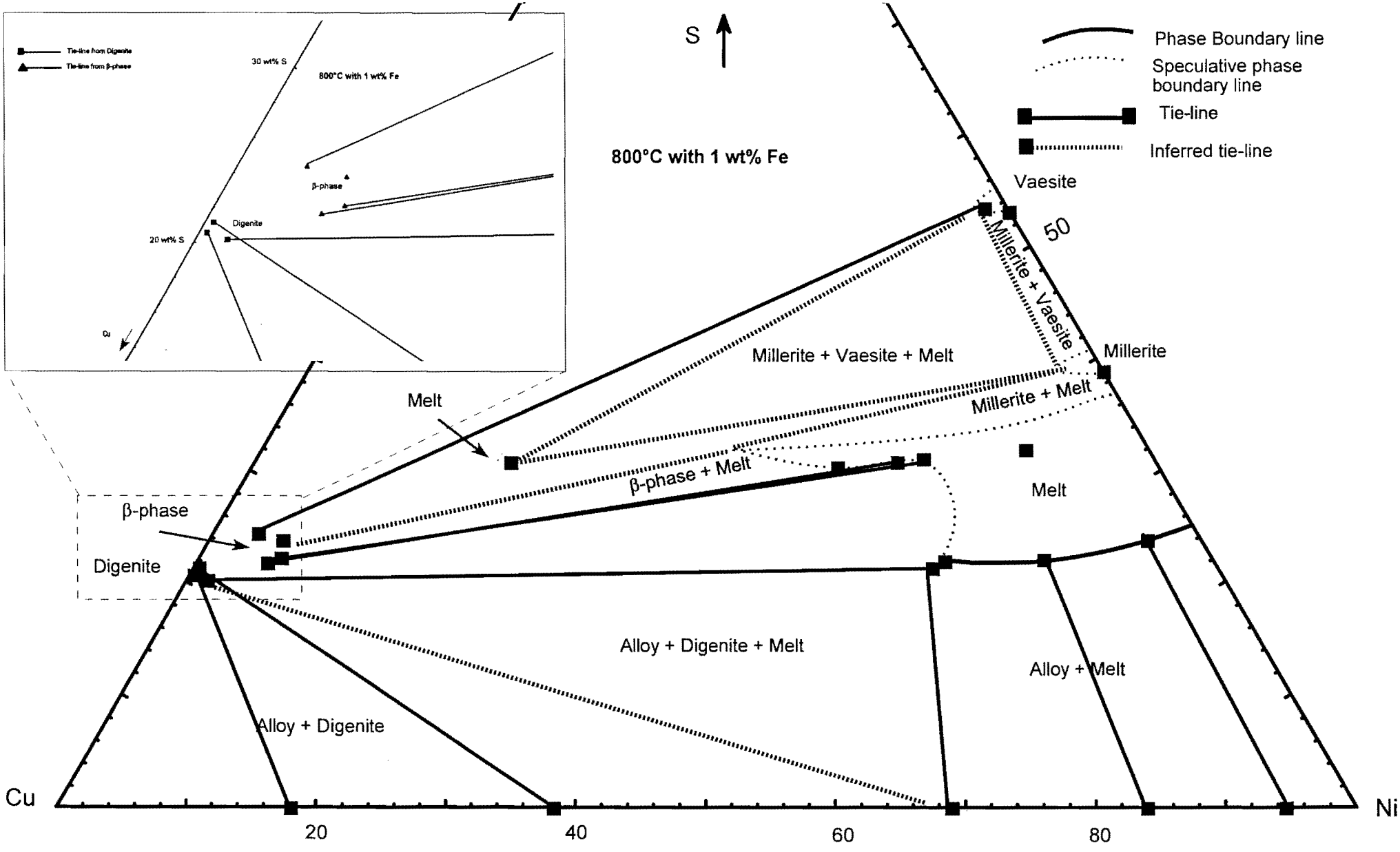

Figure 6.18: Phase relations at 800°C and 1 wt% Fe in starting compositions. The insert shows the area where digenite and β-phase plots.

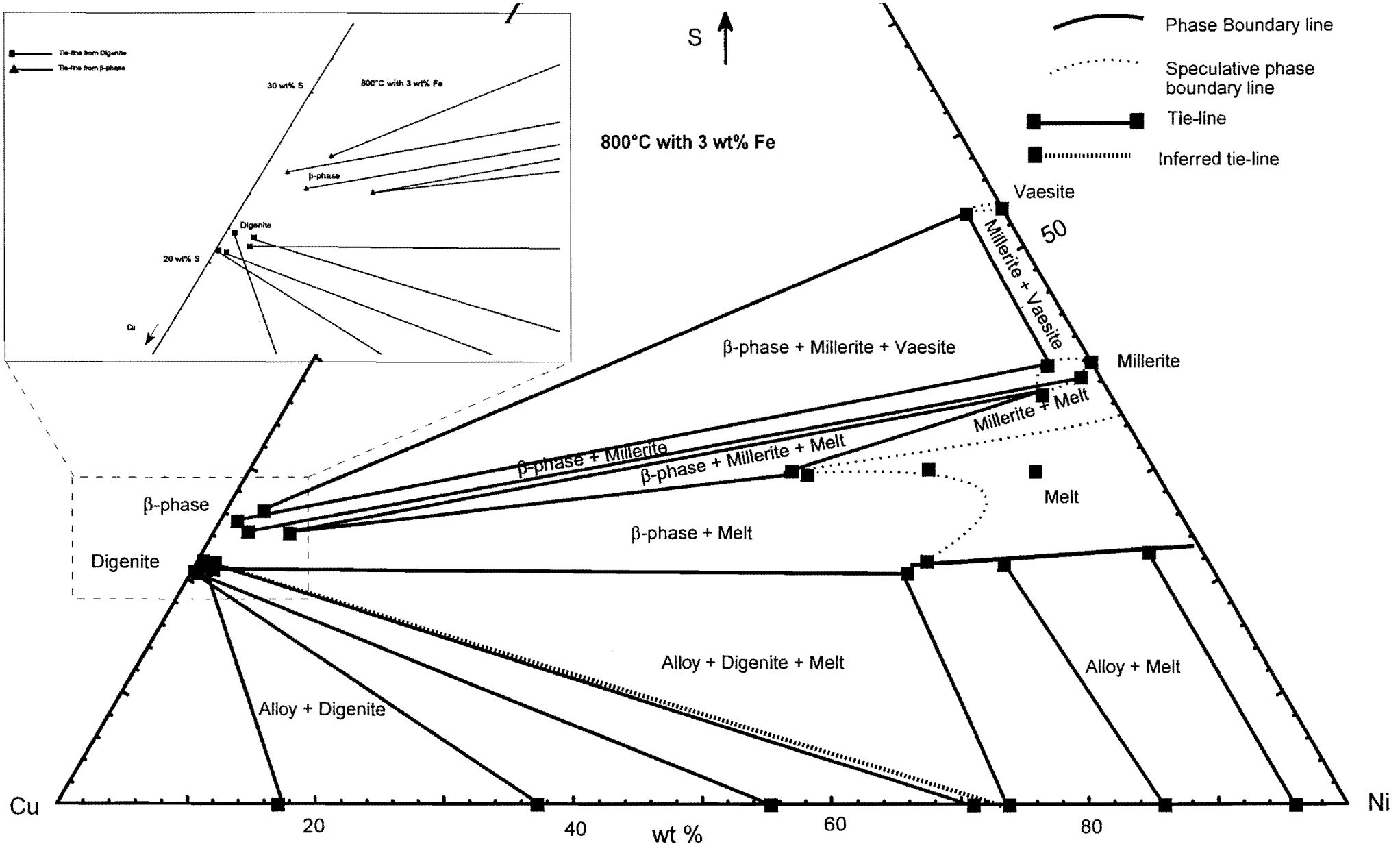

Figure 6.19: Phase relations at 800°C and 3 wt% Fe in starting compositions. The insert shows the area where digenite and β-phase plots.

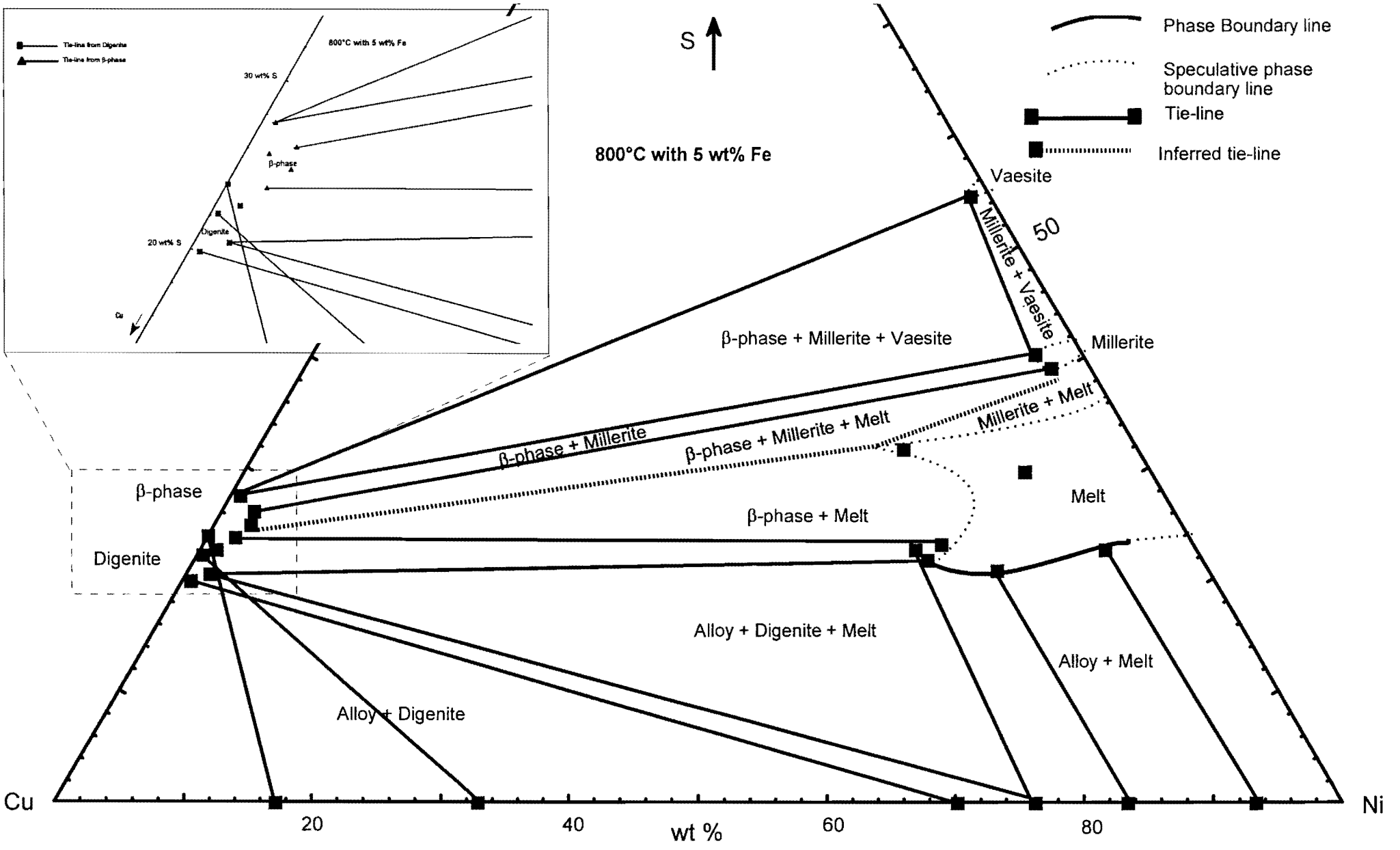

Figure 6.20: Phase relations at 800°C and 5 wt% Fe in starting compositions. The insert shows the area where digenite and β-phase plots.

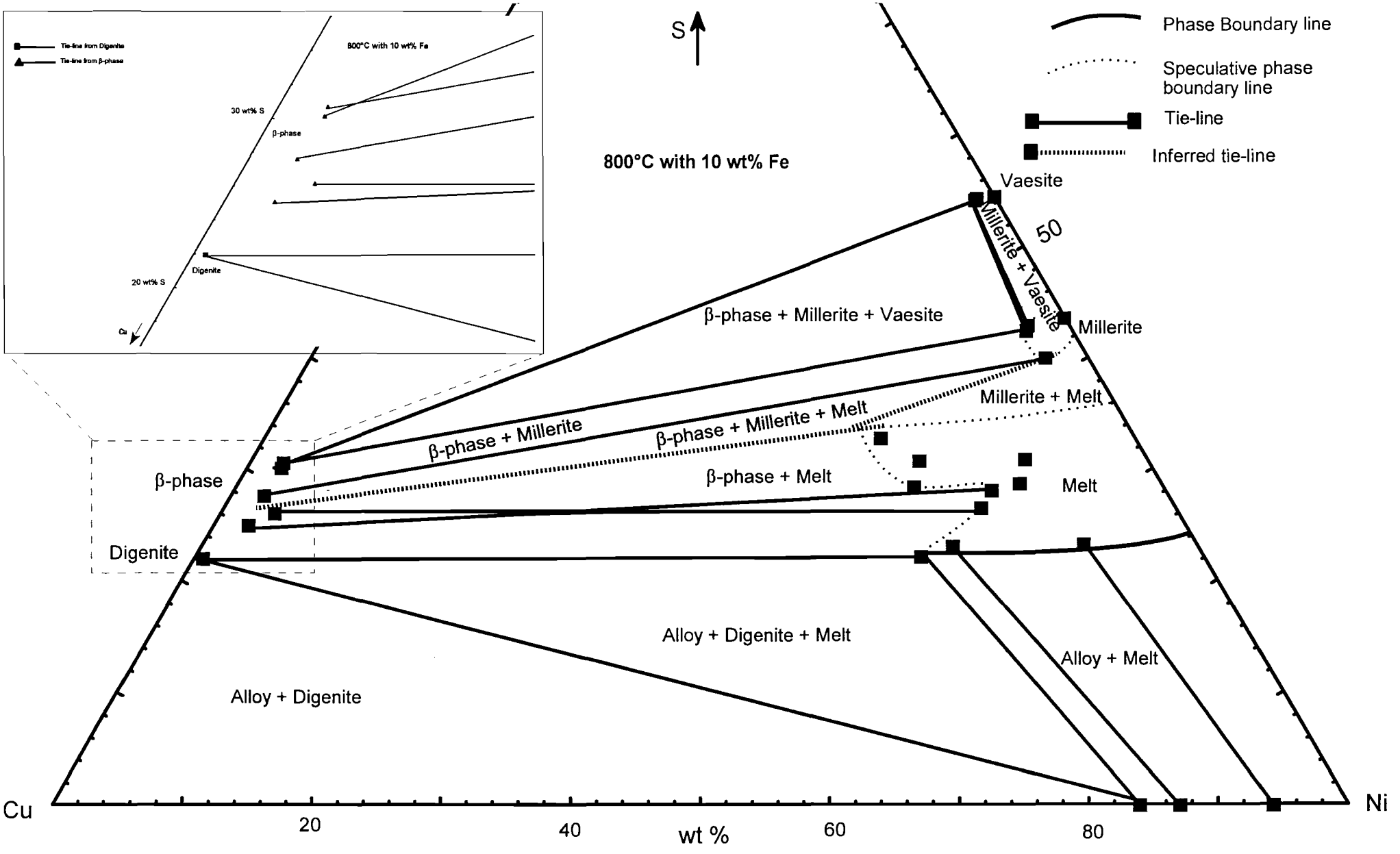

Figure 6.21: Phase relations at 800°C and 10 wt% Fe in starting compositions. The insert shows the area where digenite and -β-phase plots.

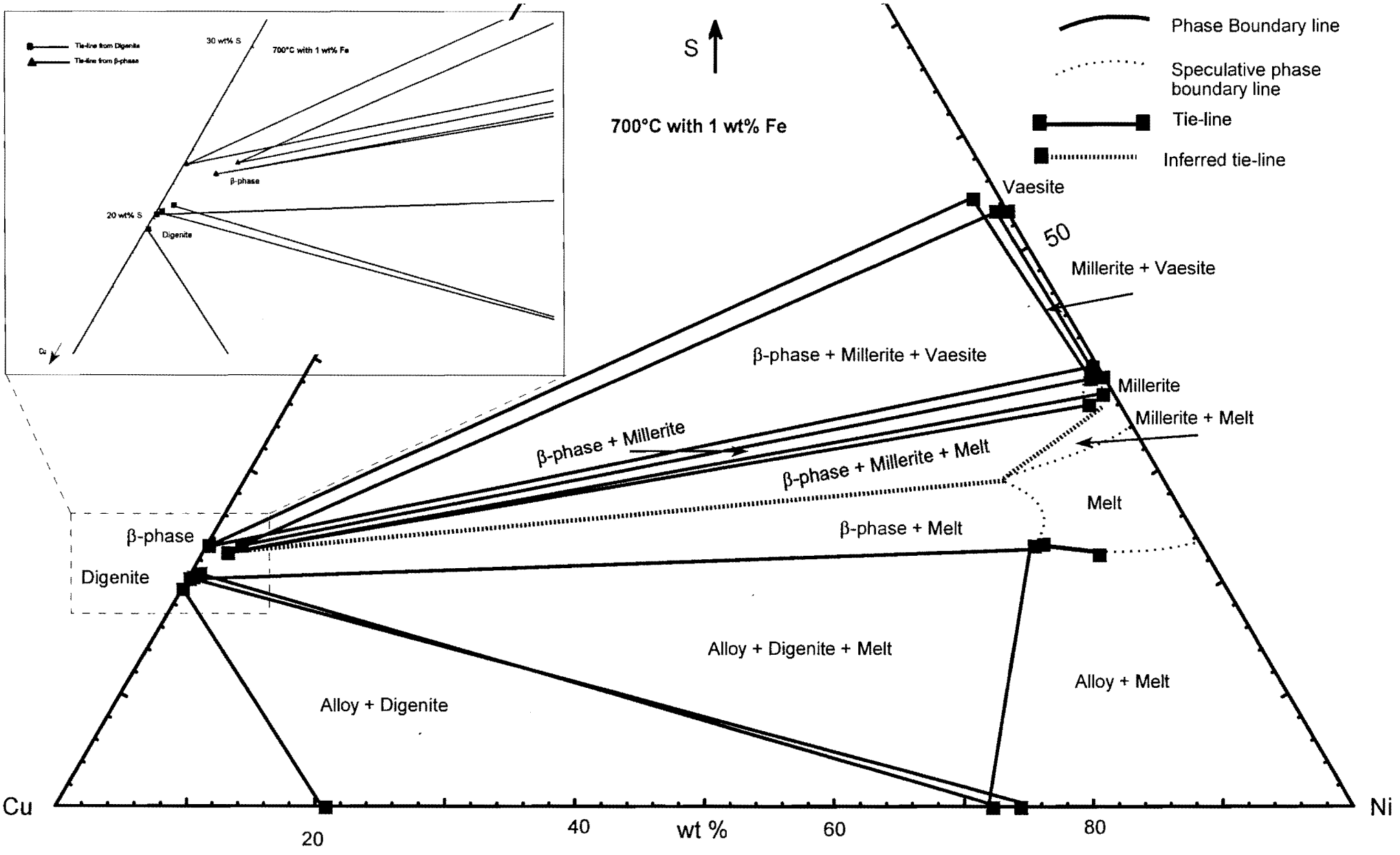

Figure 6.22: Phase relations at 700°C and 1 wt% Fe in starting compositions. The insert shows the area where digenite and β-phase plots.

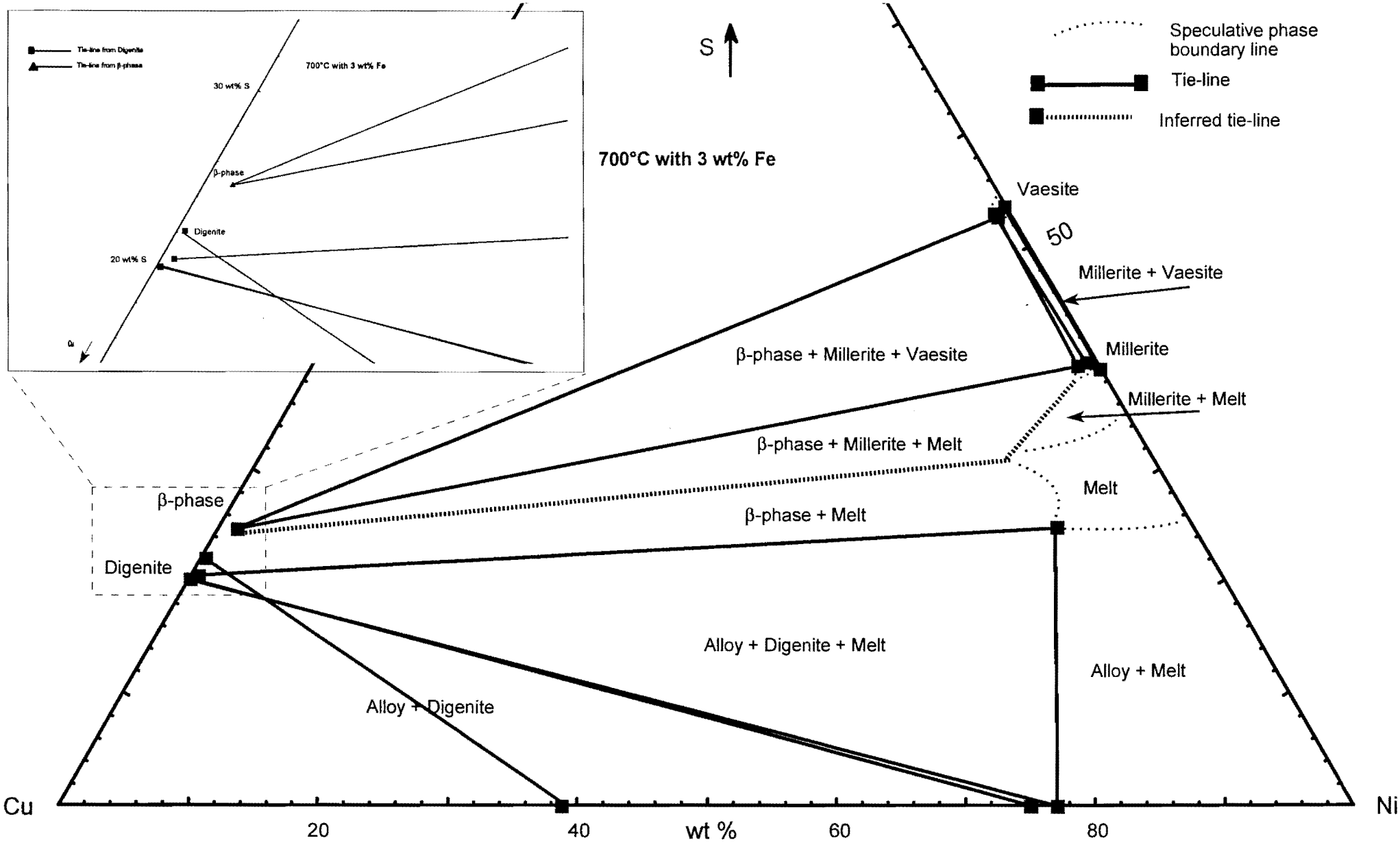

Figure 6.23: Phase relations at 700°C and 3 wt% Fe in starting compositions. The insert shows the area where digenite and β-phase plots.

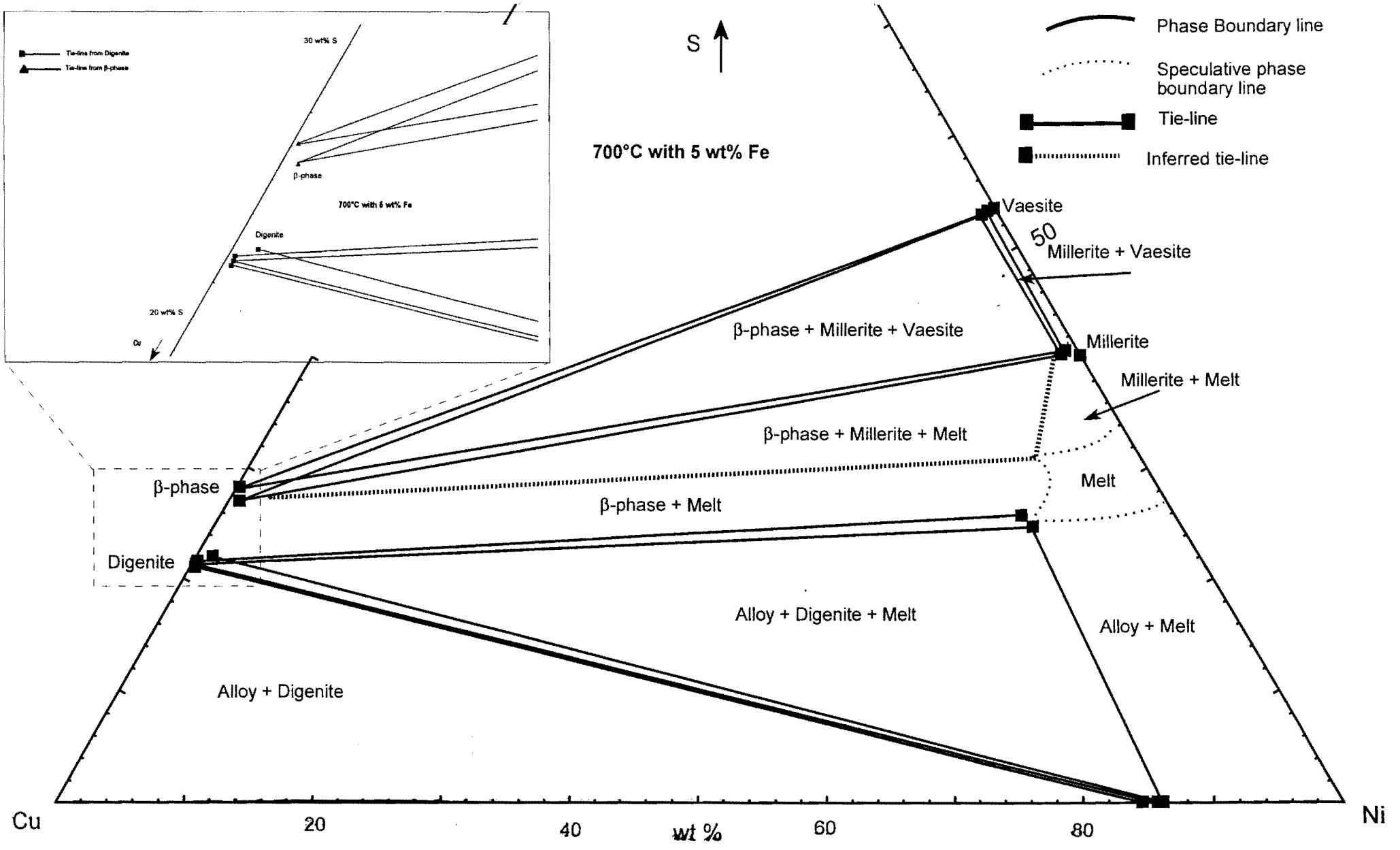

Figure 6.24: Phase relations at 700°C and 5 wt% Fe in starting compositions. The insert shows the area where digenite and β-phase plots.

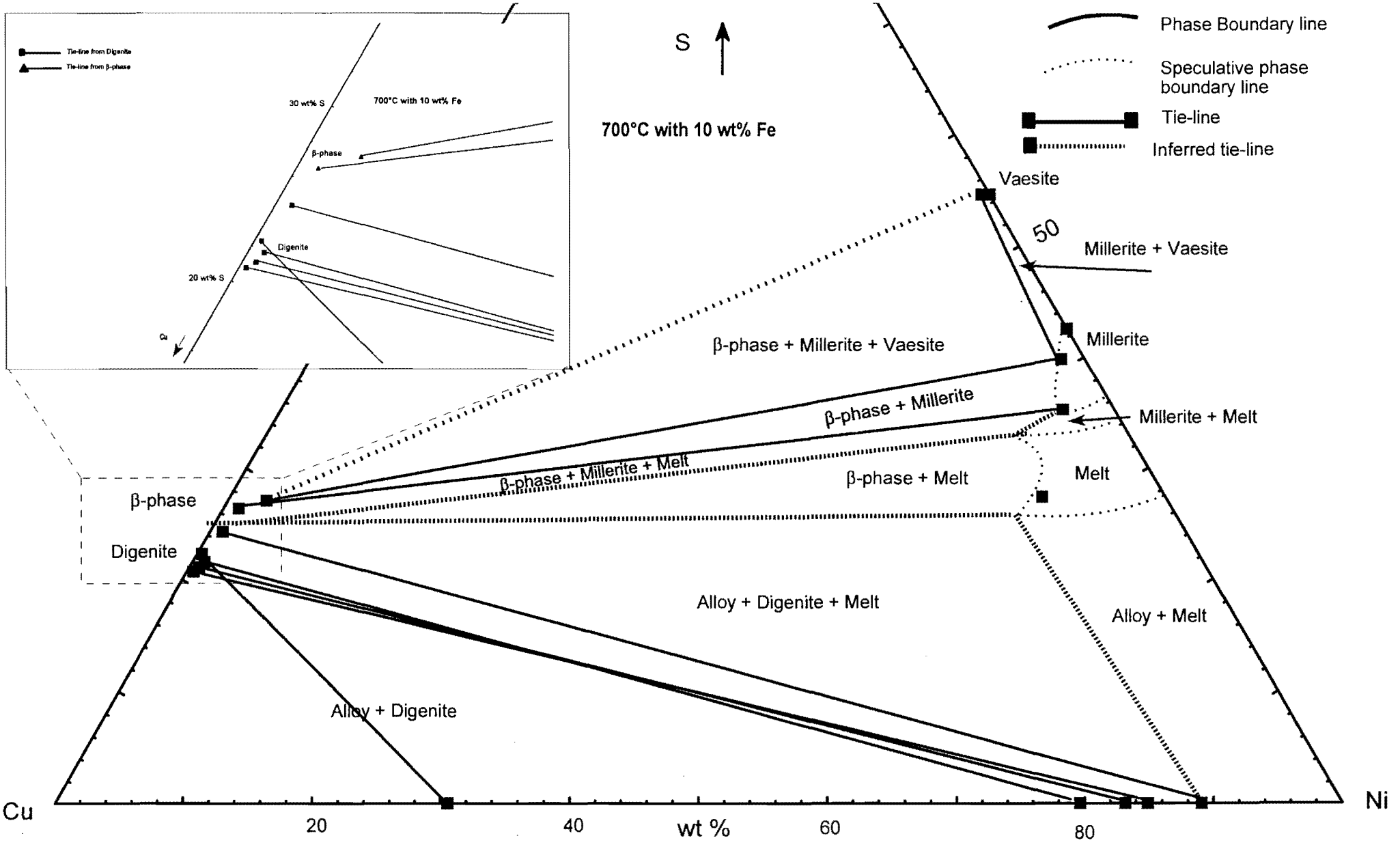

Figure 6.25: Phase relations at 700°C and 10 wt% Fe in starting compositions. The insert shows the area where digenite and β-phase plots.

7. DISCUSSION

The focus of this investigation revolves around the evolution of the projected phase diagrams with increasing Fe content and decreasing temperature, which is in the compositional framework important for slow cooling. The discussion includes the variations caused by different Fe-contents at the same equilibrium temperature, the variations at constant Fe content as a function of temperature, and the influence of the starting composition on the phase relations. The compositional changes of the cotectic alloy and cotectic melt are of special interest since these describe the evolution of the system.

Compositional changes of the various synthetic phases (alloy, digenite, β-phase, millerite and vaesite) were evaluated in relation to changes in the equilibrium temperature, the bulk composition and the mineral assemblage. Significant correlations between these variables are reported.

7.1 The Alloys

Figure 7.1 shows the Cu/Ni ratio against the Fe content of the alloys at different temperatures. No clear relationship is obvious between the Fe content, the Cu/Ni ratio, and the temperature of equilibration.

A plot of the Fe content in the starting composition against the Fe content of the alloys is seen in Figure 7.2. The higher the Fe content in the starting composition, the more Fe is present in the alloy. This is however, not a perfect linear correlation, and the higher Fe available in the bulk, the wider the range of Fe contents in the alloys. There is no correlation between the Cu/Ni ratio and the Fe content of the alloy, neither does the temperature play a role in the amount of Fe included in the alloy (Figure 7.3).

The Cu/Ni ratio against the Fe content of the cotectic alloys (Table 7.1) at the different equilibrium temperatures is presented in Figure 7.4. The Cu/Ni ratio of the cotectic alloys decrease with decreasing temperature at any given Fe content. The Fe content decreases exponentially with increasing Cu/Ni at any temperature.

7.2 The Cotectic melts

Figure 7.5 shows the Cu/Ni ratio against the Fe content of the cotectic melts at the different temperatures (Table 7.2). Three observations can be made: (1) the amount of Fe in the melt increases with the amount of Fe available in the bulk; (2) at a fixed temperature, the Fe content decreases with an increase in the Cu/Ni-ratio of the melt; and (3) similar to the cotectic alloys, the Cu/Ni ratio of the cotectic melts increases with increasing temperature. A plot of the Cu/Ni ratio against the sulphur content in the cotectic melts (Figure 7.6) indicates a slightly higher average sulphur content at lower temperatures (ranging from an average sulphur content of ~19.5 wt% at 1000°C, ~21 wt% at 900°C, ~21 wt% at 800°C and ~24 wt% at 700°C). The Cu/Ni ratios and sulphur

contents for cotectic melts at 800° and 700°C do not vary much from each other and the major compositional difference lies in the Fe content (see Figure 7.6).

Table 7.1: Average EMP data for the cotectic alloys at different temperatures and starting Fe contents.

Fe content category	Temperature (°C)	Cu wt%	Ni wt%	Fe wt%	Cu/Ni
1	1000	61.66	37.03	1.31	1.67
3	1000	52.71	43.04	4.25	1.22
5	1000	38.55	54.24	7.22	0.71
10	1000	24.04	60.83	15.13	0.40
1	900	44.48	53.52	2.00	0.83
3	900	34.26	59.51	6.23	0.58
5	900	24.56	64.91	10.53	0.38
10	900	16.12	67.47	16.41	0.24
1	800	30.39	67.64	1.97	0.45
3	800	25.06	70.28	4.65	0.36
5	800	21.90	70.28	7.82	0.31
10	800	13.85	72.58	13.57	0.19
1	700	28.07	71.53	2.41	0.39
3	700	23.16	73.42	3.43	0.32
5	700	12.70	77.35	9.95	0.16
10	700	9.39	75.76	14.85	0.12

Table 7.2: Average EMP data for the cotectic melts at different temperatures and starting Fe contents.

Fe content category	Temperature (°C)	Cu wt%	Ni wt%	Fe wt%	S wt%	Cu/Ni
1	1000	44.48	38.52	1.04	15.95	1.15
5	1000	40.25	37.06	3.51	19.18	1.09
10	1000	33.58	36.03	6.93	23.48	0.93
1	900	32.17	48.18	0.84	18.81	0.67
5	900	30.87	44.74	3.81	20.58	0.69
10	900	26.45	44.29	6.13	23.12	0.60
1	800	22.30	56.31	0.47	20.92	0.40
3	800	22.52	55.23	1.39	20.87	0.41
5	800	20.97	54.73	2.79	21.52	0.38
10	800	20.90	53.40	4.52	21.18	0.39
1	700	12.87	63.70	0.22	23.21	0.20
3	700	10.40	63.65	1.51	24.45	0.16
5	700	11.39	61.48	2.60	24.55	0.19

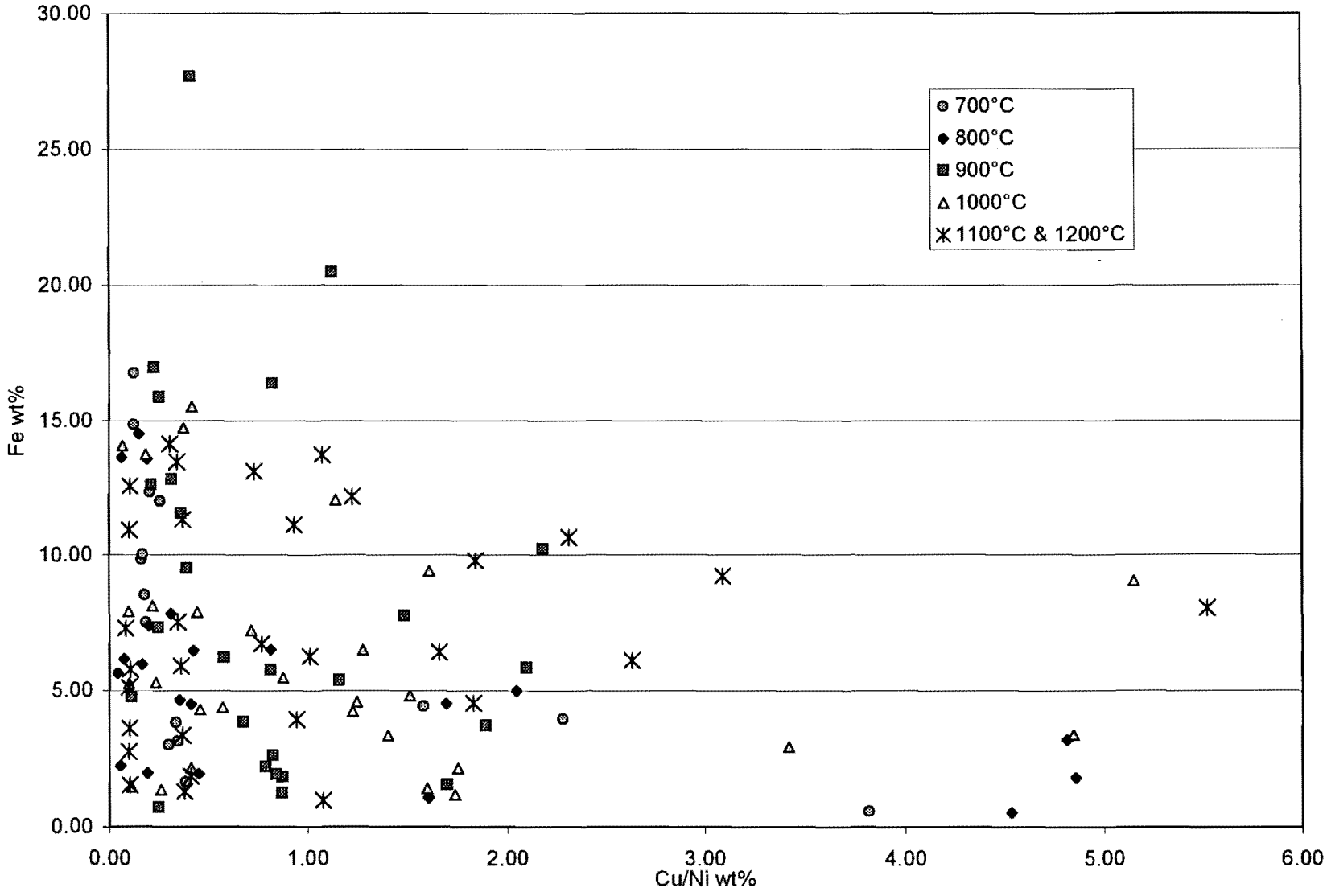

Figure 7.1: The Cu/Ni ratio against the Fe content of the alloys at different temperatures.

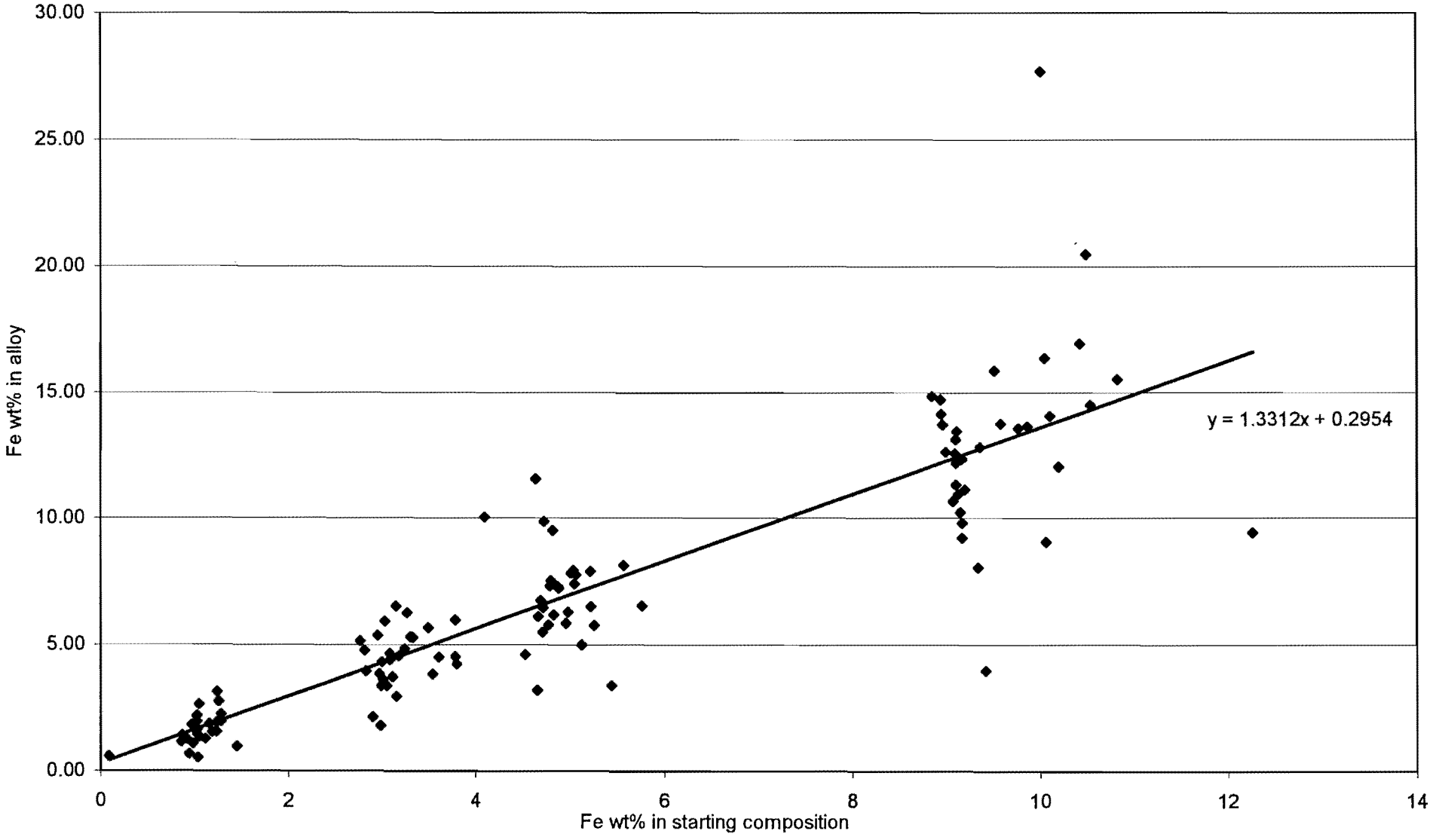

Figure 7.2: The Fe content in the starting composition against the Fe content of the alloys. Shown is a linear regression line through the population .

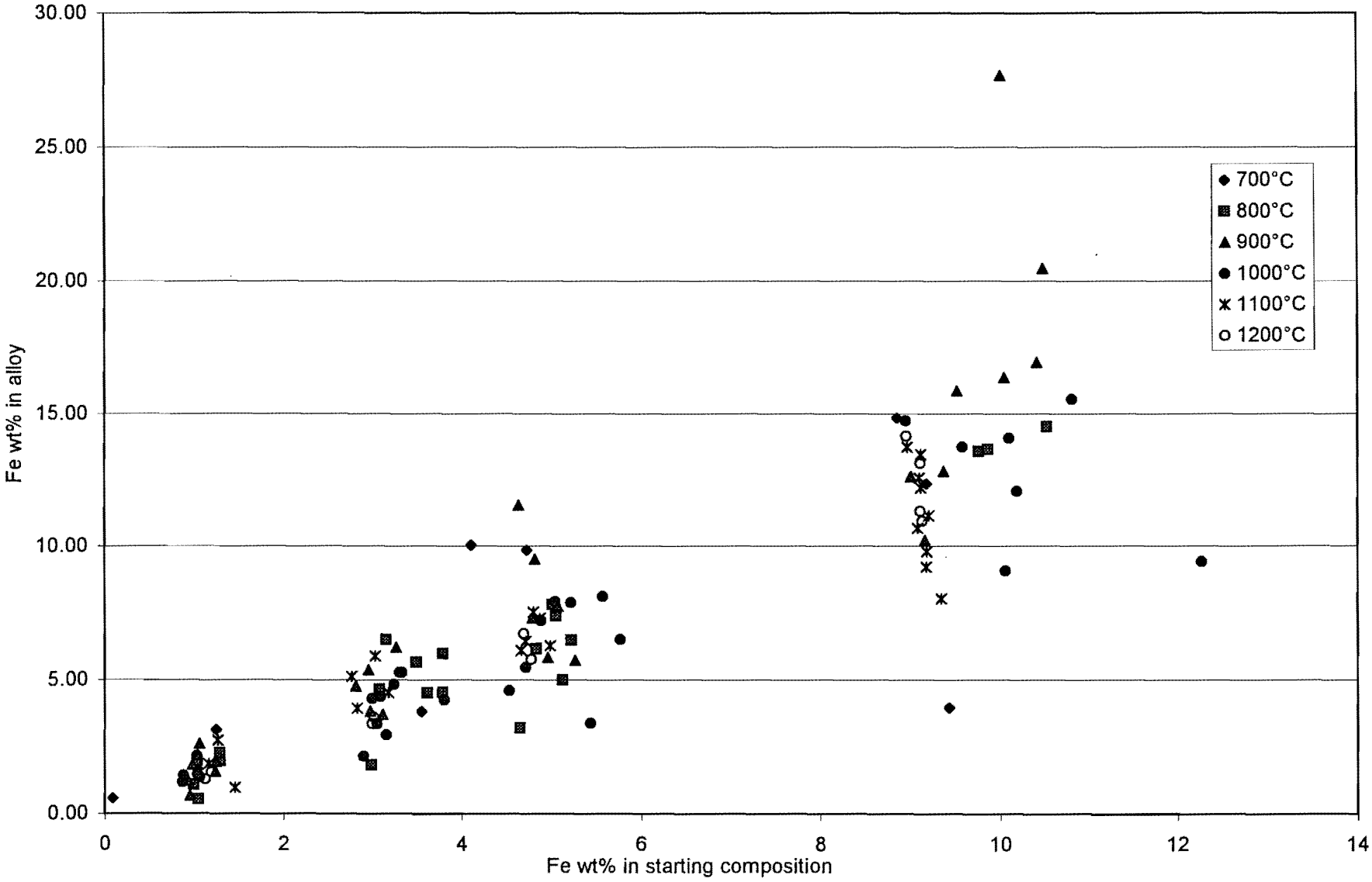

Figure 7.3: Fe in the alloy against Fe in the starting composition as a function of temperature.

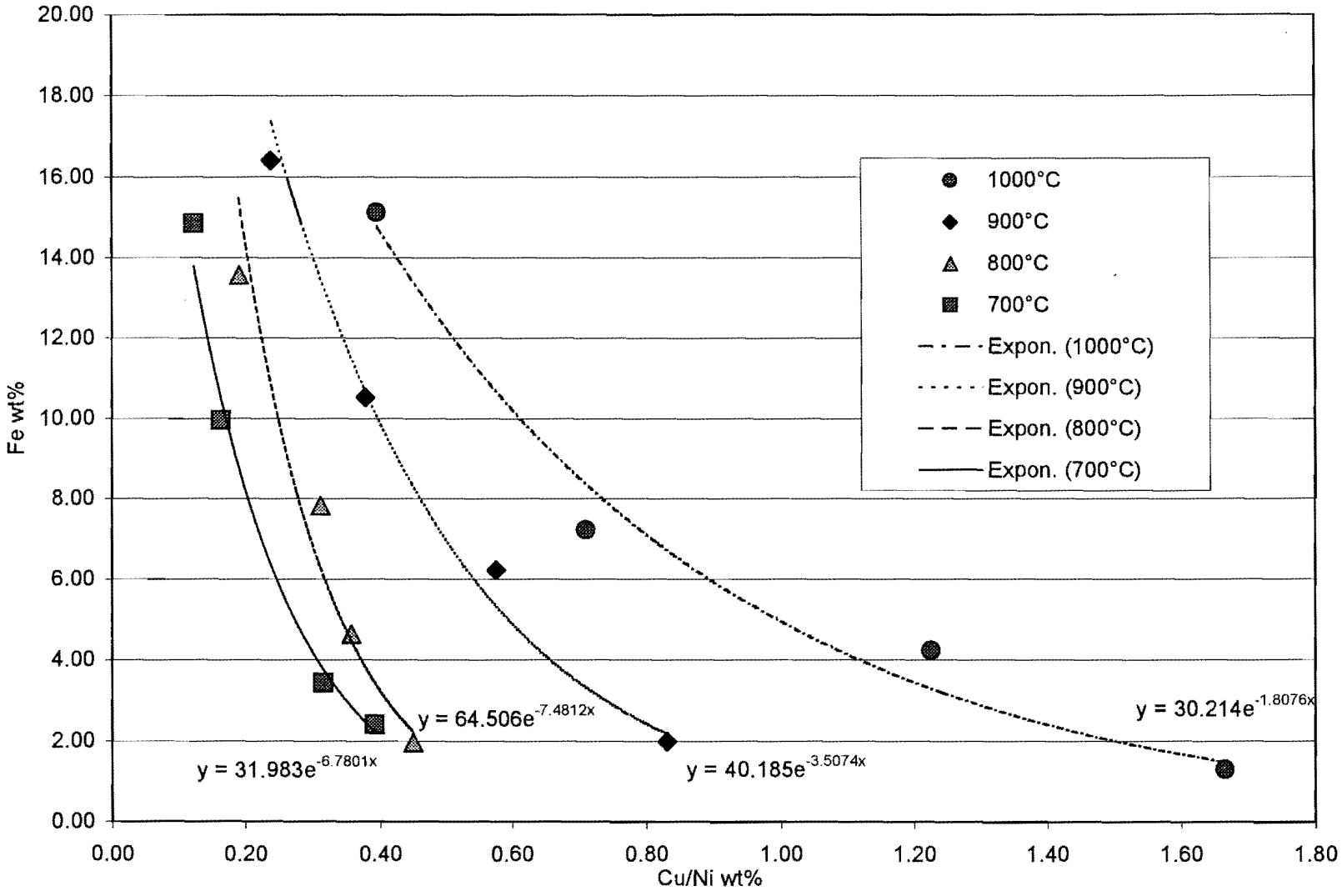

Figure 7.4: The Cu/Ni ratio against the Fe content of the cotectic alloys at the different equilibrium temperatures. Shown are the exponential regression lines for the cotectic alloys at different temperatures.

7.3 Digenite

In Figure 7.7, the Fe content against the sulphur content in digenite at different equilibrium temperatures is shown. The slope of the regression line for digenite at higher temperatures is less steep than those at lower temperatures. Linear regressions for different temperatures show an increase in sulphur content with an increase in Fe in the digenite at any given temperature. The sulphur and Fe content may be an indication that a solid solution exists between digenite and the β-phase. This aspect is discussed in sections 7.4 and 7.5.

Figure 7.8 shows the Fe content of digenite in relation to the amount of Fe in the starting composition. The higher Fe in the starting composition, the more Fe is taken up by the digenite. This is, however, not a perfectly linear relationship. The variation of the Fe content in digenite also becomes larger with the increase of the amount of Fe in the bulk. Also indicated on this diagram is the influence of temperature on the amount of Fe in the digenite. The higher the temperature, the more Fe can enter the digenite structure. The regression line for 800°C does not follow the general trend, because only one composition for digenite in the 10 wt% Fe category is available. Other plots show that the Fe in the digenite is independent of the assemblage (Figure 7.9).

The Ni and Fe content of digenite with and without exsolutions is presented in Figure 7.10. Analyses of digenite with exsolutions always included the exsolutions to represent the composition of the digenite at the temperature of equilibration. Digenite with exsolutions shows a larger variation in Ni content than the digenite without exsolutions, which has Ni contents lower than 1.23 wt%. The Fe content of both populations of digenite shows a wide variation. The presence of exsolutions can not be attributed to the amount of Fe in the digenite.

In Figure 7.11, digenite with different types of exsolutions are indicated on a Fe/Ni plot. The types are: digenite with round exsolutions that disappear towards the contact of digenite with an adjacent phase, digenite with round exsolutions that do not disappear towards the contact and digenite that contain skeletal type of exsolutions. There appears to be no distinct difference between the different types with the limited amount of data available.

Apart from the fact that metallic Cu was only observed in (alloy+digenite)- and (digenite+melt)-assemblages, there are no correlations between the starting composition, equilibrium temperature and mineral assemblage of experiments containing digenite and metallic Cu and those without metallic Cu. These Cu-rims were too small to analyze quantitatively, but the optical color strongly indicates that Cu is the main component. There is no reason to believe that the experiments containing them were in dis-equilibrium. Because they appear very infrequently and in small quantities it is believed that these metallic Cu appearances are in some way related to the process of quenching of the experiments. It is not the scope of this project to investigate this issue any further.

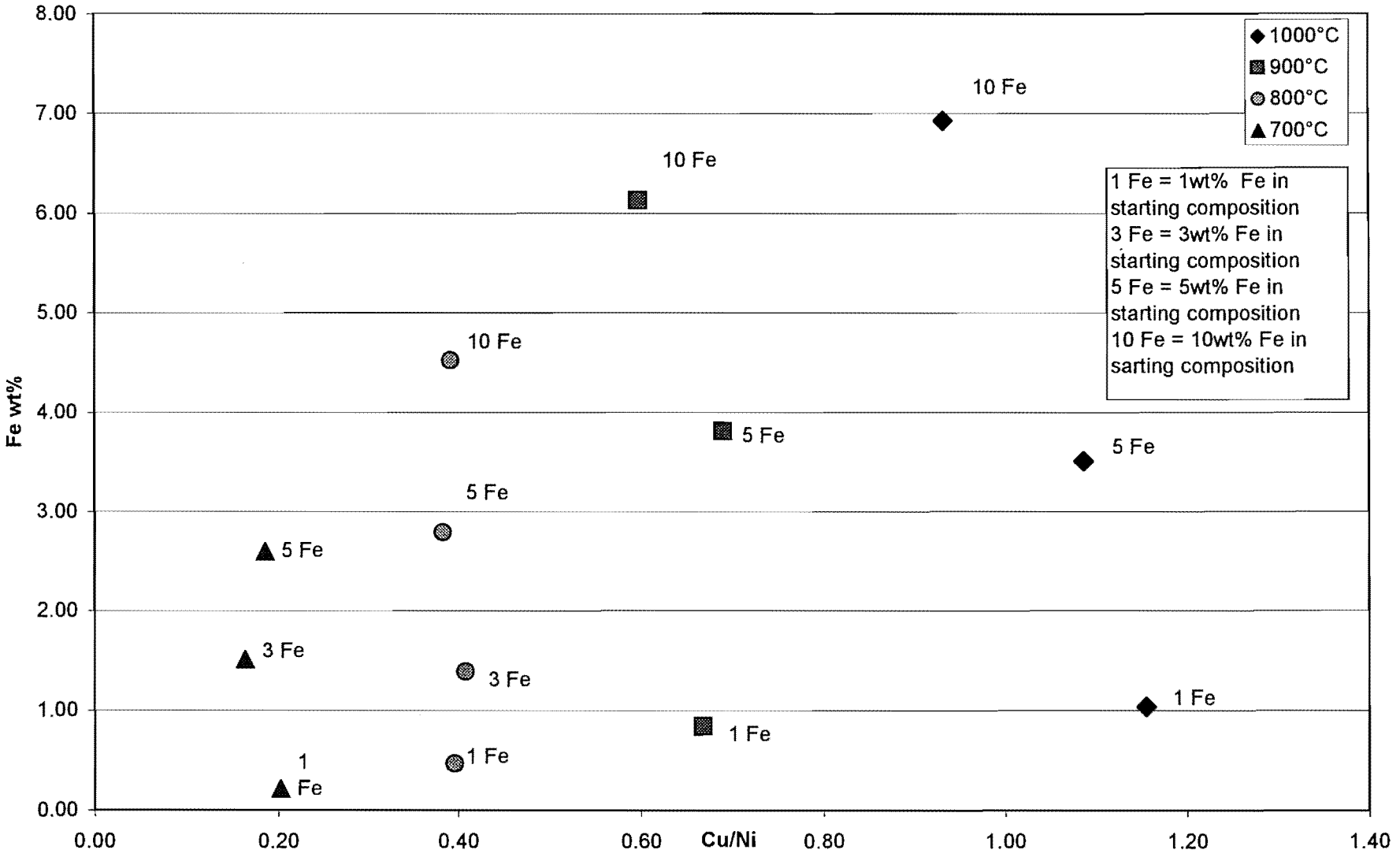

Figure 7.5: The Cu/Ni ratio against the Fe content of the cotectic melts at the different temperatures.

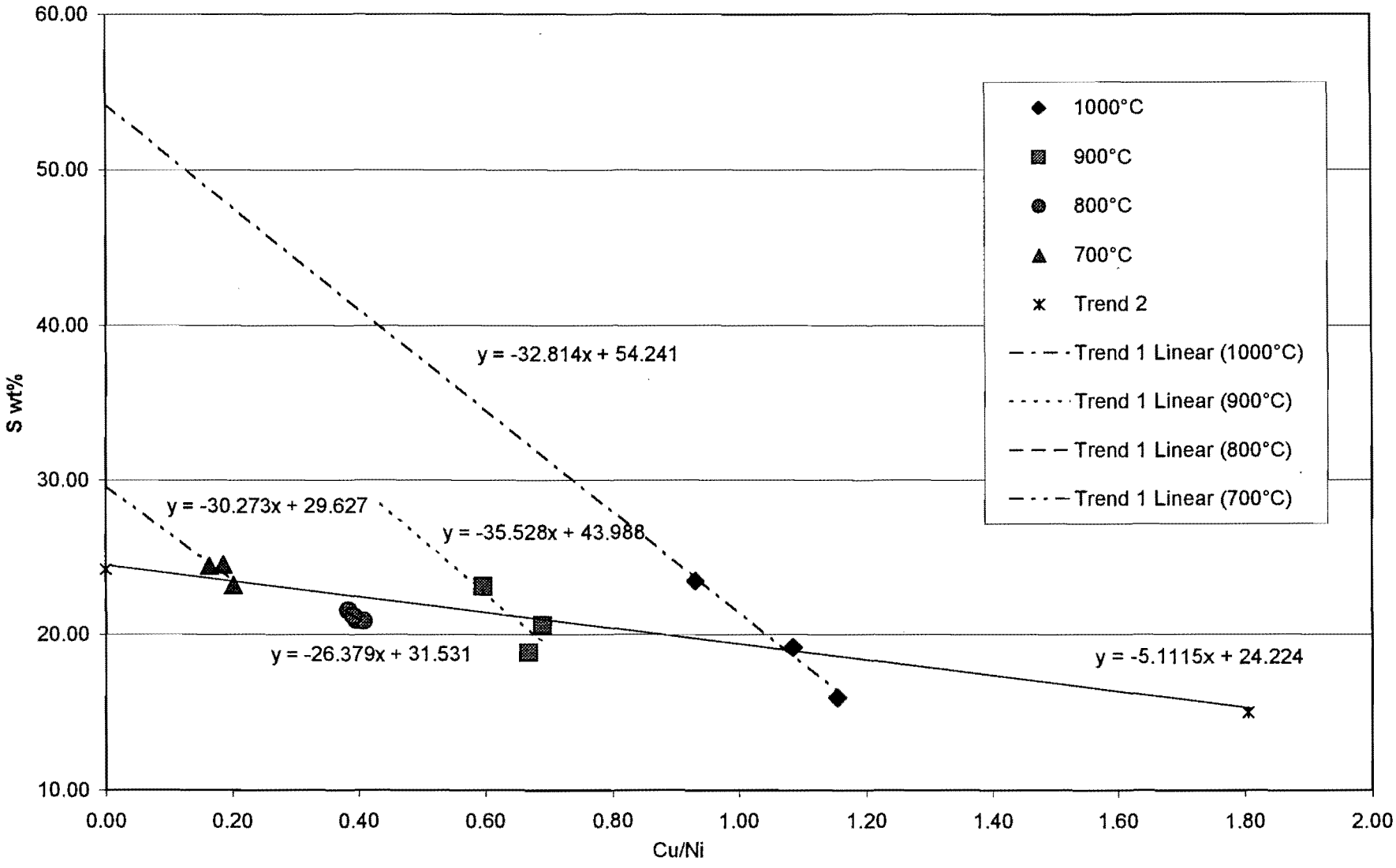

Figure 7.6: The Cu/Ni ratio against the sulphur content for the cotectic melts. Linear trend lines are indicated for each temperature as well as for the whole population.

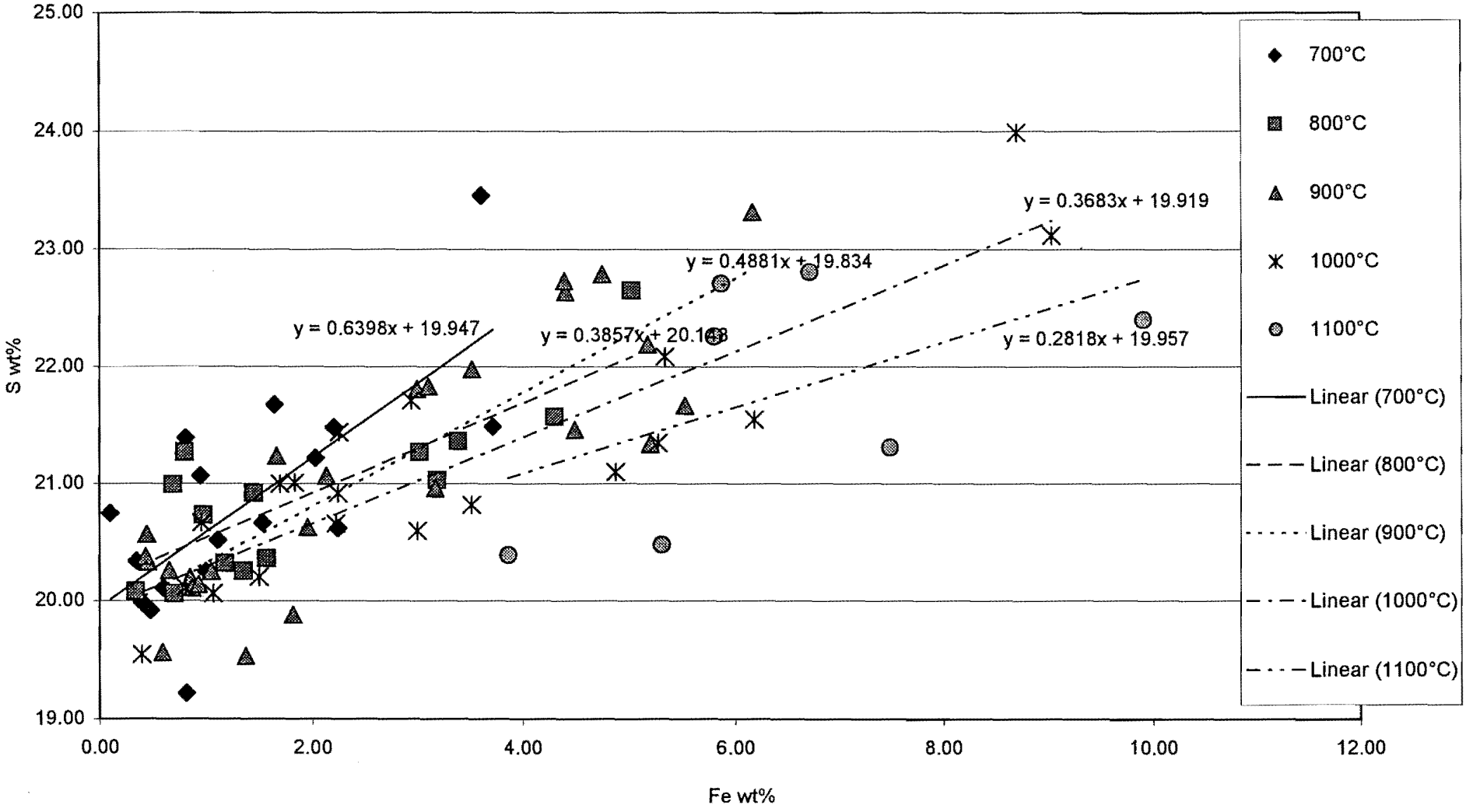

Figure 7.7 The Fe content against the sulphur content in the digenite at different equilibrium temperatures. The linear trend lines are shown at each temperature.

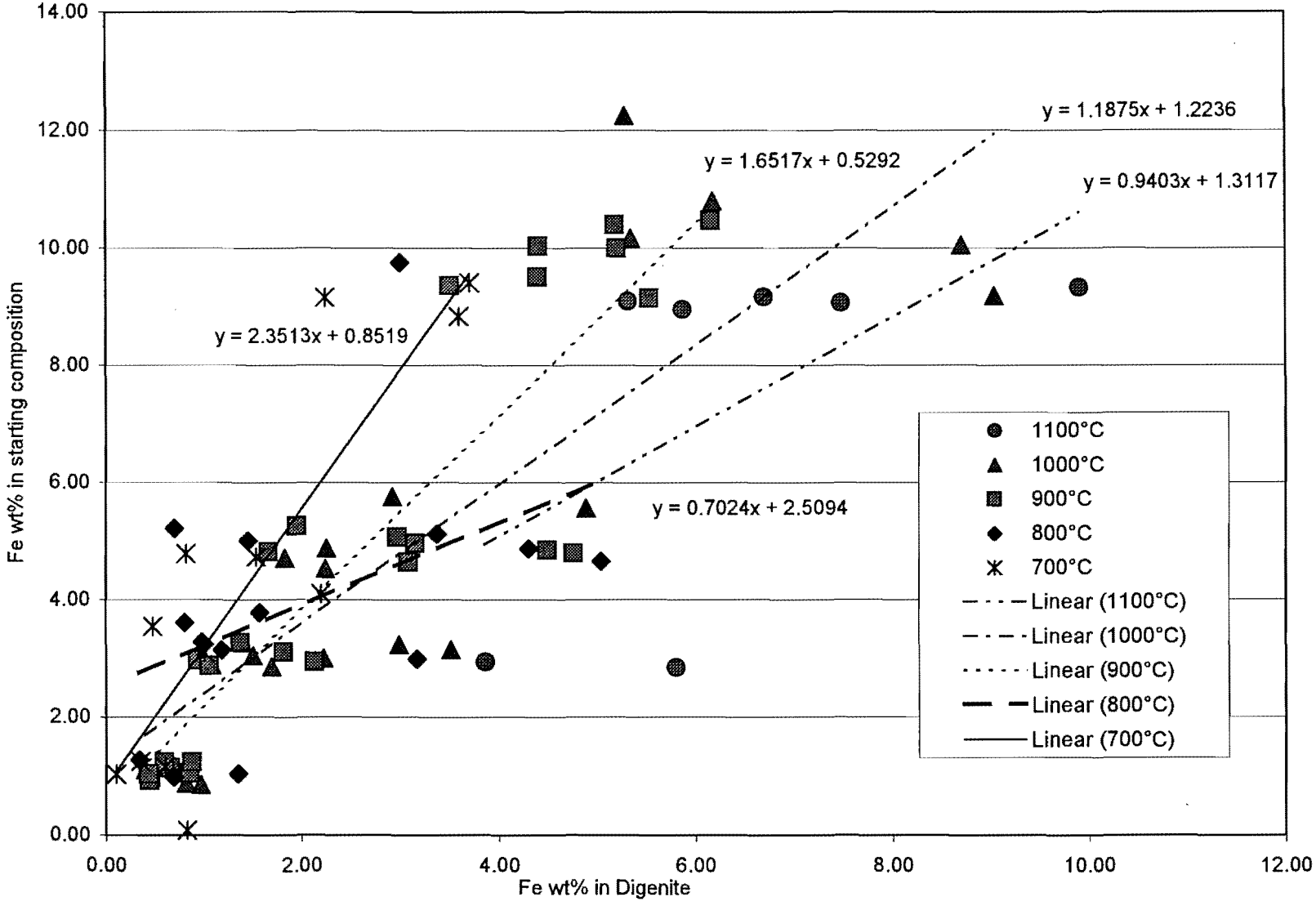

Figure 7.8 The Fe content of digenite in relation with the amount of Fe in the starting composition. Also indicated are the effect of temperature and the regression lines at different temperatures.

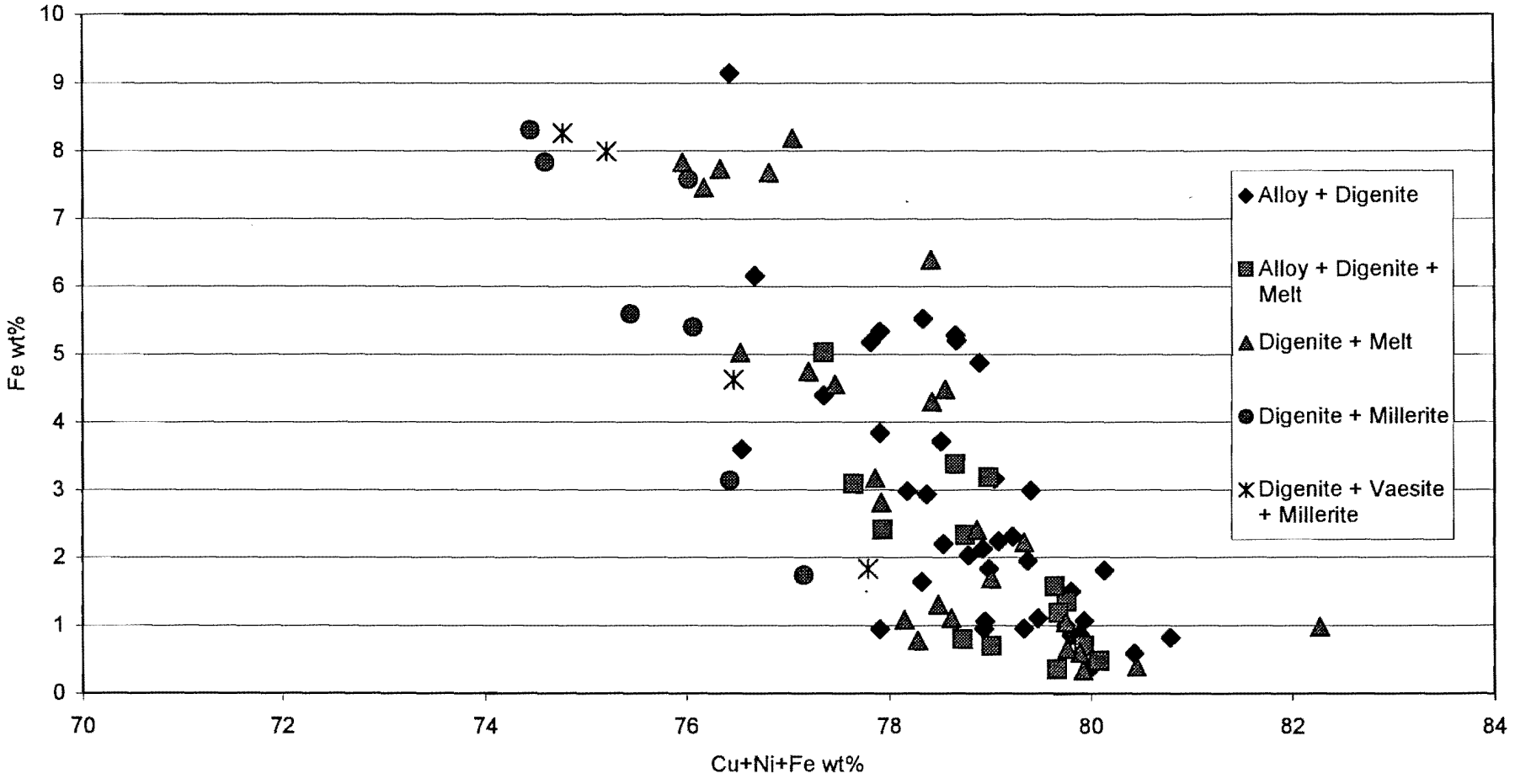

Figure 7.9: Fe content in Digenite is independent of the assemblage

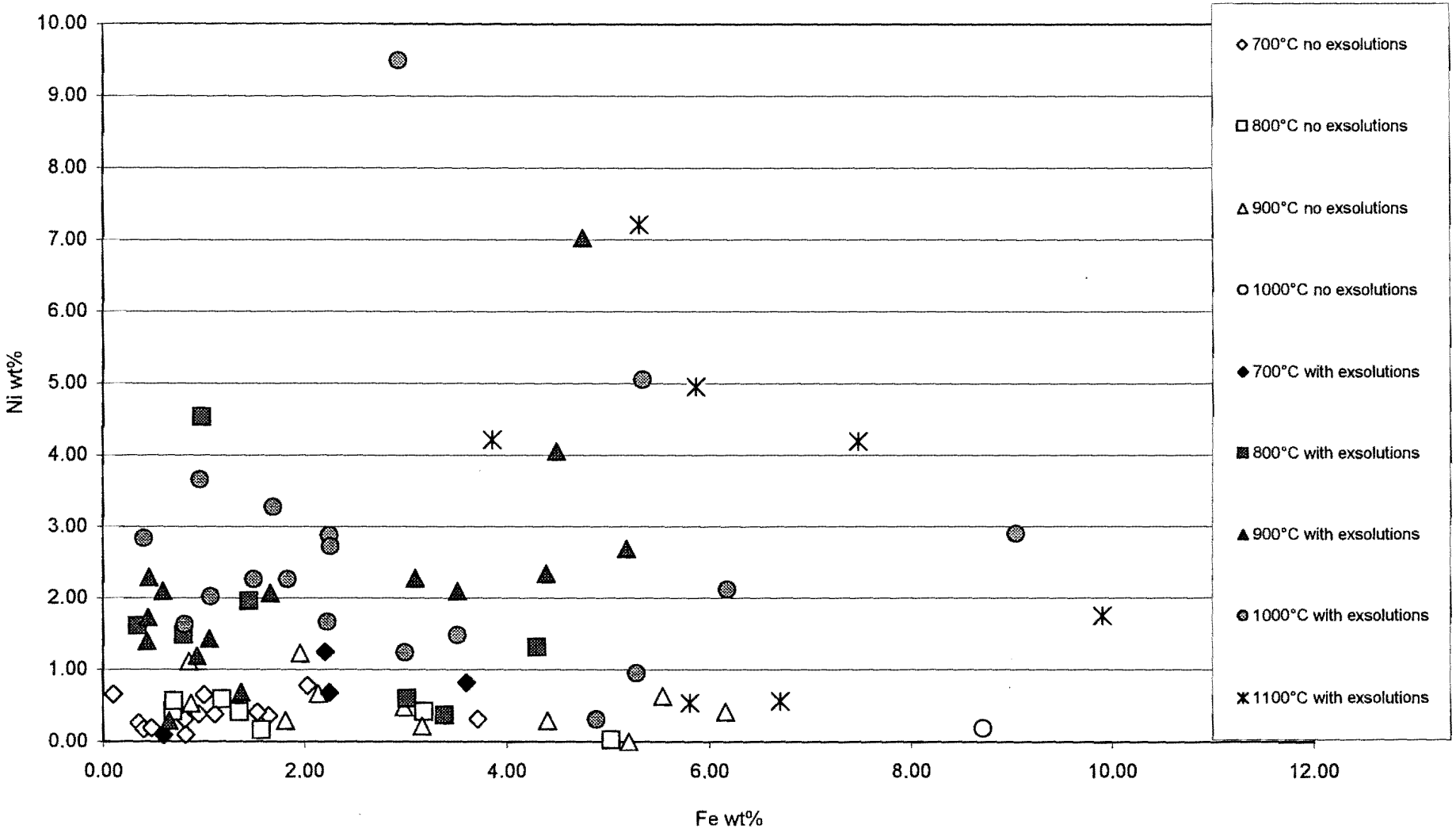

Figure 7.10 The Ni and Fe content of digenites with and without exsolutions.

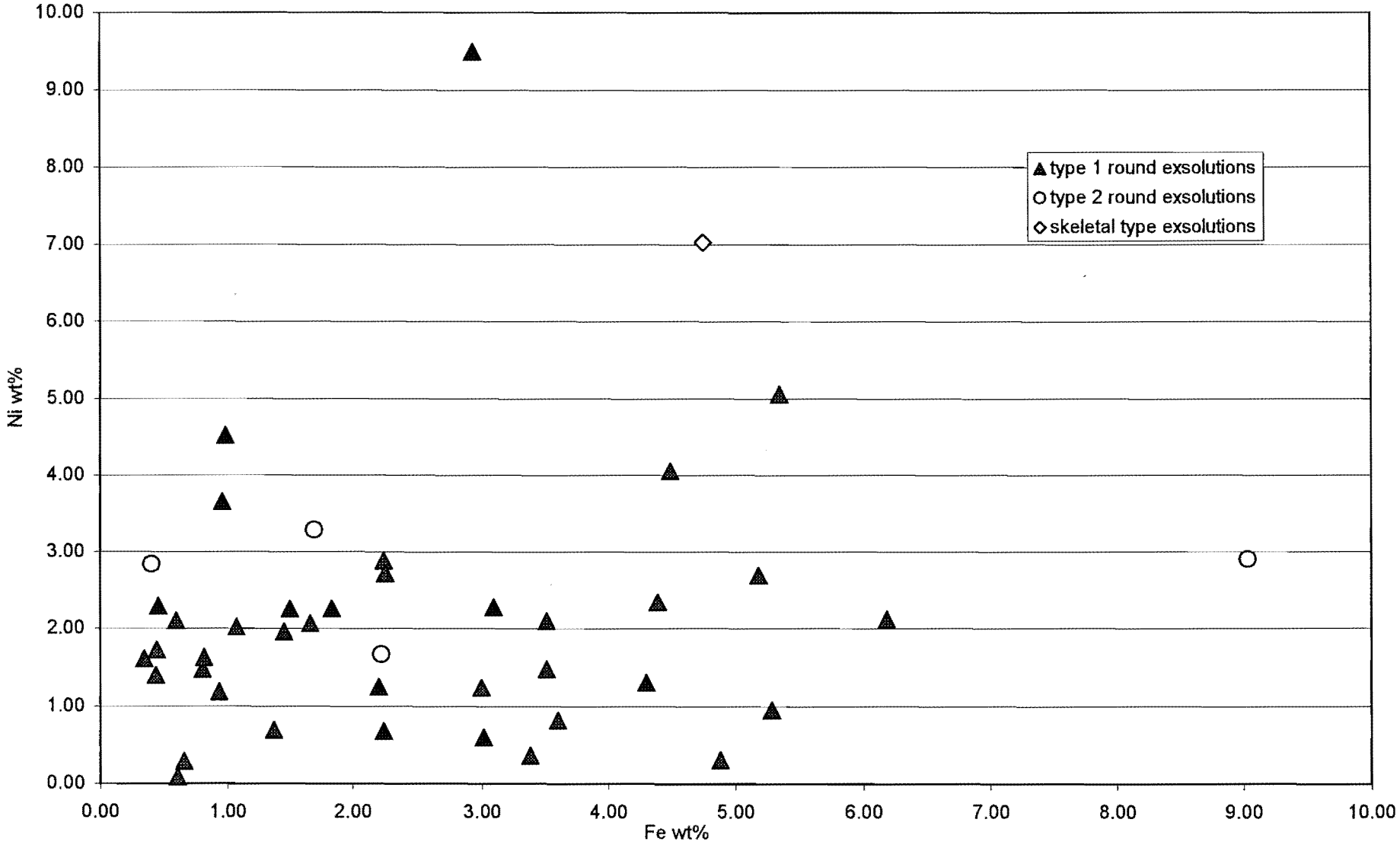

Figure 7.11 The Ni and Fe contents of digenite with different types of exsolutions.

7.4 The β-phase

EMP analyses (Table 7.3) for the β-phase were plotted together with those of digenite to show the compositional differences. Figure 7.12 displays the Cu-S relationship for digenite and the β-phase from all the experiments. The digenite data plots towards higher Cu and lower sulphur contents, while the β-phase has generally lower Cu and higher S contents. There are no other compositional differences between digenite and β-phase. A statistical evaluation between the Cu and sulphur values of digenite and β-phase follows under section 7.5.

The fact that β-phase co-exists only with millerite and vaesite suggests that it needs higher initial sulphur contents to form. With lower sulphur contents in the bulk composition, digenite will be more likely to be stable. The large compositional overlap between these two phases suggests a gradual compositional shift of digenite towards higher sulphur and lower Cu contents at lower temperatures. The empirical formula for the average β-phase is $(Cu_{1.45}Ni_{0.07}Fe_{0.12})_{1.64}S$ and that of the average digenite is $(Cu_{1.78}Ni_{0.04}Fe_{0.07})_{1.90}S$.

The difference in optical appearance may point to structural differences. For this purpose X-ray diffraction patterns were obtained from four experiments containing the β-phase (Appendix E). The aim was to determine weather there is a shift or modification in the XRD-pattern for digenite or whether there is a distinct different phase pattern present.

After careful evaluation of the XRD patterns it was determined that the Cu-sulphide phase present was not digenite, or a compositional variation of digenite. The β-phase resembles best synthetic bornite (Cu_5FeS_4). Digenite is cubic, thus isotropic whereas bornite is tetragonal below 228°C where it displays weak anisotropism, and cubic above 228°C where it is isotropic (Klein & Hurlbut, 1999). The optical appearance of β-phase also mirror that of bornite better than that of digenite. Chemically, stoichiometric bornite contains 63.3 wt% Cu, 11.2 wt% Fe and 25.5 wt% S, but shows extensive solid solution within the Cu-Fe-S system (Klein & Hurlbut, 1999). The β-phase contains on average 68.21 wt% Cu, 7.94 wt% (Fe+Ni) and 23.85 wt% S, which does not make it true synthetic bornite but possibly part of the solid solution of bornite.

Yund and Kullerud (1966) investigated the thermal stability of assemblages in the Cu-Ni-S system from 700°C to approximately 100°C, and found a synthetic phase which they called "x-bornite". This phase is close in optical appearance and composition to bornite, but contains about 0.4 wt% more sulphur. They proposed that "x-bornite" forms when sulphur-rich bornite synthesized at high temperature is annealed between 62° and 140°C. This phase was identified with natural "anomalous bornite" also described by Sillitoe and Clark (1969) that found that "anomalous bornite" in the Copiapo mining district, northern Chile contains 2 wt% less Cu and 2 wt% more sulphur than optically-normal, hypogene bornite. Other natural occurrences of "anomalous bornite" were described by Ixer et al. (1986) and Nylstrom and Wickman (1991) in supergene natural systems (generally temperatures below ~ 150°C). Durazzo and Taylor (1982) also mention "anomalous bornite" in experimental work in the bornite-chalcopyrite system at annealing temperatures between 100° and

350°C. These occurrences of "anomalous bornite" are all described in low temperature systems, and the correlation of "anomalous bornite" to the high temperature β-phase is not concluded.

7.5 Statistical Evaluation of the Composition of Digenite and β-phase

To quantify the compositional difference between digenite and the β-phase, the non-parametric Tukey-test (Tukey, 1959; Neave, 1966; and Neave, 1979) and a Kolmogorov-Smirnov-type (K-S-type) test were performed. For step-by-step overview on how the Tukey-test is performed the summary by Nelson (1975) is recommended, and for the K-S-type test the statistical books by Conover (1980) and Meddis (1975) give a good overview.

With the Tukey-test, the Cu and sulphur data for the digenite and β-phase were compared to determine whether the means for the two populations are statistically different at the 5% and 1% significance levels. This would give an indication. According to the table of critical values given by Nelson (1975), T_N for Cu should be larger than 10 for the 5% significance level and larger than 13 for the 1% significance level. The value T_N for Cu from this study is 16, which is larger than both values. Thus, the difference in the mean of the Cu values for these two populations are statistically significant. The test was not successful distinguishing between the two populations with respect to the sulphur values.

The Kolmogorov Goodness-of-fit Test was applied to first determine the normality of at least one of the populations. Although it can be derived from Figure 7.12 that neither digenite nor β-phase has a normal distribution with regard to their Cu and sulphur values, the Kolmogorov test was applied to verify this. The T value was calculated to be much larger (0.80) than the critical value at both the 95% (0.11) and 99% (0.18) confidence levels for the two-sided test. Therefore, the common t-test used for normal distributions could not be used to test the difference in distribution between the Cu values for digenite and the β-phase, and it was decided to use a non-parametric Kolmogorov-Smirnov-type test.

With the Kolmogorov-Smirnov test a significant difference between the Cu and sulphur values of the digenite and β-phase was investigated. Tests for both the Cu and sulphur distributions of digenite and the β-phase showed that a statistically significant difference between these distribution exists. The critical value for the two-sided test at a 95% confidence level is 0.28, and the T value for Cu was calculated to be 0.68. Similarly, the T value for sulphur (0.77) is also much larger than the critical value of 0.28.

The results from the Tukey- and the K-S-type test proved that there exists a, statistically significant difference between the distribution of the Cu and sulphur values for digenite and the β-phase. Therefore, based on compositional differences and the XRD analyses these two phases are not part of the same solid solution series.

Table 7.3: Average EMP data for the β-phase in weight and atomic percentage.

Experiment no.	Cu wt%	Ni wt%	Fe wt%	S wt%		Cu at%	Ni at%	Fe at%	S at%
7h4	76.51	0.13	0.24	23.11		62.34	0.11	0.22	37.32
7a4	75.19	1.77	0.95	22.09		61.65	1.57	0.89	35.90
7g5	72.80	2.62	1.74	22.84		59.24	2.31	1.61	36.84
7h1	74.11	1.85	1.83	22.20		60.65	1.64	1.70	36.01
7g1	70.46	1.38	4.63	23.53		56.89	1.21	4.25	37.65
7j3	68.21	0.26	4.71	26.82		53.70	0.22	4.22	41.86
7i3	66.42	0.80	7.99	24.78		52.93	0.69	7.24	39.14
7e4	63.69	2.66	8.98	24.67		50.67	2.29	8.13	38.91
7e5	66.54	1.03	8.13	24.30		53.20	0.89	7.40	38.51
8j4	69.83	5.62	1.07	23.48		56.46	4.92	0.98	37.63
8j2	72.04	5.46	1.11	21.39		59.24	4.86	1.04	34.86
8j3	70.72	6.35	1.08	21.84		57.91	5.63	1.01	35.45
8l1	70.45	3.37	2.40	23.79		56.82	2.94	2.20	38.03
8f3	70.77	2.52	3.14	23.58		57.16	2.20	2.89	37.75
8l2	67.20	5.68	3.93	23.19		54.29	4.97	3.61	37.13
8l3	69.51	1.15	5.40	23.94		55.90	1.00	4.94	38.16
8l5	66.94	2.70	5.58	24.78		53.41	2.33	5.07	39.19
8b4	70.79	2.12	4.56	22.53		57.59	1.87	4.22	36.33
8b5	68.74	2.76	5.03	23.47		55.45	2.41	4.62	37.52
8m2	65.86	0.65	8.26	25.23		52.28	0.56	7.46	39.70
8m3	67.39	1.21	7.73	23.68		54.16	1.05	7.07	37.72
8m4	67.44	2.41	5.59	24.56		53.91	2.09	5.08	38.92
8d1	64.32	3.81	7.83	24.04		51.45	3.30	7.13	38.12
8i3	66.44	2.42	8.19	22.95		53.64	2.12	7.52	36.72
8m5	64.46	2.31	7.83	25.40		51.07	1.98	7.06	39.89
8n2	60.16	2.41	10.56	26.88		46.98	2.04	9.38	41.60
8n5	59.33	2.27	11.22	27.18		46.20	1.91	9.94	41.95
9i3	69.31	5.80	2.81	22.07		56.56	5.13	2.61	35.70
9i5	68.50	6.19	3.17	22.14		55.83	5.46	2.94	35.77
9g2	65.08	3.63	7.46	23.83		52.18	3.15	6.81	37.87
9l4	65.16	3.98	7.68	23.18		52.48	3.47	7.04	37.01
9n3	66.79	6.14	1.13	25.94		52.95	5.27	1.02	40.76
9e3	67.61	7.91	1.35	23.13		54.72	6.93	1.24	37.11
9h3	71.39	6.11	0.78	21.73		58.53	5.42	0.73	35.31
Average	**68.21**	**3.08**	**4.86**	**23.85**		**54.90**	**2.69**	**4.42**	**37.99**
Standard Deviation.	**3.71**	**2.09**	**3.14**	**1.54**		**3.62**	**1.84**	**2.82**	**1.92**

7.6 Millerite and Vaesite

In Figure 7.13, the (Ni + Cu + Fe) and sulphur content of the millerite and vaesite from all the experiments are compared. Analyses of millerite show an average metal content of 47.67 ± 1.15 at% (range 49.38 – 54.24 at%) and an average sulphur content of 52.33 ± 1.15 at% (range 45.76 – 50.62 at%). Vaesite has an average metal content of 32.47 ± 0.49 wt% (range 66.56 – 68.55 at% metals) and an average sulphur content of 67.53 ± 0.49 at% (range 31.45 – 33.44 at%). Recalculation to atomic proportions gives a general formula of $(Ni,Cu,Fe)_{0.91}S$ for millerite and $(Ni,Cu,Fe)_{0.96}S_2$ for vaesite.

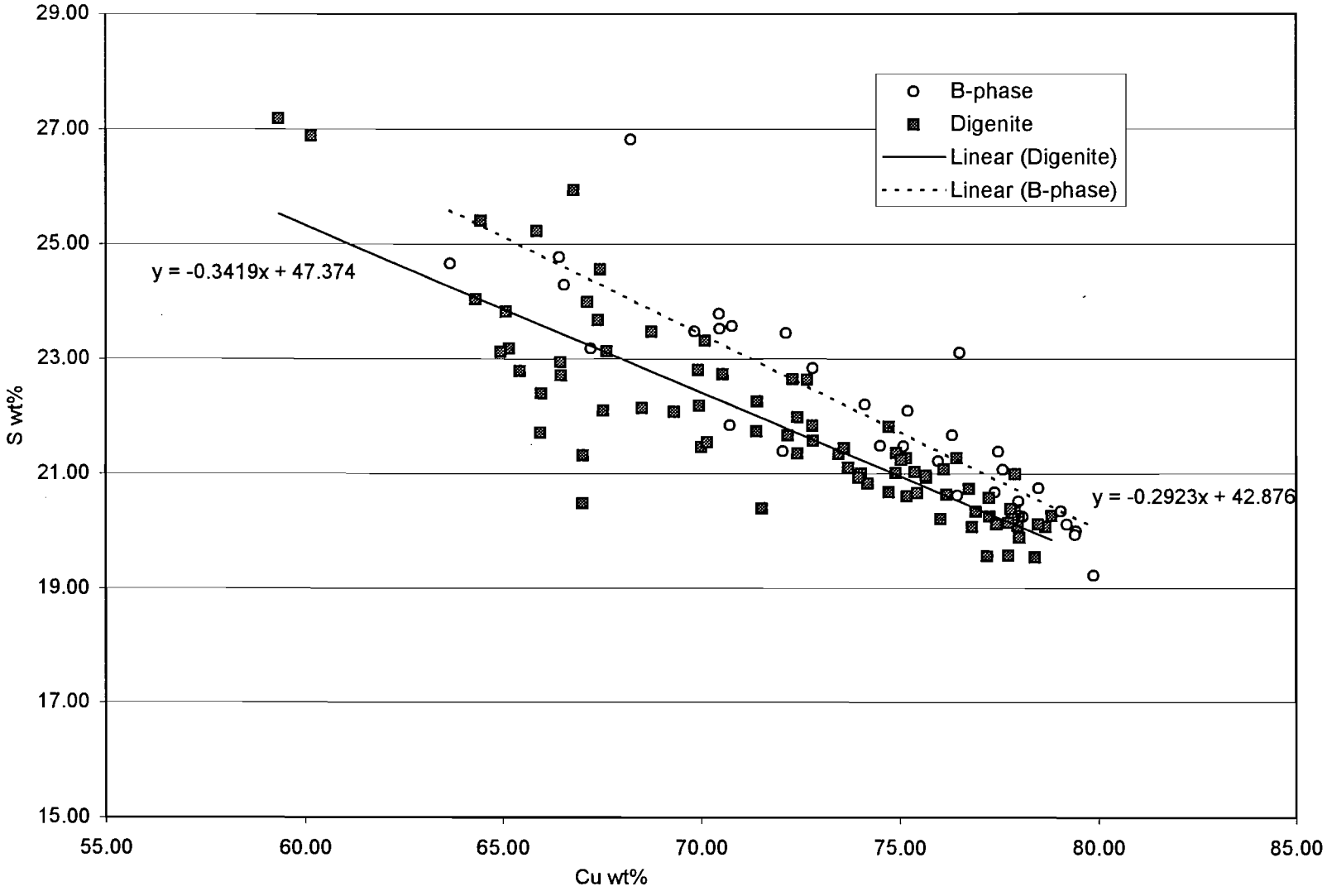

Figure 7.12: A Cu against sulphur plot for digenite and the B – phase. The linear regression lines are indicated with the relevant equations.

The relationship between the Ni and Fe-content in millerite and vaesite from all the [illegible] be seen in Figure 7.14. Vaesite shows little variation in Ni and Fe contents, and the composition is close to the stoichiometric NiS_2. Analyses of millerite show a negative correlation between Ni and Fe, and a wide variation in Fe contents.

Figure 7.15 is a plot of the Fe content in millerite against the Fe content in the starting composition. The amount of Fe in millerite is strongly dependent on the amount of Fe in the starting composition. For lower starting Fe-contents, the variation in the population is smaller than when larger quantities of Fe are available. The plot for vaesite (Figure 7.16) shows that the starting Fe content will also influence the amount of Fe in the vaesite, although only a small amount of Fe will enter the vaesite structure.

Evaluation of the millerite and vaesite data indicated that there is no significant relationship between the starting composition, equilibration temperature and assemblage.

7.7 Construction of Cooling Paths

For each bulk Fe content (i.e. 1, 3, 5 and 10 wt% Fe), a basic Cu-Ni-S ternary diagram was prepared, containing the average composition of all the sulphides and the average cotectic alloy composition at each temperature. Solidus tie-lines indicate which phases co-exist on complete solidification.

Unto the relevant diagram, the cotectic lines from each temperature isotherm (1200°C to 700°C) were superimposed. The eutectic points on each temperature isotherm were then connected to form a "cooling path isotherm". Where the detailed information lacked sufficient data the lines were inferred using the diagram of Bruwer (1996) as a guideline. The direction of cooling is indicated with arrows on the cotectic lines, each line leading towards an eutectic point. Crossing isotherms and winding cotectic(s) are a result of projection of a three-dimensional surface onto a two-dimensional plane.

7.8 Cooling Paths

The liquidus isotherms and cooling paths of a Cu-Ni-sulphide melt with different starting Fe-contents are shown in Figures 7.17 to 7.20. Indicated on the diagrams are the average compositions of phases in this system based on analyses from this study (the composition of heazlewoodite is schematic). The average compositions of these solid phases change according to the amount of Fe in the starting composition. The cotectic lines indicate the path of crystallization from 1200°C towards complete crystallization of the melt, at the relevant eutectic point. The exact positions of the eutectic points E1, E2 and E3 can not be determined from this study and these points are estimated.

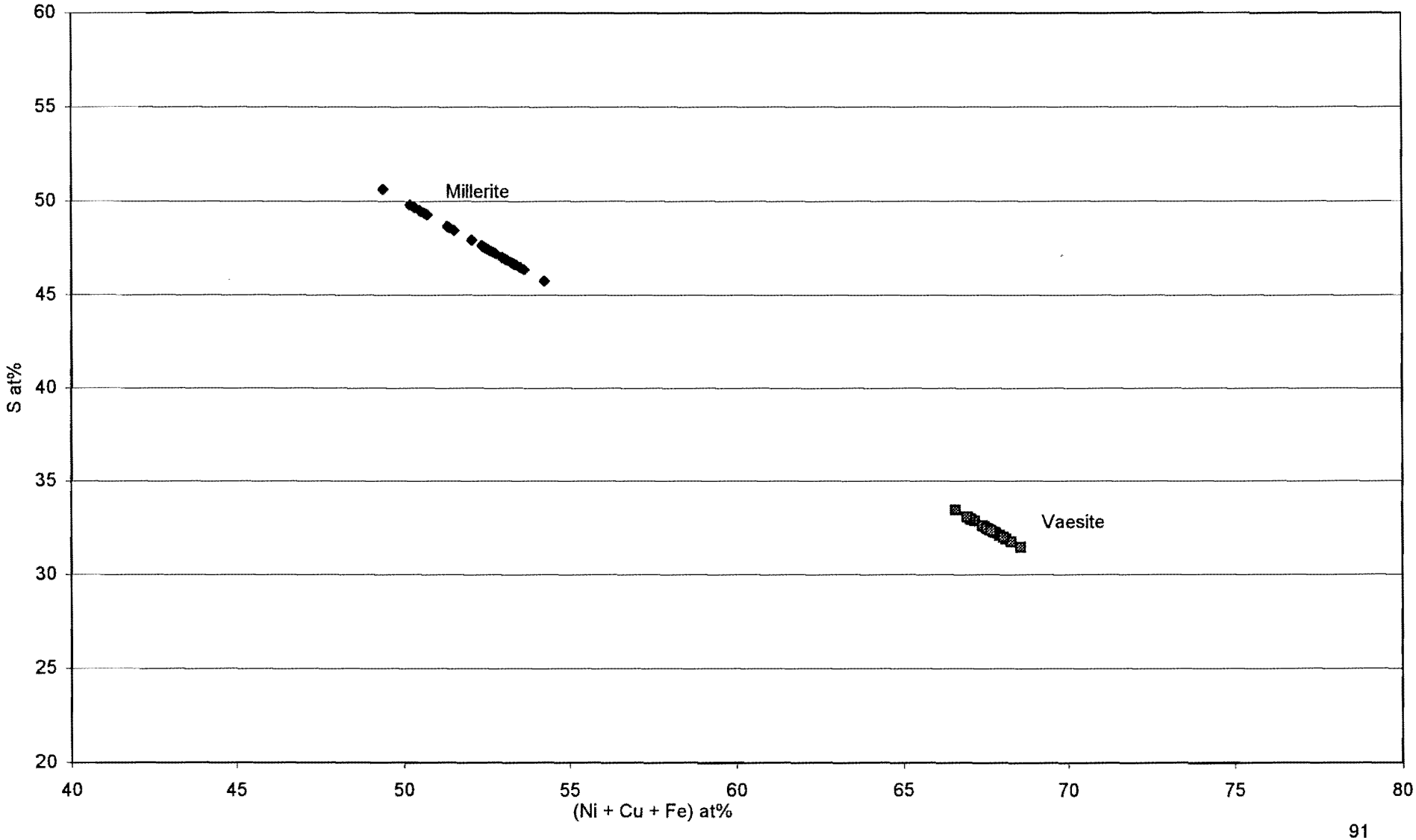

Figure 7.13: The (Ni + Cu + Fe) against the sulphur for millerite and vaesite.

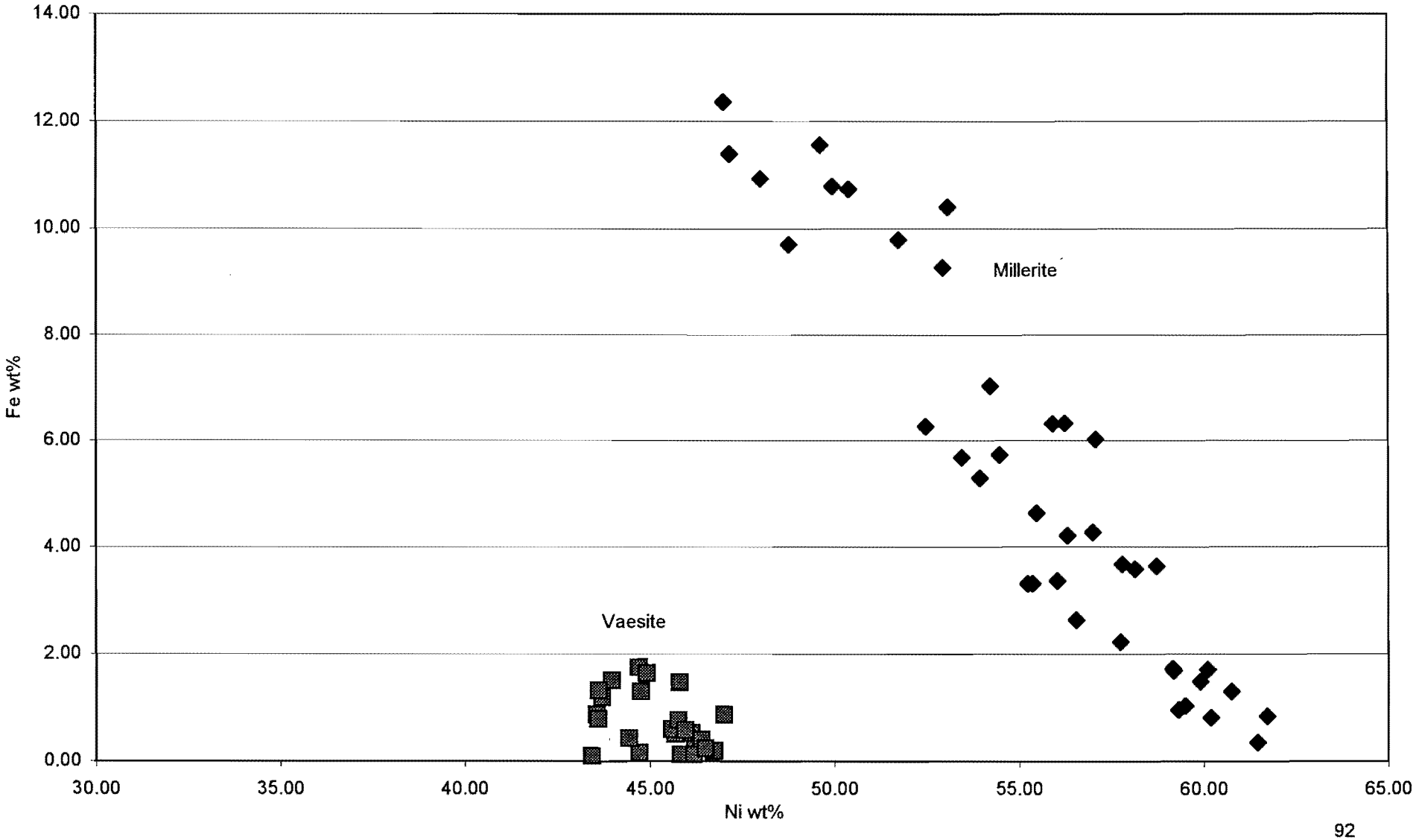

Figure 7.14: The Ni against Fe content in millerite and vaesite.

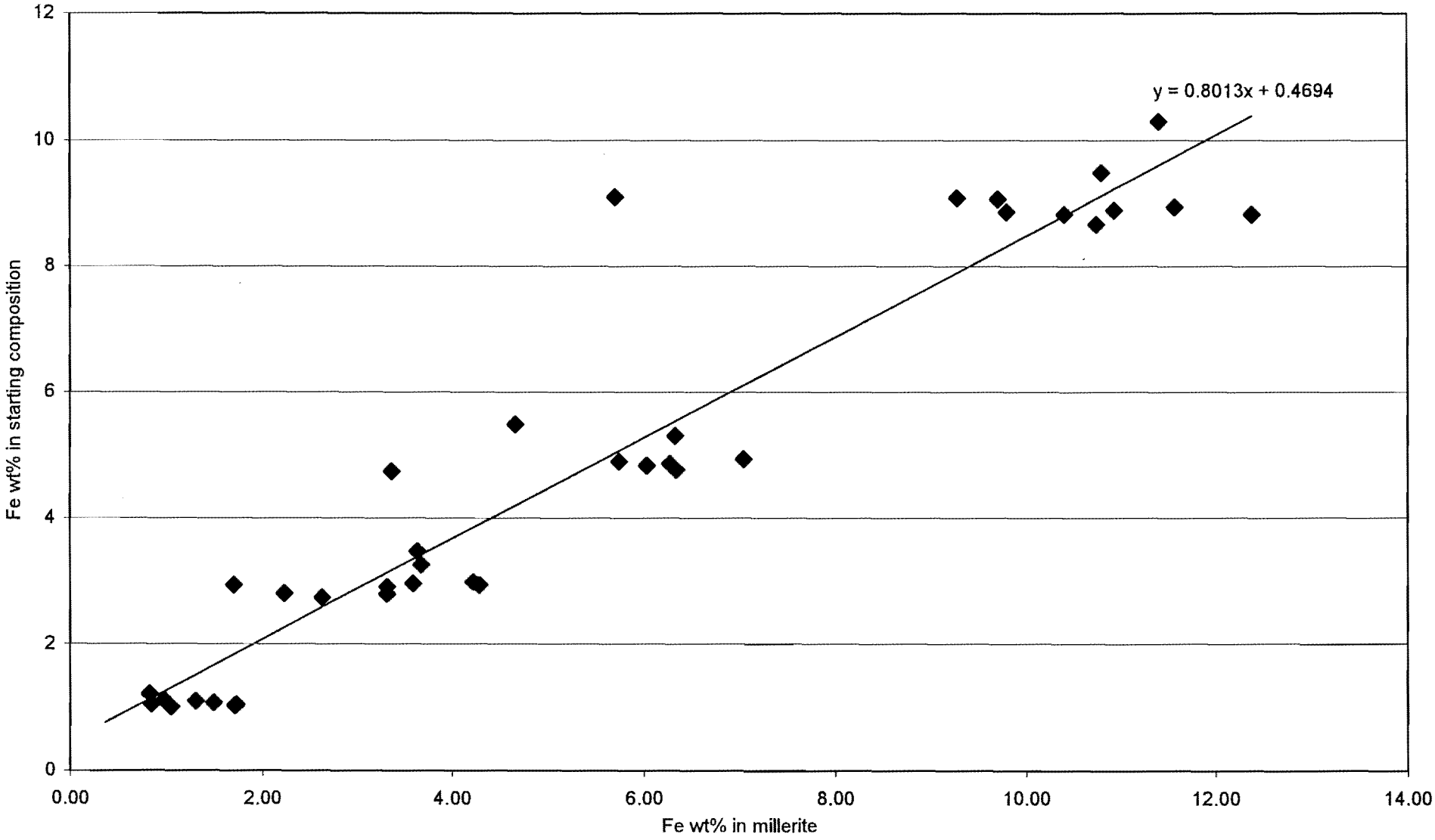

Figure 7.15: The Fe in millerite against the Fe in the starting composition. The linear regression line and equation are indicated on graph.

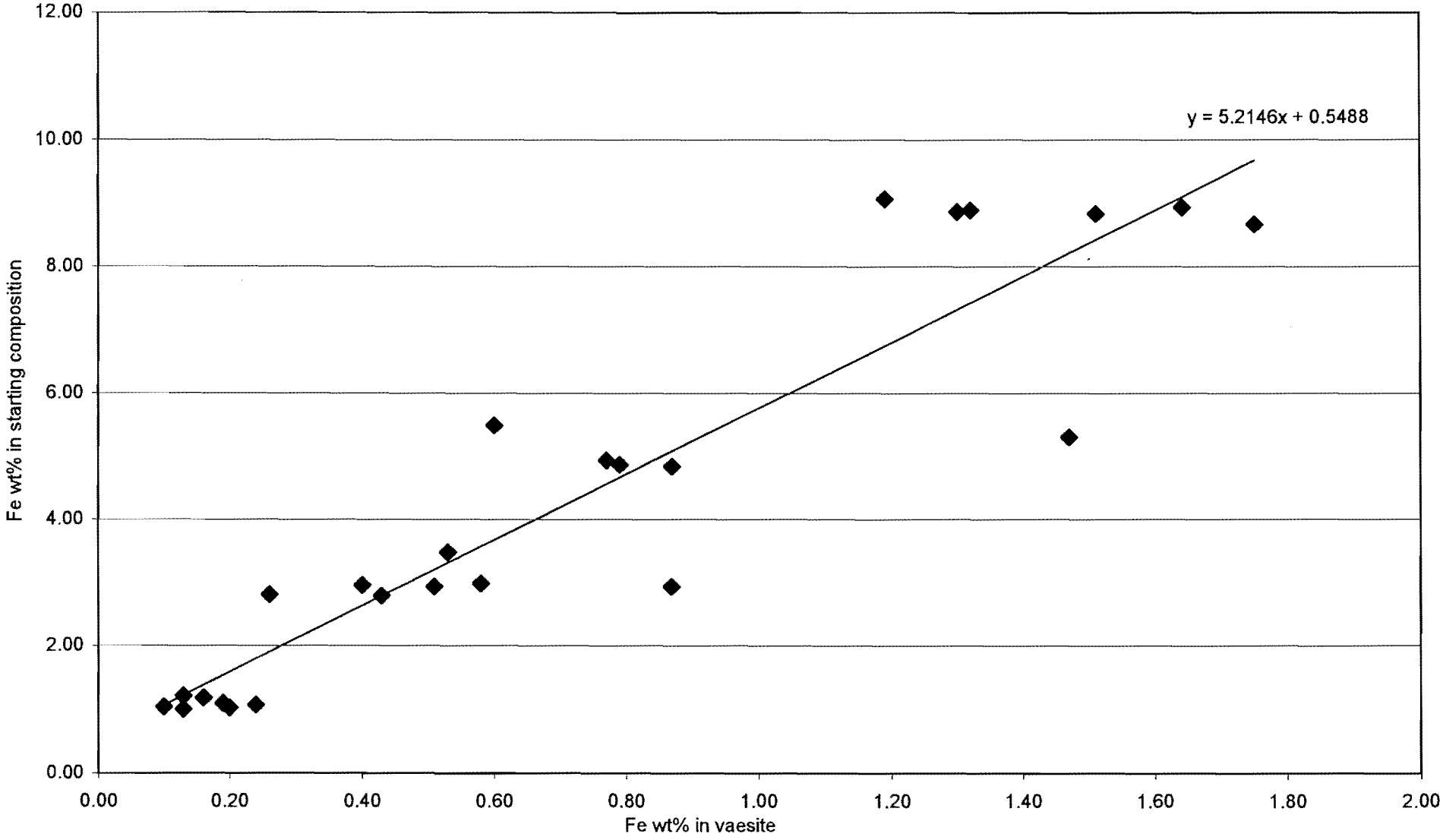

Figure 7.16: The Fe in vaesite against the Fe in the starting composition. The linear regression line and equation are indicated on graph.

Solidus tie-lines indicate the phase relations between solid phases on complete c[illegible] the phase rule, P + F = C + 1 (Ehlers, 1972), with F (degrees of freedom) = 0 for the maximum amount of phases, and C (number of components) = 4, it is derived that P (number of phases) can be up to 5. However, at any composition, a maximum of three phases were observed. Although the gas phase can not be seen, it is always present and must always be included. Therefore the maximum number of solid phases coexisting under equilibrium conditions can only be four. Due to the compositional variation of the alloy phase, the degrees of freedom (F) can be 1 in the lower part of the diagrams, which will explain why only three solid phases were observed.

Each of the triangles that defines which three phases coexist, contains an eutectic point. Three eutectic points are present: E1 in the (alloy-digenite-heazlewoodite)-field, E2 in the (β-phase+millerite+heazlewoodite)-field and E3 in the (β-phase+millerite+vaesite)-field (only in the 1 wt% Fe diagram). The eutectic point in the (digenite+β-phase+heazlewoodite)-field is undetermined by this study.

From any starting composition in the (digenite+heazlewoodite+alloy)-field, crystallization will follow a vector (away from the crystallizing phase) crossing the temperature contours until the cotectic is reached. From there, crystallization will proceed along the cotectic towards the eutectic point E1. Within a phase field, only one phase will crystallize from the melt. On the cotectic two phases will crystallize simultaneously form the melt and at the eutectic point three solid phases will coexist. The three phases would be alloy, digenite and heazlewoodite.

In the case where an alloy will crystallize first from the melt, the composition of the first crystallized alloy will change as the melt evolves, provided the alloy remains in equilibrium with the melt. On final solidification, and under equilibrium conditions, all the alloy grains will have the same composition. This is rarely, if ever, the case in slow cooled mattes under plant conditions.

From any starting composition in the (β-phase+millerite+heazlewoodite)-field, crystallization will proceed away from the crystallizing phase (crossing the temperature contours) to the cotectic and then towards the eutectic point E2, where β-phase, millerite and heazlewoodite crystallize together.

In a similar fashion, crystallization in the (β-phase+millerite+vaesite)-field, will evolve towards the eutectic point E3 where all three phases will crystallize together.

A significant comparison with the schematic phase diagrams of Craig & Kullerud (1969) and Ebel & Naldrett (1997) could not be drawn due to the lack of relevant quantitative data in the Fe deficient part of the quaternary.

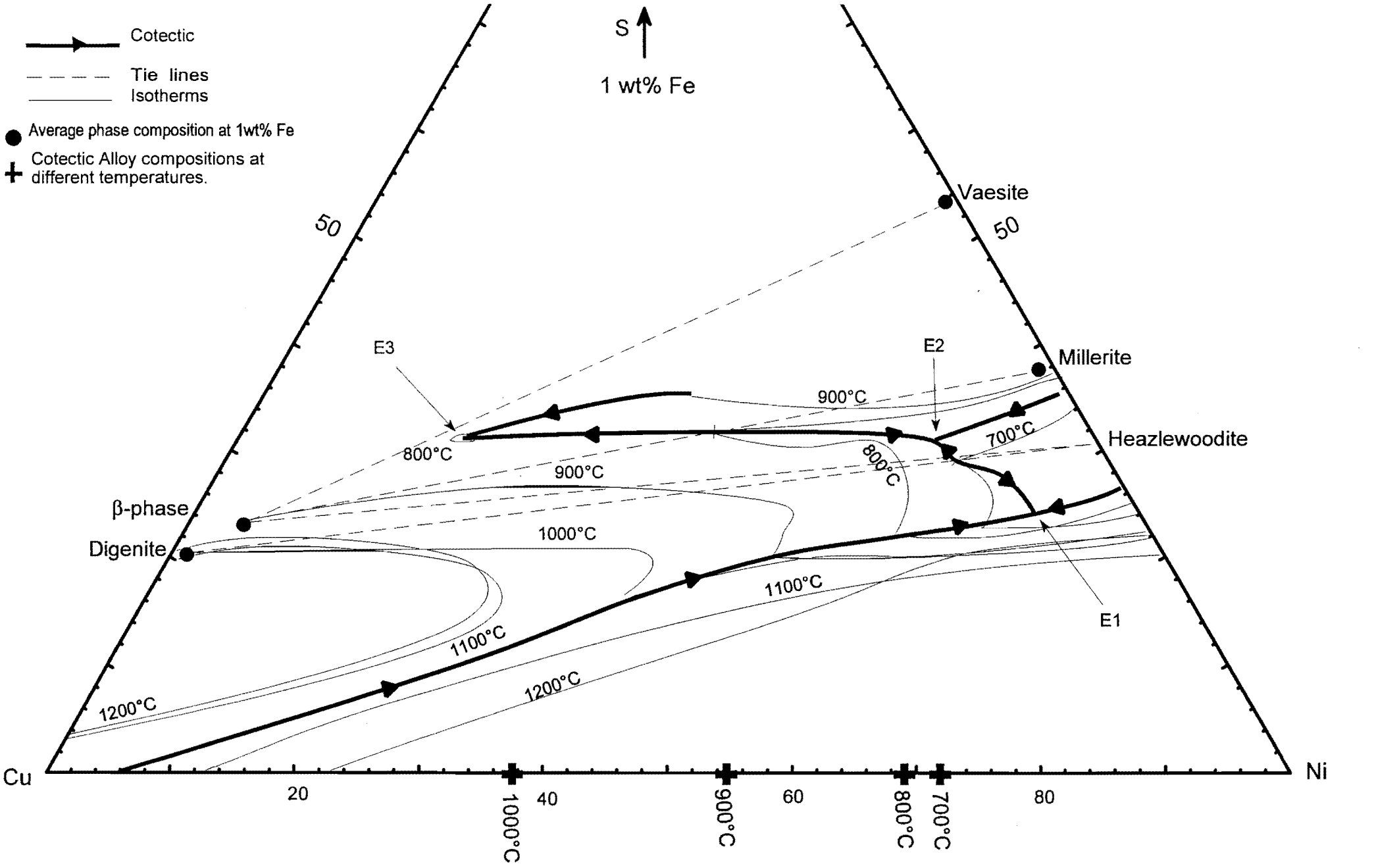

Figure 7.17: The liquidus isotherms and cooling path from 1200°C to 700°C at 1 wt% Fe in the starting composition. The composition of haezlewoodite is schematic.

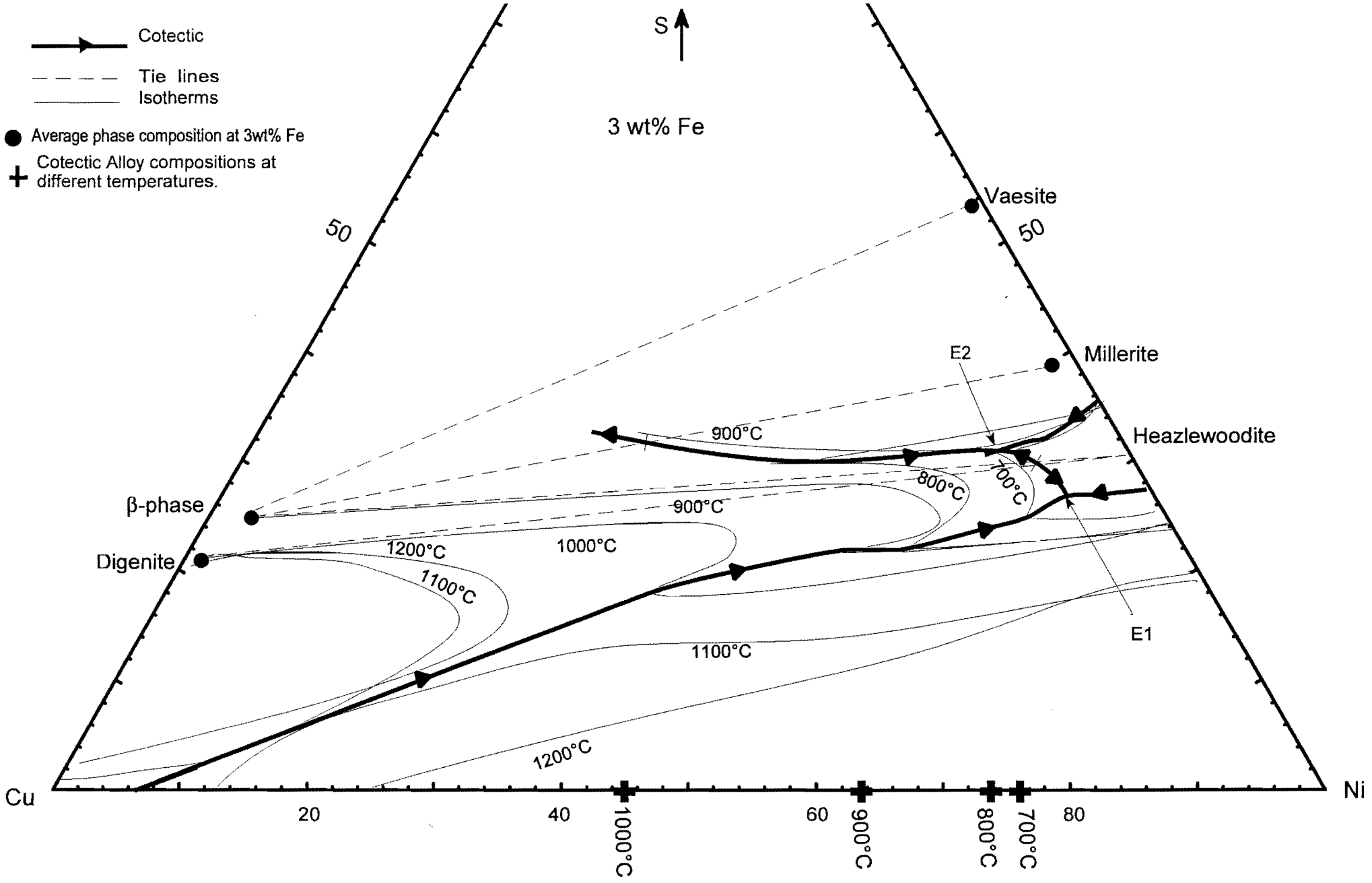

Figure 7.18: The liquidus isotherms and cooling path from 1200°C to 700°C at 3 wt% Fe in the starting composition. The composition of haezlewoodite is schematic.

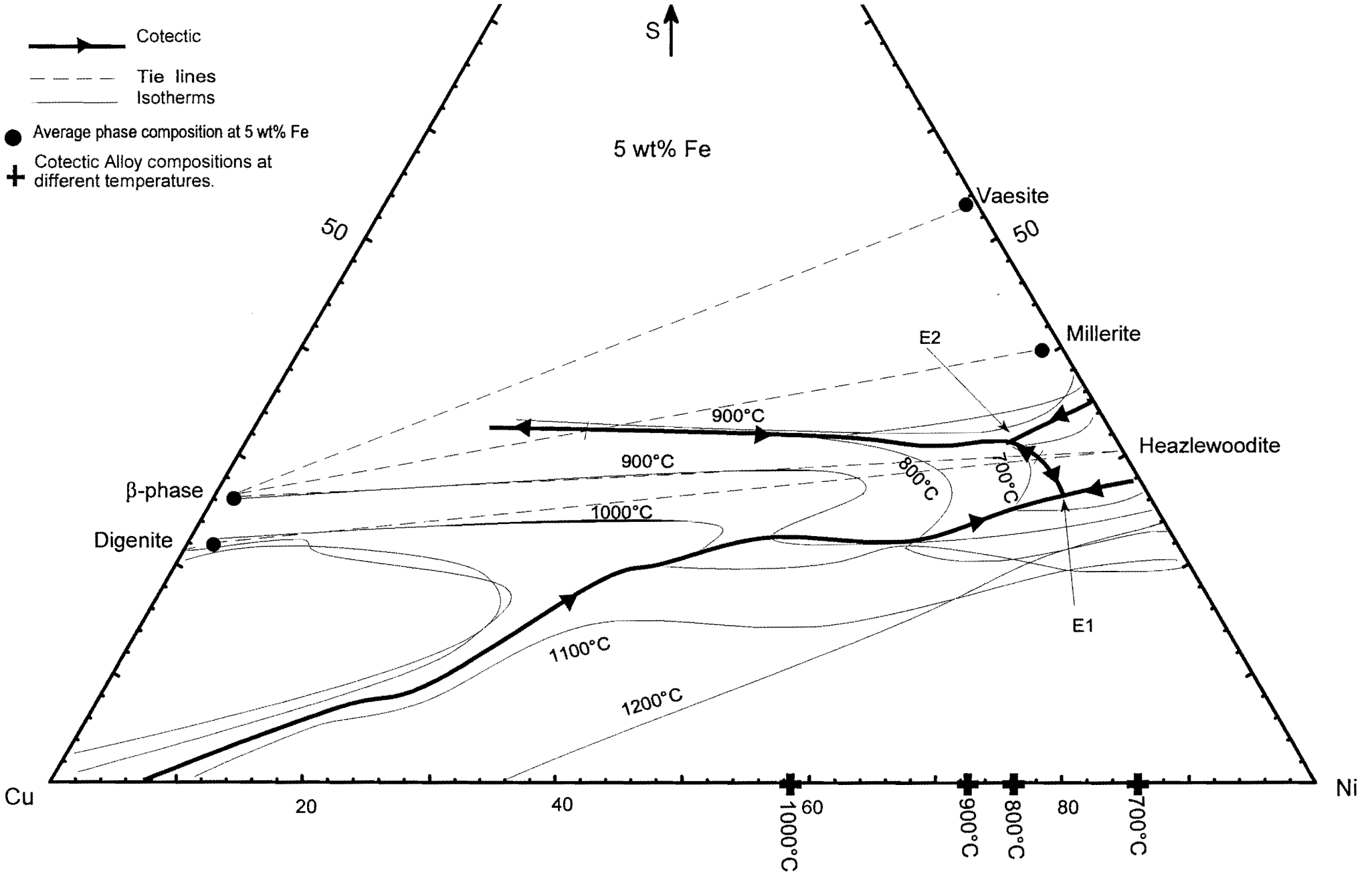

Figure 7.19: The liquidus isotherms and cooling path from 1200°C to 700°C at 5 wt% Fe in the starting composition. The composition of haezlewoodite is schematic

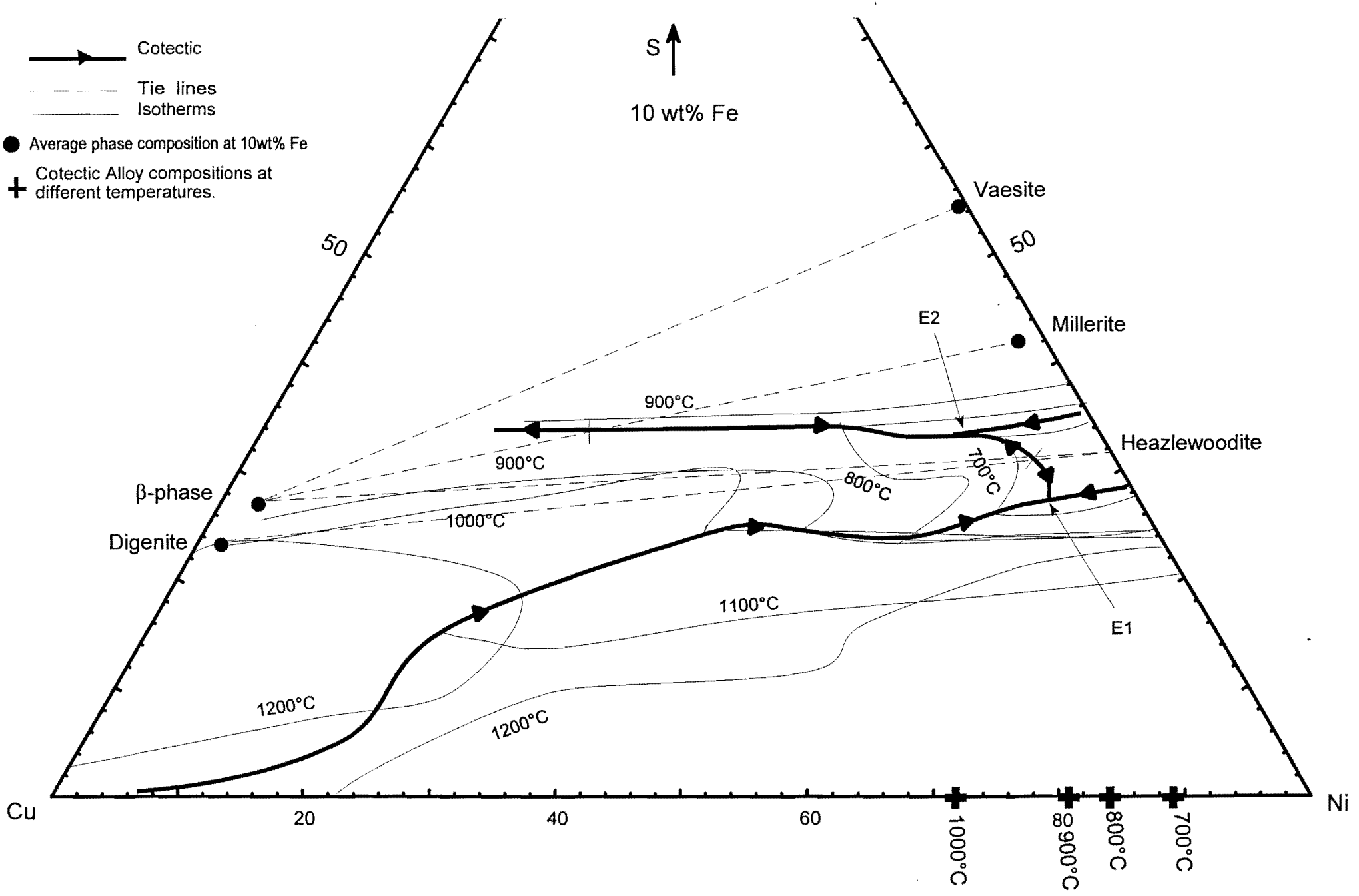

Figure 7.20: The liquidus isotherms and cooling path from 1200°C to 700°C at 10 wt% Fe in the starting position. The composition of haezlewoodite is schematic.

8. IMPLICATIONS

The successful process of slow cooling of converter matte in the beneficiation of platinum group metals requires a detailed understanding of the effect of compositional variation (mainly of the sulphur contents), because the temperature in conjunction with the bulk composition of the converted matte determine the path of crystallization. Under ideal conditions, the converter matte starts slow cooling at a temperature of 1200° - 1100°C with a composition of less than 3 wt% Fe and less than 20 wt% sulphur (Hiemstra, 1988). The average ore from the Bushveld Complex has higher Ni contents than Cu contents, which will result in the converter matte having a Cu/Ni ratio between 0.8 and 0.4 (Bruwer, 1996; Hiemstra, 1988). For economic reasons, the proportion of alloy crystallizing from the matte should not exceed 15 –20 % of the total (Sproule et al., 1960; Schouwstra et al., 1998).

Cooling from these conditions will ensure that a Cu-Ni-Fe alloy will crystallize first, collecting most of the PGMs, followed by the formation of sulphides. If the crystallization of alloy from the melt is preceded by crystallization of a sulphide, or during simultaneous crystallization of alloy and sulphide, the sulphide will compete for collection of the PGMs.

8.1 Cooling Paths for Mattes with Different Starting Compositions

Sproule et al. (1960) determined that the average eutectic alloy on complete crystallization has a composition of $Cu_{20}Ni_{80}$. The composition of the initial alloys differ, but if equilibrium conditions prevail (unlikely in a slow cooled converter matte), the composition of the first formed alloys will change until all alloys in the crystallized matte have a composition of $Cu_{20}Ni_{80}$. The Fe content of the bulk will influence the exact composition of this eutectic alloy. Because there is not a perfect linear relationship between the amount of Fe in the bulk and the amount of Fe in the alloys, the eutectic alloy composition at complete crystallization can not be easily predicted. For low Fe contents it has a composition close to that in the Fe-free system, but at higher Fe contents the composition deviates substantially from that given by Sproule et al. (1960). For the different starting Fe contents in the bulk, the composition of the cotectic alloy is indicated on the stability phase diagrams (Figures 8.1 to 8.4). Eutectic alloy compositions at solidification are completely inferred following the trend of the cotectic alloy at different temperatures.

Because the proportion of alloy in the ingot is ideally 15 – 20% of the mass, it is important to determine the influence of Fe on the amount of alloy that will crystallize. However, alloys crystallizing in the initial stages of slow cooling will have a larger grain size than the alloy forming at the eutectic point (E1) (Schouwstra et al., 1998). Fine intergrowths with sulphides at the eutectic will cause problems in the liberation of the alloy from the sulphide bulk. Therefore, the amount of alloy that form large, non-intergrown grains, which can easily be liberated during crushing, is essential. After crushing the crystallized matte, the magnetic alloy fraction is separated from the less magnetic sulphide fraction. A successful process will ensure that most of the PGE's are removed together with the alloy fraction.

This investigation looks at the influence of Fe on the slow cooling sequence of the matte. For a comparative discussion with the Fe-free system, the same starting compositions (representing that of an average converter matte) are chosen, varying only the Fe content. The crystallization paths are the same for all four diagrams, therefore, they will be discussed simultaneously.

Depending on the starting composition, three fundamentally different crystallization paths are possible, which are called A, B and C: If the starting composition falls into the (alloy)-stability field, crystallization path A will be followed on cooling of the matte. If the starting composition falls into the (digenite or β-phase)-stability field, two possible paths of crystallization can take place depending on the sulphur content. Which path (B or C) is followed, depends on the sulphur content. The critical sulphur content can be derived by a line connecting digenite and the eutectic point E1. At lower sulphur contents (than this line), path B will be followed and at higher sulphur contents path C will be followed. For starting compositions falling directly on the critical sulphur content line, the matte will crystallize digenite and at the eutectic temperature also alloy and heazlewoodite.

Best results are to be achieved if the Cu/Ni-ration is between 0.8 and 0.6 and the sulphur content between 18 and 22 wt%. Indicated on each diagram is an area that represents the typical range of converter matte compositions.

8.2 Path A

For a starting composition of X (Cu/Ni ~ 0.6 and S ~ 20 wt%), alloy will start to crystallize from the matte. Crystallization will proceed along the tie-line (X-A) until the cotectic line at composition A is reached. From A to the eutectic point E1, alloy and digenite will crystallize together. The composition of the alloy will change on cooling along the Cu-Ni join. On reaching the eutectic point E1, heazlewoodite will start to crystallize together with the alloy and digenite, until complete solidification.

8.3 Path B

For a starting composition of Y (Cu/Ni ~ 0.6 and S < critical sulphur content), digenite will start to crystallize first from the matte. Crystallization will proceed along a line directly away from digenite to point B on the cotectic line. At point B, digenite and alloy will crystallize together and follow the cotectic to the eutectic point E1. The composition of the alloy will change on cooling. At E1, heazlewoodite will also start to crystallize together with digenite and alloy until complete solidification.

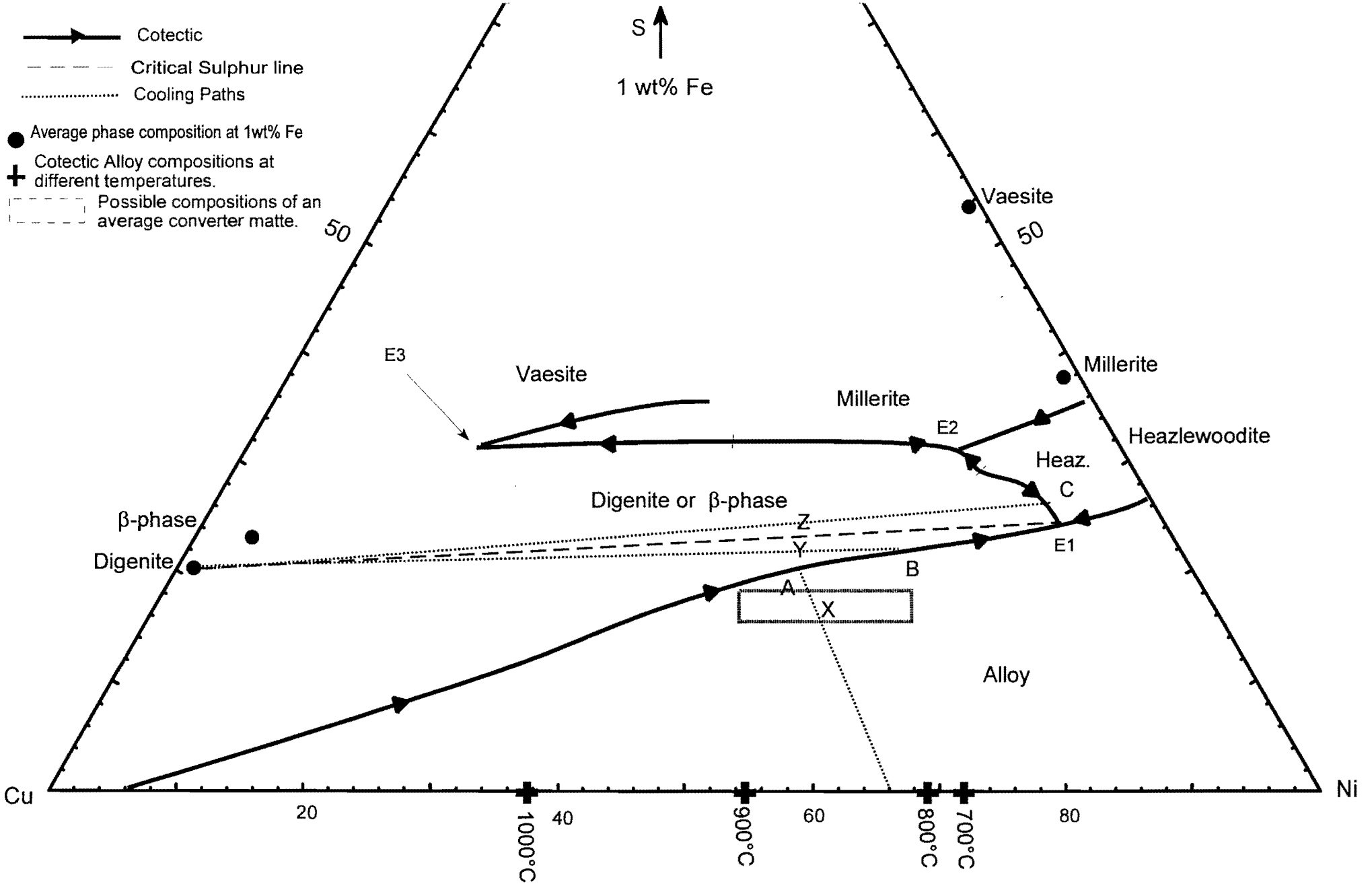

Figure 8.1: Stability phase fields and the cooling path for 1 wt% Fe in the bulk. Starting compositions for paths A, B and C are shown as X, Y and Z respectively. The composition of the cotectic alloy at the different temperatures is indicated on the Cu-Ni join.

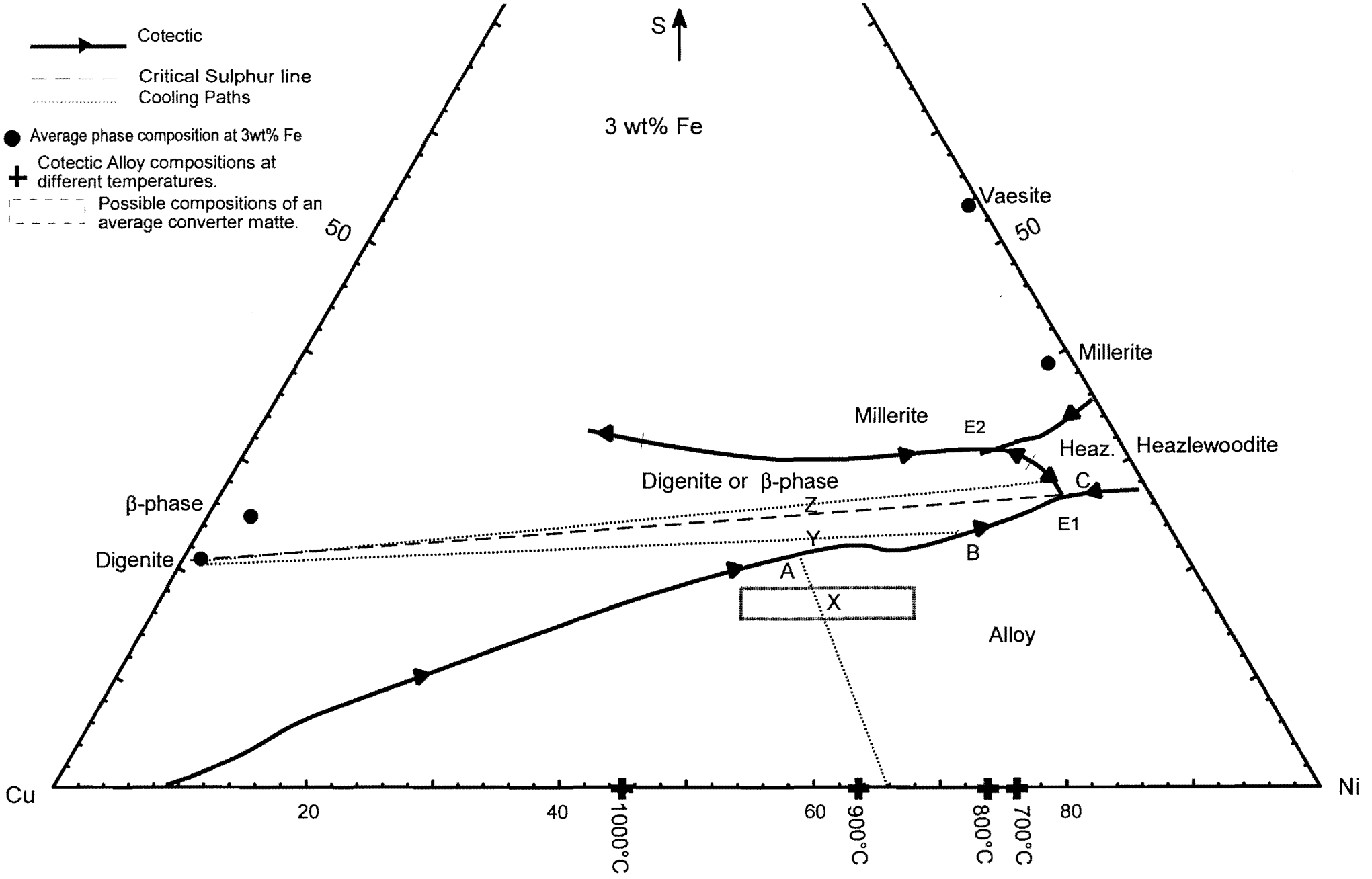

Figure 8.2: Stability phase fields and the cooling path for 3 wt% Fe in the bulk. Starting compositions for paths A, B and C are shown as X, Y and Z respectively. The composition of the cotectic alloy at the different temperatures is indicated on the Cu-Ni join.

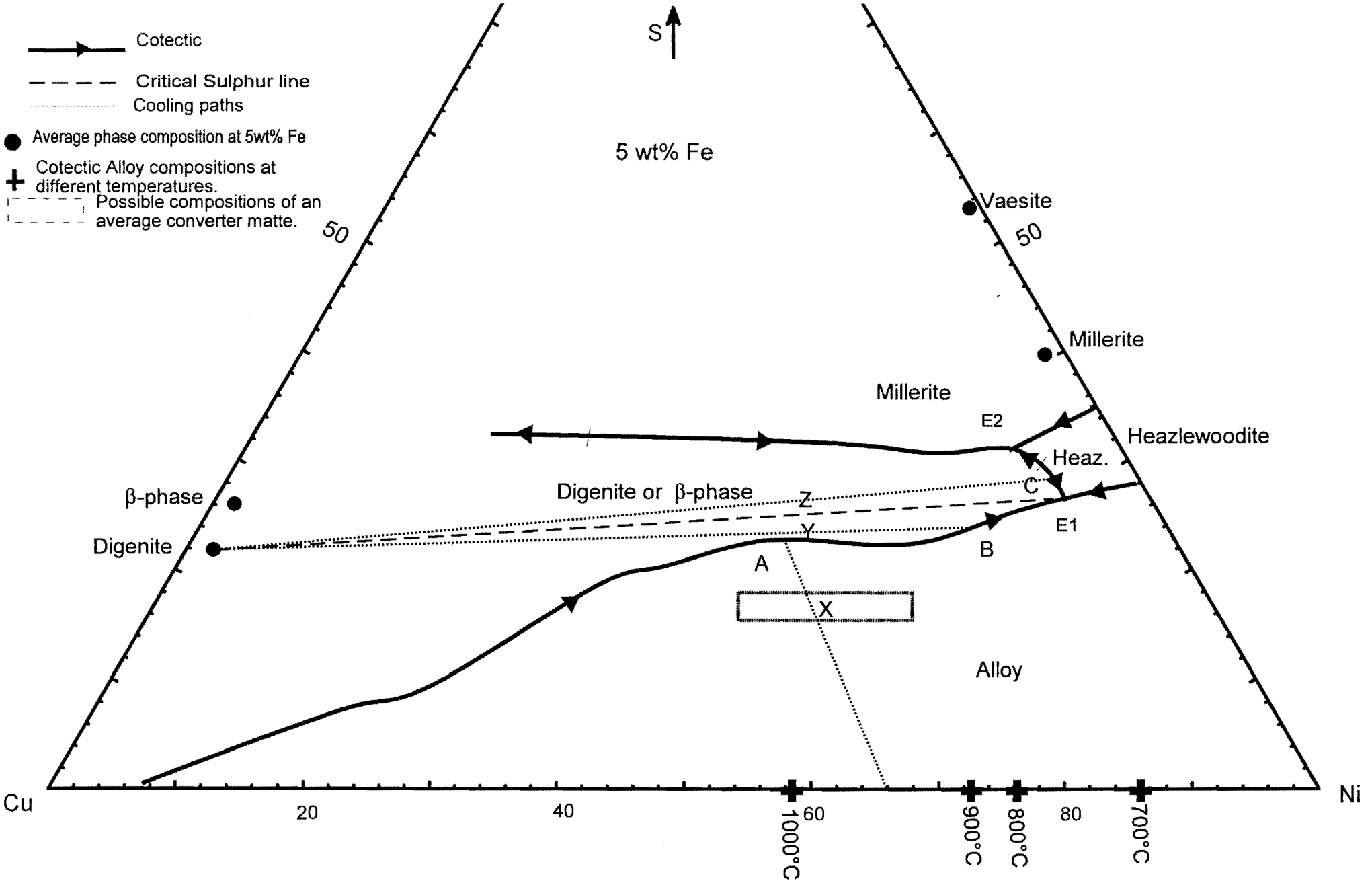

Figure 8.3: Stability phase fields and the cooling path for 5 wt% Fe in the bulk. Starting compositions for paths A, B and C are shown as X, Y and Z respectively. The composition of the cotectic alloy at the different temperatures is indicated on the Cu-Ni join.

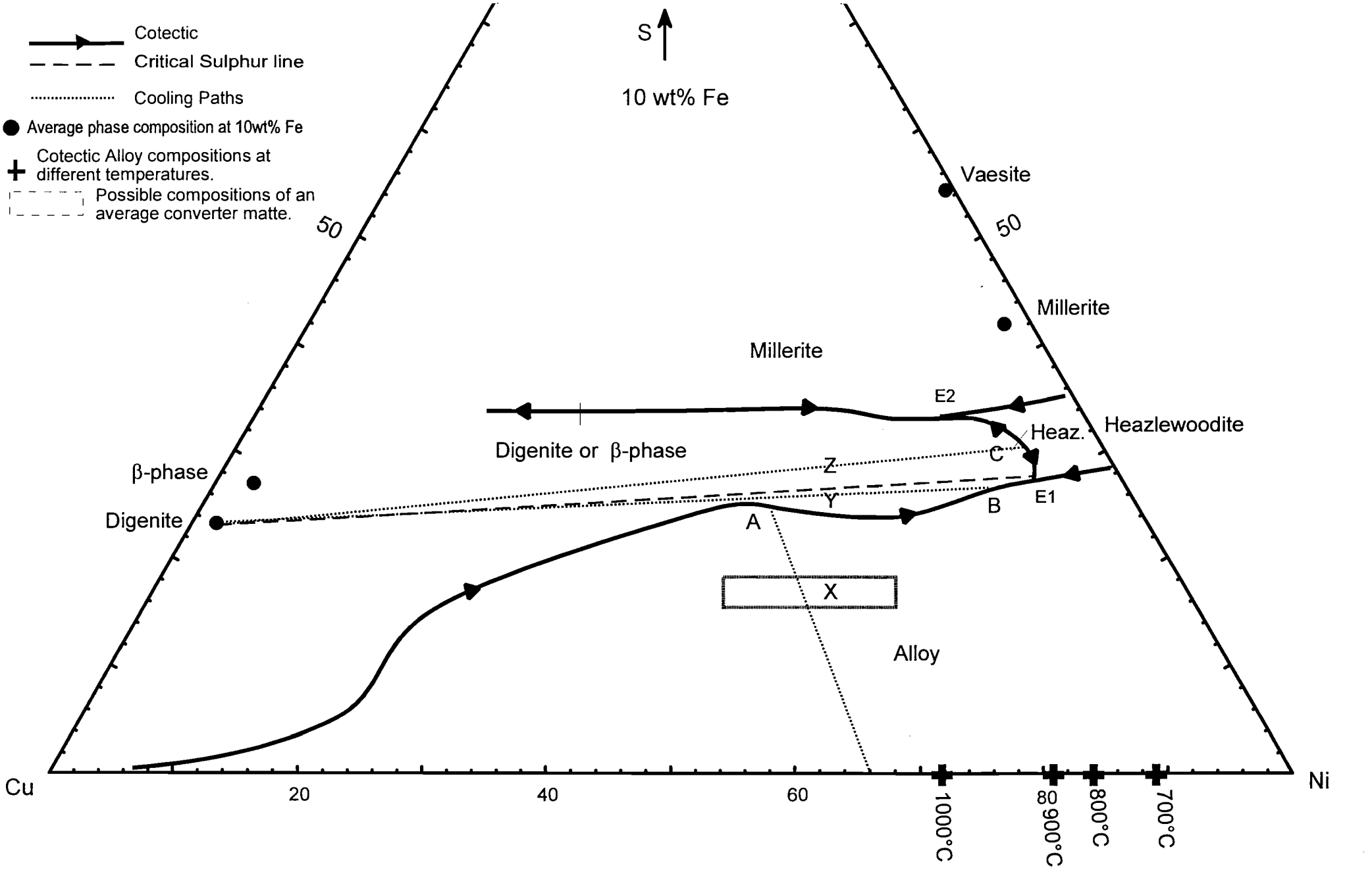

Figure 8.4: Stability phase fields and the cooling path for 10 wt% Fe in the bulk. Starting compositions for paths A, B and C are shown as X, Y and Z respectively. The composition of the cotectic alloy at the different temperatures is indicated on the Cu-Ni join.

8.4 Path C

For a starting composition of Z (Cu/Ni ~ 0.6 and S > critical sulphur content), digenite will be the first phase to crystallize from the matte. Crystallization will proceed along a line directly away from digenite to point C on the cotectic line. At this point, digenite and heazlewoodite will crystallize simultaneously and crystallization will proceed along the cotectic line to the eutectic point E1. At E1, alloy will crystallize together with digenite and heazlewoodite until complete solidification.

8.5 Effect of Fe on Path A

At a fixed Cu/Ni ratio and sulphur content, Fe will influence the amount of alloy crystallizing from the melt. The higher the Fe content in the bulk, the more alloy will form before digenite will start to crystallize. By applying the lever rule (at a starting composition of X and a fixed Cu/Ni of 0.51), the proportion of alloy crystallizing before reaching the cotectic, can be determined. The results (Figure 8.5) show a definite increase in the proportion of alloy crystallizing, as the bulk Fe content increases. It must be kept in mind that additional alloy will crystallize together with digenite as the melt cools down towards the eutectic point. At the eutectic point, alloy will continue to crystallize together with digenite and heazlewoodite, until complete solidification. Because the later crystallized alloy has to compete with simultaneous crystallizing sulphides (e.g. digenite and heazlewoodite), their texture and size will differ from that of the first alloy (Schouwstra et al., 1998).

At a sulphur content of 22 wt%, a small decrease in the Cu/Ni from 0.8 of the bulk at lower than 3 wt% Fe, will move the starting composition into the (digenite or β-phase) stability field. This shift will cause digenite to crystallize first from the melt followed by alloy at the cotectic line. At higher Fe contents, this increase in Cu has to be much larger to cause the same effect. For example, from point X the Cu/Ni must increase by ~0.4 at 1 wt % Fe in the bulk, by ~0.6 at 3 wt% Fe, by ~0.8 at 5 wt% Fe, and by ~1.3 at 10 wt% Fe, to ensure that digenite crystallizes first from the matte.

8.6 Effect of Fe on Paths B and C

From Figure 8.6 it appears as if the position of the critical sulphur content line rises with an increase in the Fe content of the bulk. This is, however, only a result of projection onto the floor of the diagram. For a Cu/Ni ratio of 0.6 the critical sulphur values vary between 24 and 25 wt% for all the different Fe contents. The variation in the position of the critical sulphur line can be explained by a shift in the position of the digenite composition field and the composition of the cotectic melt with an increase in Fe. Although not observed in this study, it stands to reason that the position of the heazlewoodite composition will also change with an increase in Fe, and therefore the phase stability line between digenite and heazlewoodite will also rise to supposedly high sulphur levels.

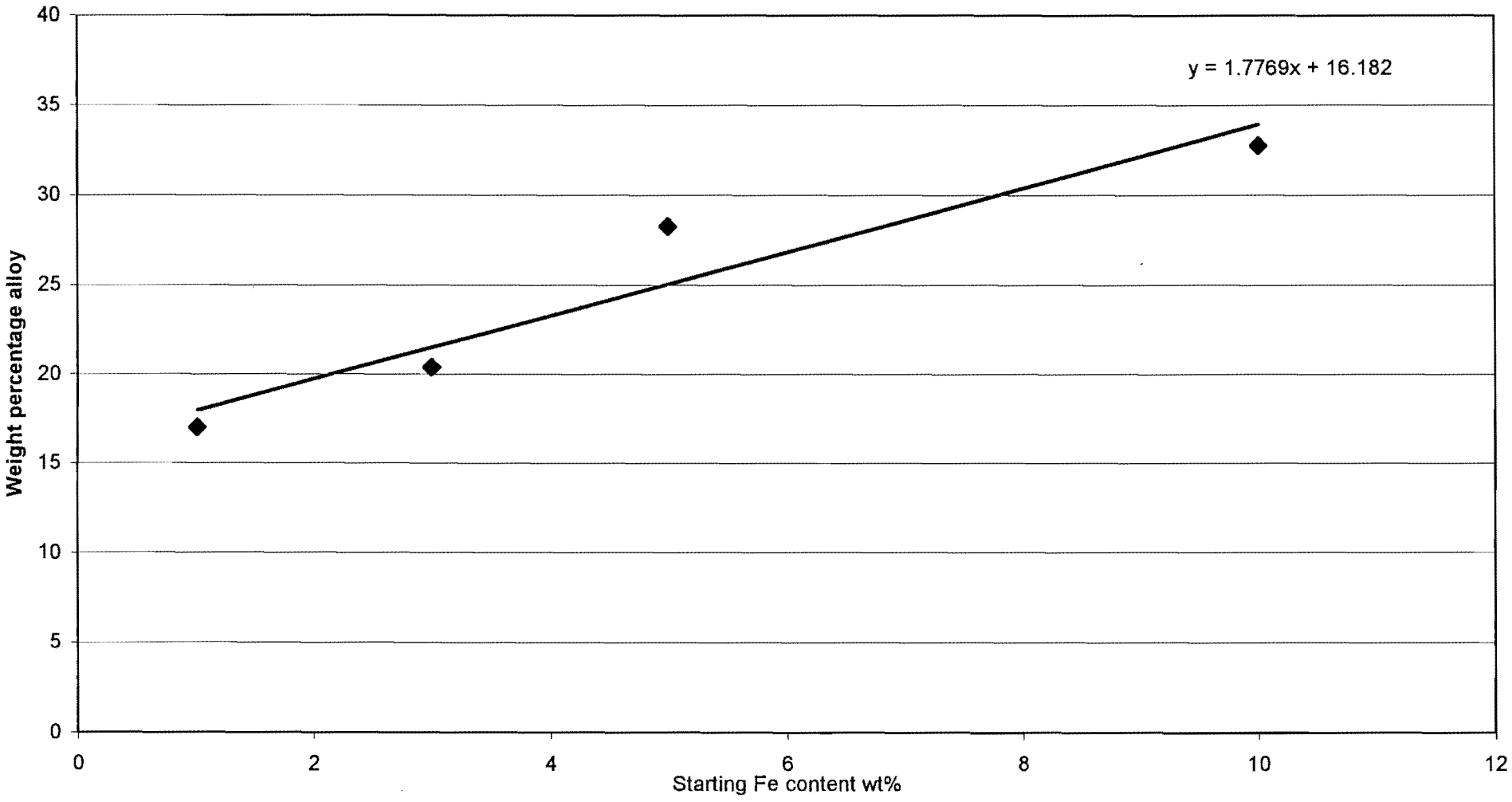

Figure 8.5:The percentage alloy crystallizing singularly form the melt at a starting composition of 20 wt% sulphur and a Cu/Ni of 0.6.

8.7 Summary

With an increase in the bulk Fe content the possibility for an average converter matte to fall into the alloy stability field improves. At Fe contents higher than 5 wt%, a small increase in Cu of the starting composition will not influence the crystallization sequence. It can be expected that the higher the amount of Fe in the bulk composition, the higher the proportion of coarse grained alloy in the total ingot (even though equilibrium conditions do not exist). However, the total amount of alloy will also increase and will influence the amount of material to be treated in the extraction of the noble elements.

An increase in Fe content will not significantly influence the crystallization path at higher levels of sulphur. The critical sulphur content (that determine the initial crystallization of either digenite / β-phase or heazlewoodite) stays virtually the same at any Fe content. This is however, subject to the exact position of the eutectic points (that were not determined by this study).

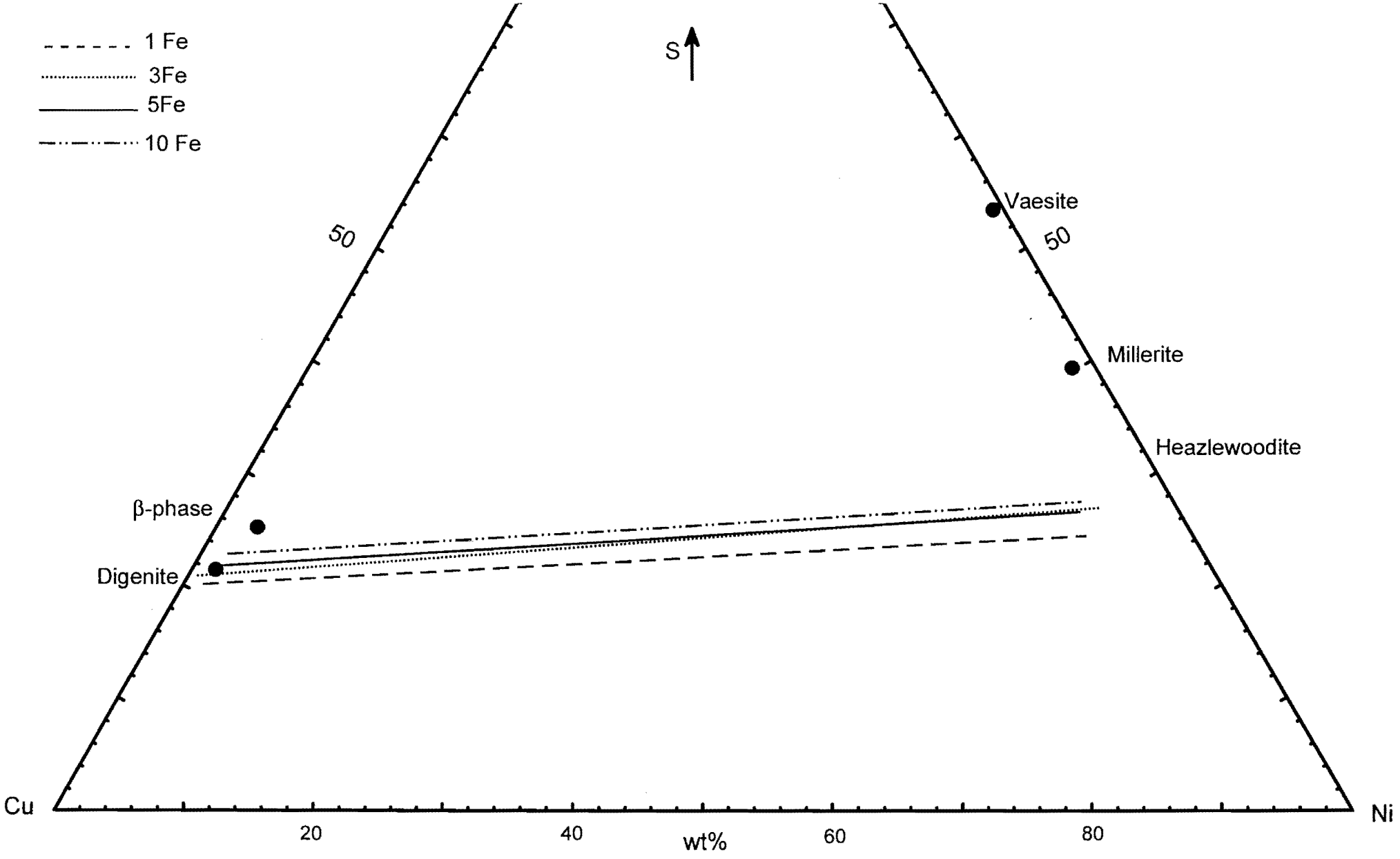

Figure 8.6: The position of the critical sulphur lines in the Cu-Ni-S ternary at variable Fe contents. Allso indicated are the average sulphide compositions.

9. CONCLUSIONS

The aim of the study is to investigate the influence of low concentrations of Fe on the Cu-Ni-S system with relevance to an average Cu-Ni-converter matte. Of particular interest are: (1) the compositions of the alloy and digenite co-existing with melt (generally referred to as the cotectic alloy, cotectic digenite and cotectic melt) at different temperatures; (2) the Fe content of sulphide and alloy phases with an addition of Fe to the starting composition, and (3) the partitioning of Fe between co-existing solid phases.

Alloy is the first phase to crystallize in an average converter matte (provided the composition is favorable) and also the primary collector of PGE's in the matte. In this investigation it was confirmed that at a fixed bulk Fe content, a decrease in temperature causes a decrease in the Cu/Ni of the cotectic alloy. Additionally, it has also been established that at a fixed temperature, an increase in the Fe content of the bulk will cause a decrease in the Cu/Ni of the cotectic alloy. Therefore, if all other parameters are kept stable, it can reasonably be accepted that an increase in the bulk Fe content will produce an increasingly Ni-rich alloy.

The composition of the cotectic melt is essential in determining the cooling path towards the eutectic point where alloy, digenite and heazlewoodite coexist. The cotectic melt in the assemblage (alloy+digenite+melt) shows an increase in Ni, Fe and sulphur content, with an increasing Fe content in the bulk. This causes the cotectic to shift towards higher sulphur contents, which results in a larger stability field for alloy. The implications are twofold: Firstly higher Fe contents increase the amount of alloy that will crystallize from the melt, and secondly it would require a larger variation in starting composition (particular the Cu/Ni) to alter the path of crystallization of a matte.

Examining the second aspect revealed that all of the stable phases are strongly influenced by the amount of Fe present in the bulk composition: The more Fe available, the more Fe will be incorporated in the crystal structures of phases. The relationship is, however, not linear and generally the more Fe available in the bulk the wider the range of Fe contents in the phase.

Lastly, in assemblages containing alloy, the alloy phase has consistently the highest partitioning coefficient for Fe. In other assemblages, Fe does not show any preference for a particular phase, regardless of the sequence of crystallization or temperature of equilibration.